

The University of British Columbia

FACULTY OF GRADUATE STUDIES

PROGRAMME OF THE
FINAL ORAL EXAMINATION
FOR THE DEGREE OF
DOCTOR OF PHILOSOPHY

of

NARENDRA KUMAR JHA

B.Sc (Hons.), Patna University, India 1955

M.Sc., Patna University, India 1957

TUESDAY, SEPTEMBER 28, 1965 AT 10:00 A.M.

IN ROOM 263, CHEMISTRY BUILDING

COMMITTEE IN CHARGE

Chairman: M. Darrach

N. Bartlett

R. C. Thompson

C. A. McDowell

R. M. Thompson

C. Reid

J. Trotter

External Examiner: R. D. Peacock

Department of Chemistry

The University of Birmingham

Birmingham 15, England

THE FLUORIDES AND OXYFLUORIDES OF OSMIUM AND
THE OXIDIZING PROPERTIES OF
THE NOBLE METAL HEXAFLUORIDES

ABSTRACT

An investigation of the attainable oxidation states of osmium in reaction with fluorine and fluorine-oxygen mixtures was carried out. The first simple heptavalent compound of osmium, osmium oxide pentafluoride, OsO_5F , was prepared by the fluorination of anhydrous osmium dioxide. This compound was characterized by analysis, X-ray single crystal and powder methods, and by infrared spectroscopy. The vapour pressure-temperature relationship and derived thermodynamic data have been evaluated. The magnetic susceptibility has been measured over the temperature range 77° to 300°K . The existence of an octavalent osmium oxyfluoride, osmium trioxide difluoride, OsO_3F_2 has been confirmed. This compound is diamagnetic and the solid is dimorphic. Preliminary structural work has indicated that the osmium is six-coordinated in this compound. A related ternary fluoride, NOOsO_3F_3 containing octavalent osmium was prepared and characterized. The results of the investigations indicate that OsO_2F_4 and higher fluorides of osmium than OsF_6 are unlikely to be stable at ordinary temperatures and pressures.

The oxidizing properties of the noble metal hexafluorides have been investigated. The reactions of platinum hexafluoride with nitrogen trifluoride, carbon monoxide, krypton, chlorine and hexafluorobenzene have been studied with the aim of preparing some unusual cations and to set an upper limit to the oxidizing power of PtF_6 . The reaction of xenon with platinum hexafluoride was further investigated in order to better characterize the reaction product. Dioxygenyl hexafluoroplatinate (V) was prepared on a large scale for a neutron diffraction study. This study was carried out by J.A. Ibers and W.C. Hamilton of the Brookhaven National Laboratory. Interpretation

of their findings is given.

Reactions of nitric oxide with OsF_6 , IrF_6 and PtF_6 were investigated to establish the oxidizing trend in the series and to prepare as complete a series of NOMF_6 salts as possible. The products NOMF_6 were characterized by analysis, magnetic measurements and X-ray powder photography. Reactions of these hexafluorides with sulphur tetrafluoride were also investigated and products containing SF_3^+ cations were obtained and characterized.

GRADUATE STUDIES

Field of Study: Inorganic Chemistry

Topics in Inorganic Chemistry	N. Bartlett W. R. Cullen
Physical Inorganic Chemistry	C. Reid H. C. Clark
Crystal Structures	J. Trotter N. Bartlett
Seminar In Chemistry	W. A. Bryce
The Chemistry of Organometallic Compounds	H. C. Clark
Topics in Organic Chemistry	J. P. Kutney D. E. McGreer R. E. I. Pincock

Related Studies:

Topics in Chemical Metallurgy	E. Peters A. M. Armstrong
Computer Programming	C. Froese

PUBLICATIONS

N. Bartlett, N. K. Jha, J. Trotter

Osmium Oxide Pentafluoride, OsOF_5
Proc. Chem. Soc., 277 (1962).

N. Bartlett and N. K. Jha

The Xenon-Platinum Hexafluoride Reaction
and Related Reactions

Hyman: Noble-Gas Compounds, University
of Chicago, 1963.

THE FLUORIDES AND OXYFLUORIDES OF OSMIUM
AND
THE OXIDIZING PROPERTIES OF THE NOBLE METAL HEXAFLUORIDES

by

NARENDRA KUMAR JHA

B.Sc. (Hons.) Patna University, India, 1955

M.Sc., Patna University, India, 1957

A THESIS SUBMITTED IN PARTIAL FULFILMENT OF THE
REQUIREMENTS FOR THE DEGREE OF
DOCTOR OF PHILOSOPHY

in the Department

of

CHEMISTRY

We accept this thesis as conforming to the
required standard

THE UNIVERSITY OF BRITISH COLUMBIA

September, 1965.

In presenting this thesis in partial fulfilment of the requirements for an advanced degree at the University of British Columbia, I agree that the Library shall make it freely available for reference and study. I further agree that permission for extensive copying of this thesis for scholarly purposes may be granted by the Head of my Department or by his representatives. It is understood that copying or publication of this thesis for financial gain shall not be allowed without my written permission.

Department of Chemistry,

The University of British Columbia
Vancouver 8, Canada

Date October 4, 1965.

ABSTRACT

An investigation of the attainable oxidation states of osmium in reaction with fluorine and fluorine-oxygen mixtures was carried out. The first simple heptavalent compound of osmium, osmium oxide pentafluoride, OsOF_5 , was prepared by the fluorination of anhydrous osmium dioxide. This compound was characterized by analysis, X-ray single crystal and powder methods, and by infrared spectroscopy. The vapour pressure-temperature relationship and derived thermodynamic data have been evaluated. The magnetic susceptibility has been measured over the temperature range 77° to 300°K . The existence of an octavalent osmium oxyfluoride, osmium trioxide difluoride, OsO_3F_2 has been confirmed. This compound is diamagnetic and the solid is dimorphic. Preliminary structural work has indicated that the osmium is six-coordinated in this compound. A related ternary fluoride, NOOsO_3F_3 containing octavalent osmium was prepared and characterized. The results of the investigations indicate that OsO_2F_4 and higher fluorides of osmium than OsF_6 are unlikely to be stable at ordinary temperatures and pressures.

The oxidizing properties of the noble metal hexafluorides have been investigated. The reactions of platinum hexafluoride with nitrogen trifluoride, carbon monoxide, krypton, chlorine and hexafluorobenzene have been studied with the aim of preparing some unusual cations and to set an upper limit to the oxidizing power of PtF_6 . The reaction of xenon with platinum hexafluoride was further investigated in order to

better characterize the reaction product. Dioxygenyl hexafluoroplatinate (V) was prepared on a large scale for a neutron diffraction study. This study was carried out by J.A Ibers and W.C. Hamilton of the Brookhaven National Laboratory. Interpretation of their findings is given.

Reactions of nitric oxide with OsF_6 , IrF_6 and PtF_6 were investigated to establish the oxidizing trend in the series and to prepare as complete a series of NOMF_6 salts as possible. The products NOMF_6 were characterized by analysis, magnetic measurements and X-ray powder photography. Reactions of these hexafluorides with sulphur tetrafluoride were also investigated and products containing SF_3^+ cations were obtained and characterized.

TABLE OF CONTENTS

	Page
Abstract	ii
List of Tables	vii
List of Figures	x
List of Plates	xi
Acknowledgements	xii
Chapter	
I INTRODUCTION	1
II EXPERIMENTAL	9
2.1 General Experimental Techniques	9
2.1.1 Fluorine handling and vacuum techniques	9
2.1.2 Fluorination reactions	15
2.1.3 Analysis	21
2.1.4 Gauges for vapour pressure and gas	
pressure measurements	28
2.1.5 Tensimetric titrations	31
2.1.6 Magnetic measurements	34
2.1.7 X-ray powder photographs	37
2.1.8 Infrared, visible and UV spectroscopy	38
2.1.9 Reagents	39
2.2 The Fluorides and Oxyfluorides of Osmium	42
2.1.9 Search for higher binary fluorides of	
osmium	42
2.2.2 Osmium oxide pentafluoride	42
2.2.3 Osmium trioxide difluoride	63
2.2.4 Nitrosyl trioxytrifluoroosmate(VIII)	69

Chapter	v	Page
II		
2.2.5	The search for OsO_2F_4	69
2.3	The Oxidizing Properties of the Noble Metal Hexafluorides	71
2.3.1	Platinum hexafluoride and oxygen	71
2.3.2	Platinum hexafluoride and xenon	74
2.3.3	Reactions of platinum hexafluoride with (i) Kr (ii) NF_3 (iii) CO (iv) C_6F_6 and (v) Cl_2	81
2.3.4	Reactions of rhodium hexafluoride with (i) Xe and (ii) Kr	84
2.3.5	Iridium hexafluoride and chlorine	85
2.3.6	Reactions of the hexafluorides of osmium, iridium and platinum with nitric oxide	86
2.3.7	Reactions of the hexafluorides of osmium, iridium and platinum with sulphur tetrafluoride	102
2.3.8	Nitrosyl hexafluoro-niobate and tantarate	107
2.3.9	Magnetic properties of platinum hexa- fluoride	107
III	DISCUSSION	113
3.1.	The Fluorides and Oxyfluorides of Osmium	113
3.1.1	Higher oxidation states of osmium	113
3.1.2	Osmium oxide pentafluoride	115
3.1.3	Osmium trioxide difluoride	128
3.1.4	Nitrosyl trioxytrifluoroosmate(VIII)	130

Chapter	Page
III	
3.1.5 Interrelationships of osmium fluorides	130
3.2 The Oxidizing Properties of the Noble Metal Hexafluorides	132
3.2.1 Dioxygenyl hexafluoroplatinate(V)	132
3.2.2 Xenon - noble metal hexafluorides adducts	138
3.2.3 The reactions of nitric oxide with the noble metal hexafluorides	143
3.2.4 The reactions of sulphur tetra- fluoride with the noble metal hexafluorides	154
3.2.5 Other oxidizing reactions of the noble metal hexafluorides	158
Appendix	
I	163
II	167
III	170
IV	176
References	178

LIST OF TABLES

Table		Page
I	The highest valent oxides and fluorides of the second and third transition series	2
II	Analytical data for OsO_3F_2 and AOsO_3F_3 salts	3
III	Effective molecular volumes of the orthorhombic form of the hexafluorides of the third transition series	5
IV	Vapour pressure data for OsOF_5	47
V	Some thermodynamic data for OsOF_5	48
VI	X-Ray powder data for OsOF_5 (orthorhombic)	49
VII	X-Ray powder data for OsOF_5 (cubic)	50
VIII	Magnetic data for OsOF_5	52
IX	Infrared data for OsOF_5	55
X	Magnetic data for the mixture NOOsF_6 , NOWOF_5	62
XI	X-Ray powder data for OsO_3F_2 (orange-yellow form)	66
XII	X-Ray powder data for NOOsF_6	88
XIII	Magnetic data for NOOsF_6	91
XIV	X-Ray powder data for NOIrF_6	94
XV	Magnetic data for NOIrF_6	96
XVI	X-Ray powder data for NOPtF_6 (rhombohedral)	98
XVII	X-Ray powder data for $(\text{NO})_2\text{PtF}_6$	100
XVIII	X-Ray powder data for SF_3OsF_6 and SF_3IrF_6	108
XIX	X-Ray powder data for NONbF_6 and NOTaF_6	109
XX	Magnetic data for PtF_6	111
XXI	Intramolecular distances and valency angles for OsOF_5 molecule	116

Table		Page
XXII	Comparison of some thermodynamic data for ReF ₆ , ReOF ₅ , OsF ₆ and OsOF ₅	119
XXIII	Comparison of the molecular volumes of orthorhombic and cubic forms of PtF ₆ , OsF ₆ , IrF ₆ and OsOF ₅	120
XXIV	Magnetic properties of some d ¹ complexes	121
XXV	Infrared data for OsOF ₅ compared with those for ReF ₆ and OsF ₆	124
XXVI	Magnetic properties of some d ² complexes of osmium	127
XXVII	Alternative formulations for O ₂ PtF ₆ and the lattice energy, ionization potential and electron affinity data	134
XXVIII	Internuclear distances and molecular orbital electron configurations of some diatomic species	135
XXIX	Comparison of NOPtF ₆ (rhomb.) and O ₂ PtF ₆ (rhomb.) and NOPtF ₆ (cub.) and O ₂ PtF ₆ (cub.) molecular volumes.	137
XXX	Comparison of the infrared data for Xe(PtF ₆) _x , KPtF ₆ and O ₂ PtF ₆	139
XXXI	Comparison of unit cell parameters and molecular volumes of NOMF ₆ salts of the third transition series	146
XXXII	Magnetic data for some d ³ [MF ₆] species	147
XXXIII	Magnetic data for some d ⁴ [MF ₆] species	149

Table		Page
XXXIV	d-Electron configuration of hexafluorides and hexafluoro-anions(V) of the second and third transition series	153
XXXV	Comparison of molecular volumes of some SF_3^+ and NO^+ salts.	158

LIST OF FIGURES

Figures		Page
1	A general purpose fluorine line	12
2	(a) Adapters for Kel-F trap	14
	(b) Adapters for high pressure fluorine	14
3	A flow system for fluorination with elemental fluorine	17
4	Apparatus for fluorination with bromine tri-fluoride	20
5	Apparatus for hydrolysis of osmium compounds	24
6	The diaphragm gauge	30
7	Apparatus for Tensimetric titrations	33
8	Plot of $\log P_{mm}$ vs. $1/T$ for $OsOF_5$	46
9	Plot of $1/\chi_A$ vs. T for $OsOF_5$	54
10	Infrared spectra of $ReOF_5$, $OsOF_5$ and IOF_5	56
11	Infrared spectra of $OsOF_5$ and WF_6	57
12	Apparatus for the reaction of $OsOF_5$ with NO in WF_6 solution	60
13	Plot of $1/\chi_A$ vs. T for the 1:1 mixture $NOOsF_6$, $NOWOF_5$	64
14	Apparatus for large scale synthesis of O_2PtF_6	73
15	Plot of $1/\chi_A$ vs. T for $NOOsF_6$	92
16	The molecular structure of $OsOF_5$	117
17	Interrelationships of osmium fluorides	131
18	Comparison of effective molecular volumes of MF_6 and $[MF_6]^-$ species of the second and third transition series	152

Figure		Page
19	Bonding in the noble metal hexafluorides	155

LIST OF PLATES

Plate		Following Page
I	X-Ray powder photographs of some NOMF_6 salts and O_2PtF_6	146
II	X-Ray powder photographs of SF_3OsF_6 , SF_3IrF_6 and NOOsF_6	158

ACKNOWLEDGEMENTS

I wish to express my sincere gratitude to Professor N. Bartlett for his keen interest and constant guidance throughout this work. I would like to thank Mr. S. Beaton, my colleague for providing a sample of cubic NOPtF_6 , for permitting me to quote some of his results, for proof reading this thesis and for helpful discussions. I am also indebted to Mr. Emil Matter, of the workshop of the Chemistry Department of the University of British Columbia, for making the many pieces of metal apparatus required in this work. I very much appreciate the help given by Mr. B. Sarkar and Miss K. Lalita in drawing the diagrams. I am also grateful to the National Research Council, Ottawa for the award of a Studentship during the years 1962-1965.

Chapter I

INTRODUCTION

Fluorine is well known for its reactivity. It is the most oxidatively reactive of all the chemical elements; indeed it combines exothermically with most of them and often excites the highest attainable oxidation state of the element. Its reactivity is attributable to the low dissociation energy of molecular fluorine,^{1,2} its small atomic size³ and the exothermicity of its bonds to other elements.⁴

Although much is now known of the fluorides of the commoner elements, the fluorine chemistry of the platinum metals (ruthenium, rhodium, palladium, osmium, iridium and platinum) has received much less attention than it deserves. Appreciable advancement has, however, been made in the past few years including the preparation of several new fluorides, the recharacterization of some of those already known, and better characterization of the structure and bonding of the established fluorides by way of electron diffraction,^{5,6} crystallography,^{7-9,32} magnetochemistry¹⁰ visible, ultraviolet and infrared spectroscopy,¹¹⁻¹⁵ nuclear magnetic¹⁶⁻²⁰ and electron spin resonance^{21,22} spectroscopy.

Notable among the recently prepared fluorides are the hexafluorides of platinum,²³ technetium,²⁴ ruthenium²⁵ and rhodium²⁶ and one heptafluoride, that of rhenium.²⁷ The recharacterization included one of the first volatile metal hexafluorides to be prepared, osmium hexafluoride. This fluoride was first described in 1913²⁸ but was incorrectly identified as osmium octafluoride and was so known for the next forty five years.²⁹ Osmium octa-

fluoride was regarded as the prime example of the ability of fluorine to excite the highest valency and highest coordination. Undoubtedly the uncritical acceptance of the erroneous octafluoride formulation was conditioned by the ready formation and high stability of the tetroxide of osmium. Since all eight valence electrons of osmium are presumably involved in bonding in the tetroxide, the possibility of them all being used to bond fluorine could not be easily denied.

The established highest valent oxides and fluorides of the second and third transition series are given in Table I.

Table I

The Highest Valent Oxides and Fluorides of the Second and Third Transition Series.

Fluorides	MoF ₆	TcF ₆	RuF ₆	RhF ₆	PdF ₄	AgF ₂
Oxides	MoO ₃	Tc ₂ O ₇	RuO ₄	RhO ₂	Pd ₂ O ₃	AgO
Fluorides	WF ₆	ReF ₇	OsF ₆	IrF ₆	PtF ₆	AuF ₃
Oxides	WO ₃	Re ₂ O ₇	OsO ₄	IrO ₃	PtO ₃	Au ₂ O ₃

It is apparent that both fluorine and oxygen excite the same highest formal oxidation state except for the elements Ru, Os, Rh, Pd and Tc. Rhodium and palladium attain their highest states of oxidation most readily with fluorine. The converse is the case for ruthenium and osmium, both of which form tetroxides. There is, therefore, no indication from this simple correlation that higher fluorides of osmium than OsF₆ should not exist. Moreover, a comparison of osmium with rhenium (the preceding element), which forms a heptafluoride, lends some

support to the view that osmium may form a heptafluoride. However, the marked decrease in thermal stability, with increase in the atomic number of the transition metal, in each hexafluoride series,⁵ indicates that osmium heptafluoride would be much less stable towards dissociation than the heptafluoride of rhenium.

The work of Hepworth and Robinson³⁰ indicated that Os (VIII) could occur in oxyfluoride systems. They reported osmium trioxide difluoride OsO_3F_2 , and complex salts of general formula AOsO_3F_3 with A, as monovalent metal (K, Cs and Ag). The description of the compounds, however, was brief and their analytical identification rested only on fluorine analysis. The identification of osmium trioxide difluoride and its complex salts predated the correct identification of the "octafluoride" of osmium. In the absence of other evidence and on the basis of analytical evidence alone, this oxyfluoride could be formulated as OsO_2F_2 and the complex salts as AOsO_2F_3 as shown in Table II.

Table II

Analytical Data for OsO_3F_2 and AOsO_3F_3 Salts.

OsO_3F_2		AgOsO_3F_3	
Found:	F, 13.5%; 14.2%.	Found:	F, 13.8%; Ag, 26.7%
OsO_3F_2 requires F,	13.8%.	AgOsO_3F_3 requires F,	14.1%; Ag, 26.8%
OsO_2F_2 requires F,	14.6%.	AgOsO_2F_3 requires F,	14.7%; Ag, 27.9%

(Cont'd)

TABLE II (cont'd)

KOsO_3F_3	CsOsO_3F_3
Found: F, 20.0%; E 317.	Found: F, 15.1%; E 454.
KOsO_3F_3 requires F, 17.0%; E 334.	CsOsO_3F_3 requires F, 13.3%; E 428.
KOsO_2F_3 requires F, 17.9%; E 318.	CsOsO_2F_3 requires F, 13.8%; E 412.

Confirmation of these findings was, therefore, desirable. No other oxyfluorides of osmium except an ill-characterized osmium oxide tetrafluoride, OsOF_4 ³¹ were known prior to the present work. Allowing that the highest valence attainable in a stable binary fluoride of osmium is six, the oxyfluoride OsOF_6 appears improbable. The possible existence of the oxyfluorides OsO_2F_4 and OsOF_5 , however, cannot be readily denied. In order to better evaluate the factors which limit the formal oxidation state of osmium, an investigation of the osmium-oxygen-fluorine system was, therefore, undertaken together with a simultaneous search for a higher binary fluoride of osmium than the hexafluoride. The results of this investigation and their significance form a major part of this thesis.

The third transition series elements are of particular interest in that hexafluorides of the elements from tungsten to platinum are known.⁷ These hexafluorides have been well characterized physically. The molecules have octahedral symmetry and the solids are molecular. They are, therefore, readily volatile. In the vapour phase the metal to fluorine distance in these hexafluorides is essentially constant, being about 1.83⁰Å as found by electron diffraction.⁵ At low temperatures these molecules are close packed in an orthorhombic crystal structure, the

effective molecular volumes³² varying as shown in Table III.

Table III

Effective Molecular Volumes of the Orthorhombic Form of the Hexafluorides of the Third Transition Series.³²

WF ₆	ReF ₆	IrF ₆	PtF ₆
108.5	106.6	105.4	104.6 Å ³

All of them show a solid-solid transition at $\sim 0^{\circ}\text{C}$ from a close packed orthorhombic to a less dense body centred cubic form⁶. In the gas phase the molecules with non-bonding electronic configurations d^1 and d^2 show a dynamic Jahn-Teller effect arising from a coupling of electronic and vibrational motion^{5,13,25,33}. The visible and ultraviolet spectra of these hexafluorides have been well interpreted in terms of ligand field theory with due consideration given to the high spin-orbit coupling, characteristic of the heavier elements.¹¹ Excellent general reviews have recently appeared on the hexafluoride molecules.^{5,6}

Although the chemical investigation of the hexafluorides has hitherto been sparse, the spontaneous liberation of fluorine at ordinary temperatures from the hexafluorides of platinum,²³ ruthenium²⁵ and rhodium²⁶ clearly indicated their high oxidizing potential. This potential remained largely unexplored until 1962. The discovery of dioxygenyl hexafluoroplatinate(V), $\text{O}_2^+ [\text{PtF}_6]^-$ by Bartlett and Lohmann³⁴ and its identification in that year, established platinum hexafluoride to have a surprisingly high electron affinity; a value in excess of 160 kcal/mole.

This is considerably greater than the highest known electron affinity of any element or compound. The oxidation of xenon,³⁵ the first ionization potential of which is the same as that of oxygen, 12.2 e.v.,³⁶ further supported these conclusions. The 1:1 xenon-platinum hexafluoride adduct was formulated by Bartlett as $\text{Xe}^+ [\text{PtF}_6]^-$ by analogy with the $\text{O}_2^+ [\text{PtF}_6]^-$ compound.

The entities $\text{O}_2^+ [\text{PtF}_6]^-$ and $\text{Xe}^+ [\text{PtF}_6]^-$ are of structural interest. The formulation $\text{O}_2^+ [\text{PtF}_6]^-$ has been well founded by Bartlett and Lohmann.³⁴ Their preliminary structure determination of O_2PtF_6 was derived from X-ray powder data, since single crystals of this compound were not available. The low X-ray scattering factor of the light atoms, oxygen and fluorine, compared with platinum, together with the limited data, prevented determination of the O-O distance in O_2^+ cation with significant accuracy. A neutron diffraction study of a polycrystalline sample did, however, hold high promise of significant accuracy but called for a large, pure, well crystalline sample. Some effort was devoted successfully towards this end. The formulation $\text{Xe}^+ [\text{PtF}_6]^-$ of the 1:1 reaction product of Xe and PtF_6 required further substantiation. At the outset even the oxidation state of the platinum in this compound had not been established with certainty. Moreover, a survey of the compounds of xenon³⁷ indicates that xenon has even valence in all its simple compounds, e.g. XeF_2 , XeF_4 , XeF_6 , XeO_3 , XeOF_4 etc., whereas the formulation $\text{Xe}^+ [\text{PtF}_6]^-$ requires an odd valence of xenon.

The oxidation of molecular oxygen and xenon indicated the lower limit of the oxidizing power of platinum hexafluoride.

The upper limit remained to be assessed. In the present work, its reactions with a variety of elements and compounds were studied toward this end.

At the outset it was believed that the hexafluoride of platinum was merely the most powerfully oxidizing in the series and a smooth trend in oxidizing power with increasing atomic number of the transition metal, was anticipated. Furthermore, it was recognized that each of the second transition series hexafluorides was more powerfully oxidizing than its third transition series relative. A more systematic examination of the oxidizing power of the hexafluorides of each series was, therefore, undertaken. Nitric oxide, which has a much lower ionization potential than molecular oxygen ($I_{\text{NO}} = 9.25 \text{ e.v.}^{36}$), was considered to be a useful reagent for this survey. Ruthenium hexafluoride and rhodium hexafluoride, both of which liberate fluorine at ordinary temperature and are even less stable than PtF_6 , were considered most likely to have oxidizing potential comparable to that of the platinum compound.

Not only did an investigation of NO-MF_6 reactions appear to be useful as an indication of the relative oxidizing power of the fluorides but the investigation also presented the possibility of preparing new salts of general formula NOMF_6 . It was presumed that such salts would be structurally akin to O_2PtF_6 . Although a previous investigation³⁸ had shown that iridium hexafluoride reacts with nitric oxide to give a quadri-valent salt, $(\text{NO})_2\text{IrF}_6$, it nevertheless appeared possible that the quinquevalent salt, NOIrF_6 , could be isolated with proper

control of the interaction.

The hexafluorides are strong fluorinating agents and hence their oxidizing power can also be investigated by investigating their fluorination reactions.⁵ It had been reported that IrF_6 fluorinates sulphur tetrafluoride to the hexafluoride and is itself reduced to quinquevalent iridium to yield the adduct, $\text{SF}_4, \text{IrF}_5$,³⁸ which can be formulated as $\text{SF}_3^+ [\text{IrF}_6]^-$. The reactions of SF_4 with these hexafluorides were, therefore, also investigated in the present work.

Chapter II

EXPERIMENTAL

2.1 GENERAL EXPERIMENTAL TECHNIQUES

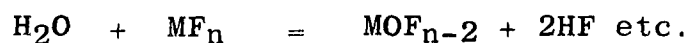
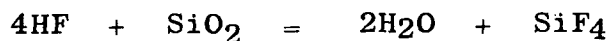
2.1.1 Fluorine Handling and Vacuum Techniques

(i) Materials of construction

The materials chosen for the construction of the system for handling fluorine in the present work were monel, nickel, copper and iron. Gaskets for high temperature work were of aluminum, otherwise they were of teflon. Kel-F traps were used wherever possible in preference to quartz or Pyrex glass. As a window material in infrared spectroscopy, silver chloride was preferred to sodium chloride and potassium bromide, because of its lower reactivity to fluorides and fluorine.

(ii) Purification of fluorine

The fluorine supplied commercially has a purity of 98%, a major impurity being hydrogen fluoride (0.2%). It is desirable to remove this hydrogen fluoride as it causes corrosion of glass or silica containers with eventual decomposition of any reactive fluorides by the cycle of reactions:



Hydrogen fluoride was removed by passing fluorine through a brass tube packed with porous sodium fluoride pellets. The activity of the sodium fluoride was maintained by periodic heating at 250^o-300^o, while purging with dry nitrogen.

Traces of hydrogen fluoride not removed by the

scrubber were condensed from the gas stream by a trap cooled in liquid oxygen. Liquid oxygen could not be used with pressures of fluorine in excess of 40 p.s.i. since fluorine condenses at liquid oxygen temperature under these conditions.

(iii) Disposal of fluorine

In order to protect the vacuum pumps from attack by fluorine a soda lime scrubber was included in the fluorine system.

(iv) Vacuum pumps

Two vacuum pumps were incorporated in the fluorine supply line. The first, a mechanical pump (Welch DUOSEAL), was used for initial evacuation of the apparatus and removal of excess fluorine. The second was a mechanical and oil diffusion pump combination, which was used for production of pressures of the order of 10^{-5} mm. of Hg or lower.

(v) Apparatus for handling fluorine

30,000 p.s.i. Autoclave Engineering compression fittings made of monel were used to build the fluorine system. These fittings consisted of various lengths of 3/8 in. O.D., 1/8 in. I.D. tubing linked by crosses, tees and straight and L-valves. Great versatility of design was possible and the system could be easily demounted, cleaned and reassembled.

A typical assembly suitable for both high and low pressure fluorine work and containing fluorine purification and disposal units is shown in Figure 1. Suitable barricades were used for the fluorine cylinder and high pressure fluorine sections. The fluorine pressures were measured with Bourdon

type gauges. A simple low viscosity fluorocarbon oil bubbler served to warn of the blocking of lines or vessels and acted as a safety valve.

(vi) Adapters for high and low pressure fluorine

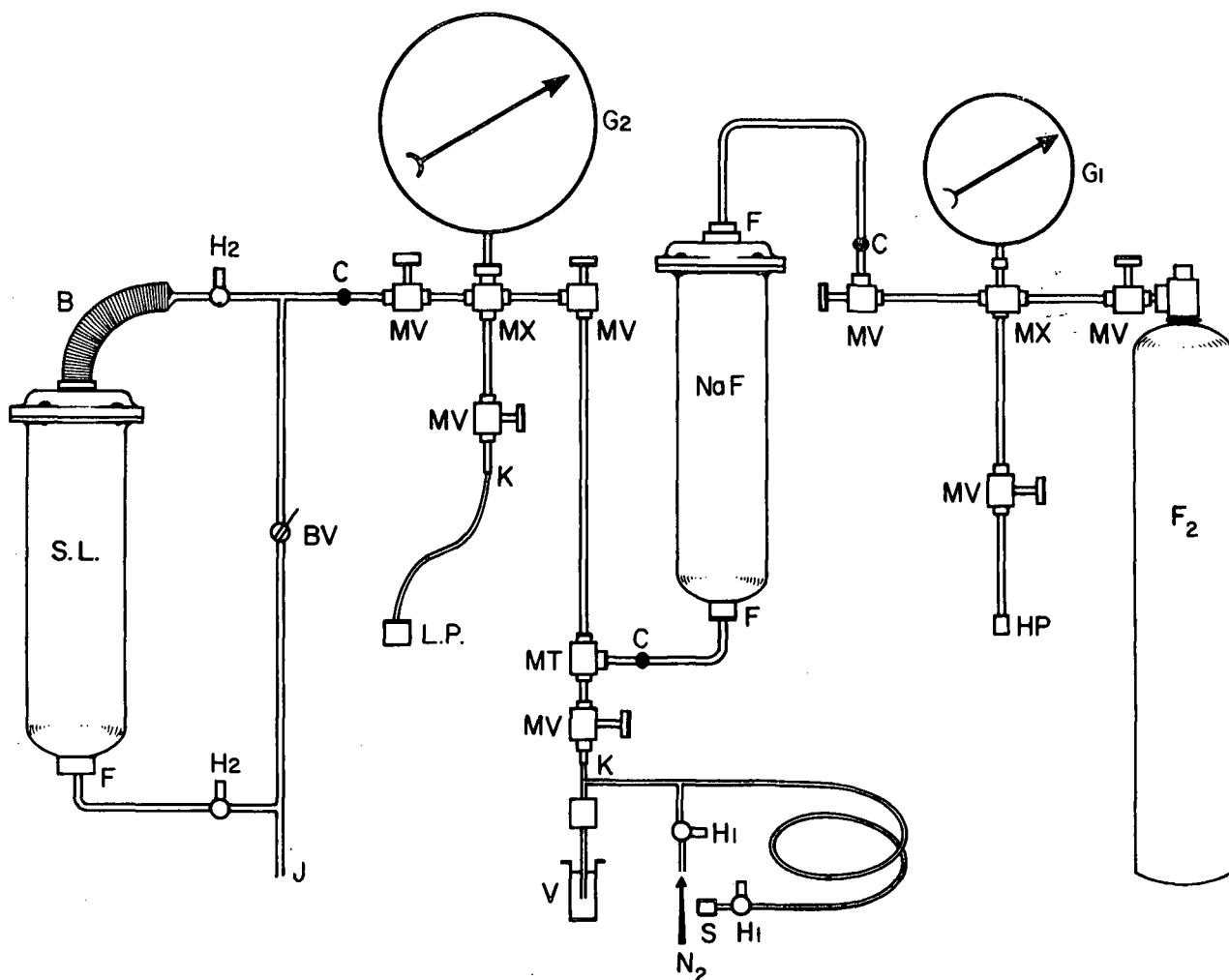
Specially constructed adapters (Figure 2) of monel metal provided with teflon gaskets were used for taking high pressure fluorine into reaction vessels. These adapters were silver soldered to the high pressure metal tubing.

For low pressure fluorine, 1/4 in. monel Swagelok compression fittings with teflon front ferrules and nylon or teflon back ferrules were used to join lengths of 1/4 in. metal tubing. These fittings could also be adapted for connecting 7 mm. glass or quartz tubing to 1/4 in. metal tubing. One side of the compression fitting was drilled to take the glass. This adaption dispensed with the need for rather fragile Kovar seals.

(vii) Storage and reaction vessels

The vessels for storing the volatile and reactive fluorides were made of monel or nickel sheet, 1/32 in. thick. They were cylindrical cans of 2 in. diameter and 3 in. length and were provided with Hoke A431 valves joined by solder tube fittings.

These cans were also used for the fluorination reactions with elemental fluorine at moderately high pressures (up to 150 p.s.i.). For higher pressures, thick-walled reaction vessels were used. For high temperature work yielding involatile products the vessels were provided with heavy gauge lid gasketed



MV, 30,000 p.s.i. monel valve; MX, Monel cross; MT, Monel tee; G₁ Monel Bourdon gauge, 400 lb.p.s.i.; G₂, Monel Bourdon gauge, 1000 mm. Hg; C, 30,000 p.s.i. seamless monel tubing 3/8 in. o.d., 1/8 in. i.d., silver soldered to 3/8 in.o.d. copper tubing; F, 3/8 in. flare fitting; K, 3/8 in. 30,000 p.s.i. tubing, silver soldered to 1/4 in. monel tubing; H₁ and H₂ Hoke A431 and A432 valves, respectively; B, Flexible copper bellows; SL, Soda lime tower; BV, 3/8 in. bore teflon-seated ball valve; J, Connection for vacuum pumps; HP, High-pressure fluorine outlet; LP, Low-pressure fluorine outlet via "Swagelok" compression fittings; S, "Swagelok" outlet for apparatus requiring fluorine diluted with nitrogen.

Figure 1. A General Purpose Fluorine Line.

with aluminum and securely bolted to the body.

(viii) General purpose vacuum system

A general purpose vacuum system for handling the volatile fluorides and studying their reactions was built using $\frac{1}{4}$ in. monel, nickel and copper tubing, Hoke A431 valves and Kel-F traps. The Hoke valves were joined to the tubes through solder tube fittings. Two types of connector were used to join the tubes. The first consisted of monel welding unions in straight connectors, elbows, tees and crosses. They were used in those parts of the system which required minimum cleaning. The second were Swagelok compression fittings which consisted of straight unions, elbows, tees and crosses. Swagelok fittings were also used for connecting glass or quartz to metal as described previously.

Kel-F traps (15 cm. long, 1 mm. thick and 20 mm. O.D., obtained from Argonne National Laboratory, Illinois) were attached to the metal system by means of the special adapters shown in Figure 2. The Kel-F traps were, by virtue of their resistance to chemical attack, of great value in the manipulation of reactive fluorides. Moreover, these traps could be detached, cleaned and used again.

(ix) Valves

The main difficulty encountered in handling fluorine and reactive fluorides was the fouling up of the valves used in the system. All valves in time developed a "leak through" which arose from poor contact of the stem-tip with the seat of the valve. The cause of this was the deposition of solids

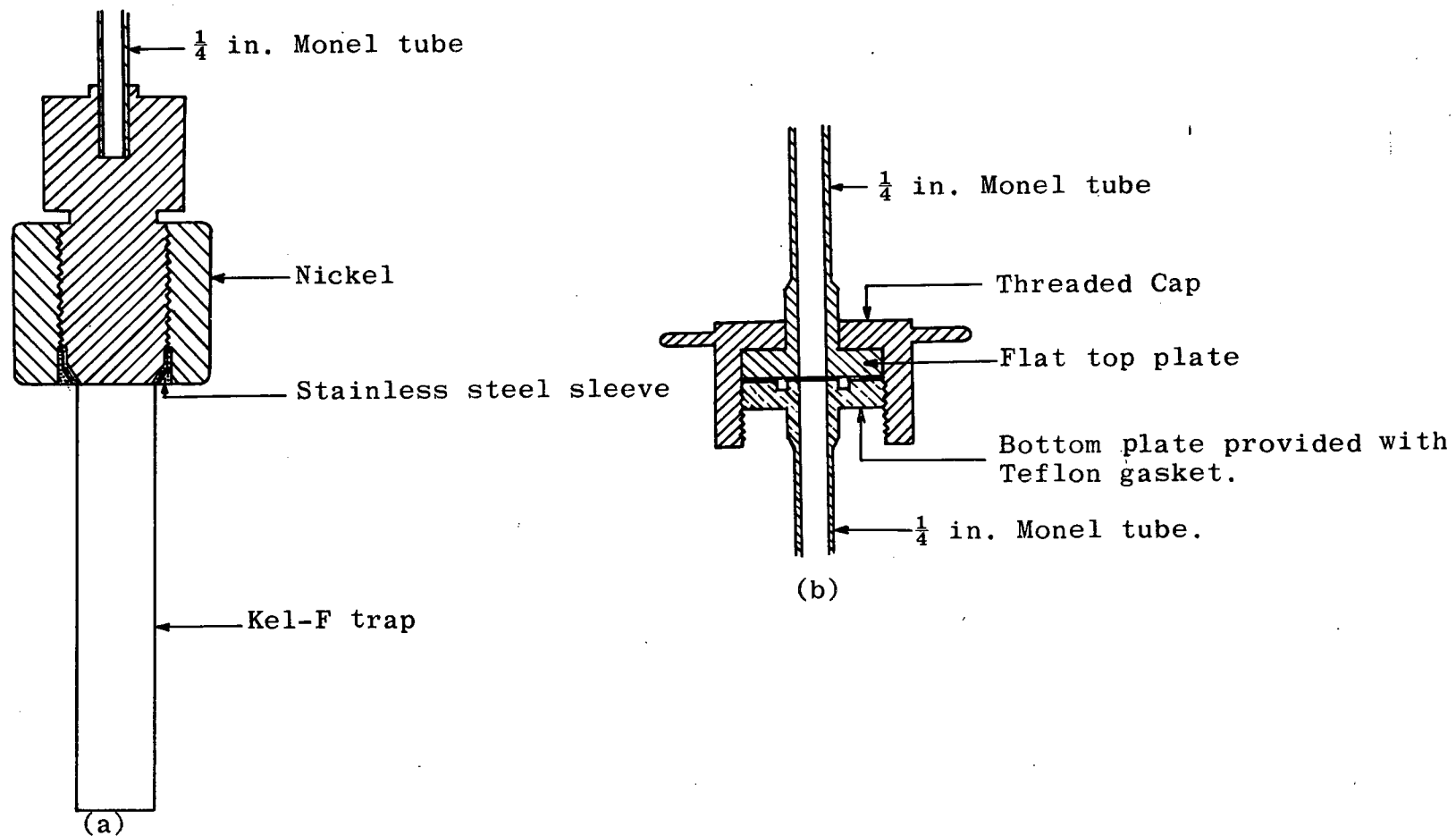


Figure 2. (a) Adapters for Kel-F Trap.

(b) Adapters for High Pressure Fluorine.

(nickel fluoride from the valve material and other involatile fluorides from the decomposition of the reactive fluorides) at the stem-tip and seat.

30,000 p.s.i. Autoclave Engineering valves were found to be quite satisfactory in overcoming this difficulty in that they could be demounted, cleaned and used again. However, they are heavy and bulky and were unsuitable in many applications, e.g. when accurate weighing of the vessel was required.

Among the small valves used were (a) Whitey valves which were brass-bodied or stainless steel bodied and with metal-tipped or Kel-F tipped stems. They were designed to take 1/4 in. tubing with the help of compression fittings. These valves were, however, found to be good for low pressure work only and they developed "leak through" rather rapidly. They could be demounted, cleaned and reassembled but those reassembled did not always give satisfactory service. (b) Hoke A431 valves which were brass-bodied and had bellows seals and were provided with a stainless steel Vee stem. They were satisfactory for moderately high pressure work (~ 250 p.s.i) and had appreciably longer life than the Whitey valves. After much use they developed "leak through" and often also developed a bellows leak. These valves could not be restored to useful service.

2.1.2 Fluorination Reactions

(i) Fluorination with elemental fluorine

Fluorination with elemental fluorine was

usually done in one of two ways: fluorination in a closed system in a monel can with high pressure fluorine (~ 150 p.s.i.) and fluorination in a flow system in a quartz or Pyrex apparatus with low pressure fluorine diluted with an inert gas like nitrogen.

A general closed system high pressure fluorination is described here. A reaction vessel, loaded with the material to be fluorinated, was connected to the high pressure side of the fluorine system. It was evacuated and then filled with fluorine at the desired pressure. The vessel was then heated in a furnace at the required temperature for the desired time. At the end of the heating period, the vessel was quenched, if necessary. It was then cooled in acetone - dry ice mixture or to lower temperatures, if necessary, to retain the volatile product and excess fluorine was pumped off through the fluorine scrubber.

The procedure for a typical flow system fluorination was as follows. The apparatus which is shown in Figure 3, consisted of a quartz reaction tube and a series of glass traps joined to it on one side by a cone and socket and on the other side by a graded seal. The material to be fluorinated was contained in a nickel boat in the quartz tube. As the apparatus was made of silica and glass, great care was taken to dry it. Thorough drying was achieved by prolonged evacuation of the apparatus which was simultaneously heated with a flame adjusted to maintain the glass temperature below the softening point. All traps in the apparatus were cooled in liquid oxygen and the apparatus was filled with diluent gas nitrogen or oxygen

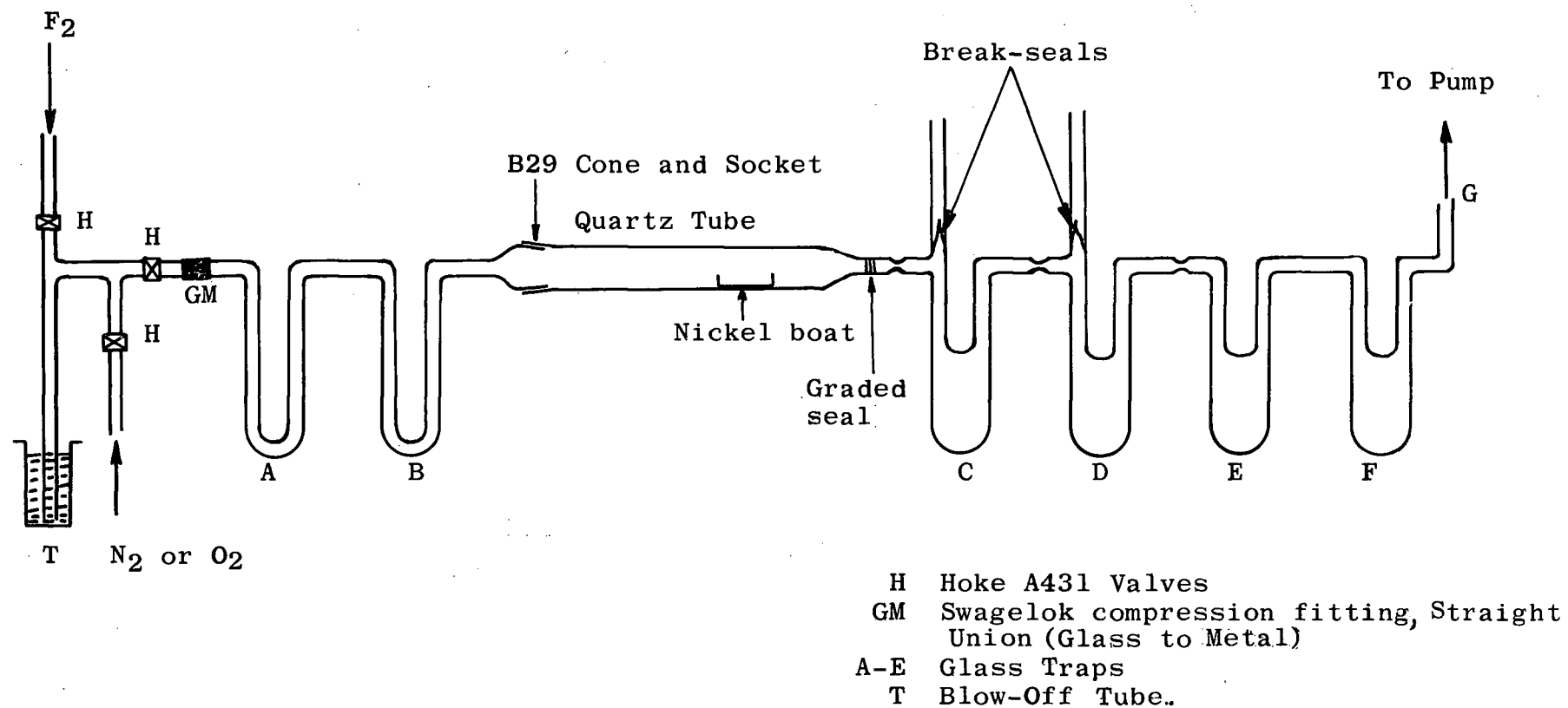


Figure 3. A Flow System for Fluorination with Elemental Fluorine

(the latter used in oxyfluorination) which had been dried by passing first through a sulphuric acid bubbler and subsequently through liquid oxygen cooled traps A and B. The blow-off tube T in the system indicated when the apparatus was filled with one atmosphere of gas, after which the apparatus was opened to the atmosphere through end G. Traps E and F prevented ingress of moisture; C and D, provided with break seals, were used to collect the volatile products of the reaction. A mixture of fluorine and nitrogen (or oxygen) was passed, the ratio of fluorine to other gas being roughly estimated with the aid of the blow-off tube. The reaction was carried out by appropriate heating of the material in the nickel boat by means of a Bunsen flame or electric furnace. Volatiles condensed in traps C and D. On completion of the reaction, the fluorine supply was shut off and the apparatus purged with the diluent gas to displace fluorine. It was then evacuated and the products were sealed off under vacuum in traps C and D.

(ii) Reactions with bromine trifluoride and iodine pentafluoride

Bromine trifluoride and iodine pentafluoride are associated liquids at room temperatures and are good solvents, particularly for ionic fluorides. Bromine trifluoride parallels the behaviour of fluorine in oxidative fluorinations. Iodine pentafluoride is thermodynamically more stable than BrF_3 and accordingly has a lower oxidizing power and is therefore of value in the preparation of low valence fluorides and complex fluorides.

Bromine trifluoride as supplied commercially was quite pure and was used without further purification.

Iodine pentafluoride was found to be impure. It was bluish in colour, presumably due to monovalent iodine.³⁹ It was purified by room temperature fluorination in a monel can.

An apparatus of glass or metal, depending on the nature of the reactants, was used for reactions with bromine trifluoride and iodine pentafluoride. In the case of glass apparatus, the reaction vessel was a silica bulb attached to the system through a graded seal and in the case of a metal system, the reaction vessel was a Kel-F trap.

The glass apparatus used in a typical reaction with bromine trifluoride in which a volatile compound was fluorinated is shown in Figure 4. The apparatus was evacuated and dried thoroughly. The break seal of bottle B containing the reactant was broken in the usual way and the reactant was condensed into the reaction bulb, C. Bulb B was then sealed off from the apparatus. Bromine trifluoride was condensed into trap A and the cylinder of BrF_3 was disconnected from the rest of the apparatus by sealing off at constriction 1. The fluoride from trap A was then condensed into reaction bulb C. Traps D and E were cooled in liquid oxygen and dry air was slowly admitted into the apparatus. These traps prevented any moisture from entering the reaction bulb from the atmosphere. The reaction bulb was then allowed to warm to room temperature. Usually, with bromine trifluoride, vigorous reaction took place at this stage with evolution of bromine and other gases. The

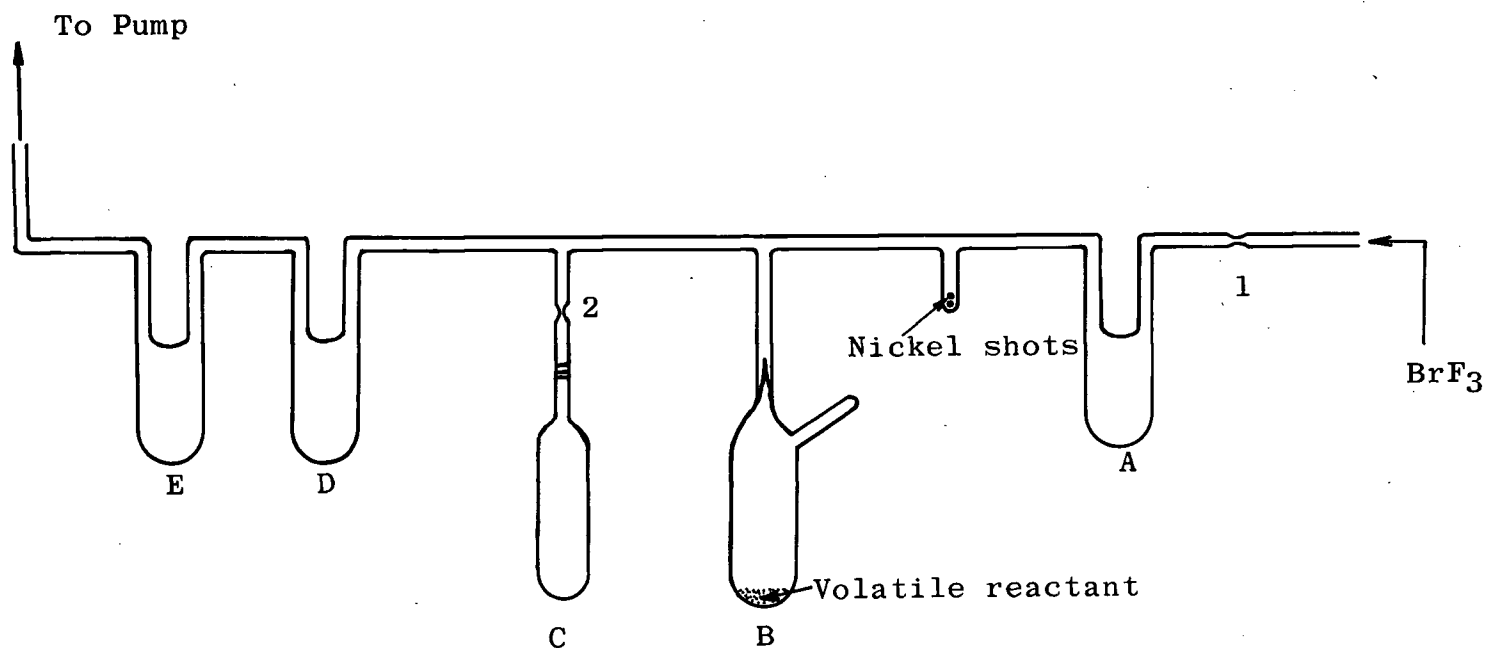


Figure 4. Apparatus for Fluorination with Bromine Trifluoride.

reactants were refluxed, when necessary, by warming the reaction bulb with a hot air blower or a small luminous flame. After the reaction was complete, the apparatus was evacuated and the excess reactant (BrF_3) and volatile products were distilled off into traps D and E. The product in the reaction bulb was completely freed from BrF_3 by heating the bulb for several hours in a small furnace at an appropriate temperature. Afterwards the reaction bulb was sealed off at constriction 2*. The excess bromine trifluoride was destroyed by pouring it into an excess of dry carbon tetrachloride. (In the iodine pentafluoride experiments the excess of the reagent was destroyed by pouring it into an excess of concentrated sulphuric acid).

2.1.3 Analysis

The general analytical techniques used for the estimation of metals and fluorine were pyrohydrolysis and conventional analysis following alkaline hydrolysis.

(i) Pyrohydrolysis

In the pyrohydrolysis method, the fluorine containing compound was initially hydrolysed by moist air at room temperature and finally by steam at elevated temperatures, giving hydrogen fluoride and an oxide of the metal. The hydrogen fluoride evolved was absorbed in water and the fluoride in this solution was estimated. The metal oxide was reduced to the metal and weighed. This method was fruitfully applied

*During the course of the reaction care was taken to remove any plug formed by solids in the arms of the traps by melting it with a hot air blower.

for the estimation of fluorine and metals in the compounds of platinum and iridium.

The apparatus used for pyrohydrolysis was the same as that used by Lohmann⁴⁰ and was similar to that described by earlier workers.^{41,42}

The usual procedure for pyrohydrolysis was as follows. The empty platinum boat was heated to 300° in a stream of steam followed by heating in a stream of hydrogen at the same temperature and was weighed to a constant weight. The sample for pyrohydrolysis, approximately 0.3 g., was transferred to the platinum boat in a dry box and the boat reweighed. It was then quickly transferred to the pyrohydrolysis tube. The hydrolysis was carried out by first passing moist nitrogen over the sample, both the steam generator and the pyrohydrolysis tube being at room temperature. The temperature of water in the steam generator and the temperature of the furnace were then gradually raised until eventually steam was passing over the sample at 300°. The hydrogen fluoride was collected by bubbling the gases coming out of the steam condenser through 50 mls. of water contained in a conical flask and by collecting the distillate in the same flask. Washings from the condenser were also collected. The fluoride ion concentration in the solution was estimated by titration of hydrofluoric acid with 0.1 NaOH using phenolphthalein as an indicator. It was also checked by precipitation as lead chlorofluoride.

For the determination of the metal left as oxide in the platinum boat in the pyrohydrolysis tube, hydrogen

was passed and the excess was burnt as it emerged, from the pyrohydrolysis tube. The metal oxide was reduced to metal at a high temperature in hydrogen, and after the reduction, the hydrogen was displaced by nitrogen. The apparatus was cooled before the boat was taken for weighing.

(ii) Alkaline hydrolysis:

This was used where the pyrohydrolysis method could not be applied, as in the analysis of osmium compounds which gave rise to the volatile oxide, OsO_4 .

To prevent the loss of any osmium tetroxide produced in the hydrolysis, the hydrolysis was done in a closed system. An apparatus as shown in Figure 5 was used for this purpose. A typical procedure for the hydrolysis is described here. A sample was sealed off in an evacuated small thin walled glass bulb of small diameter provided with a long neck, and weighed. About 75 mls. of 2N NaOH solution were taken in the flask E. The sample bulb was placed in B, which fitted snugly, the neck protruding through the tap C. Cap A was replaced and the air in the apparatus was pumped out through tap D. Tap D was closed and the apparatus was turned upside down so that the neck of the bulb was immersed in the alkaline solution. The neck was broken by turning tap C. (To assure a clean break, the neck was scratched with a file prior to weighing of the bulb). The resultant solution was diluted to a known volume and aliquots were taken for osmium and fluorine analysis. The weight of the sample was found by weighing the broken sample bulb and the glass pieces in the apparatus.

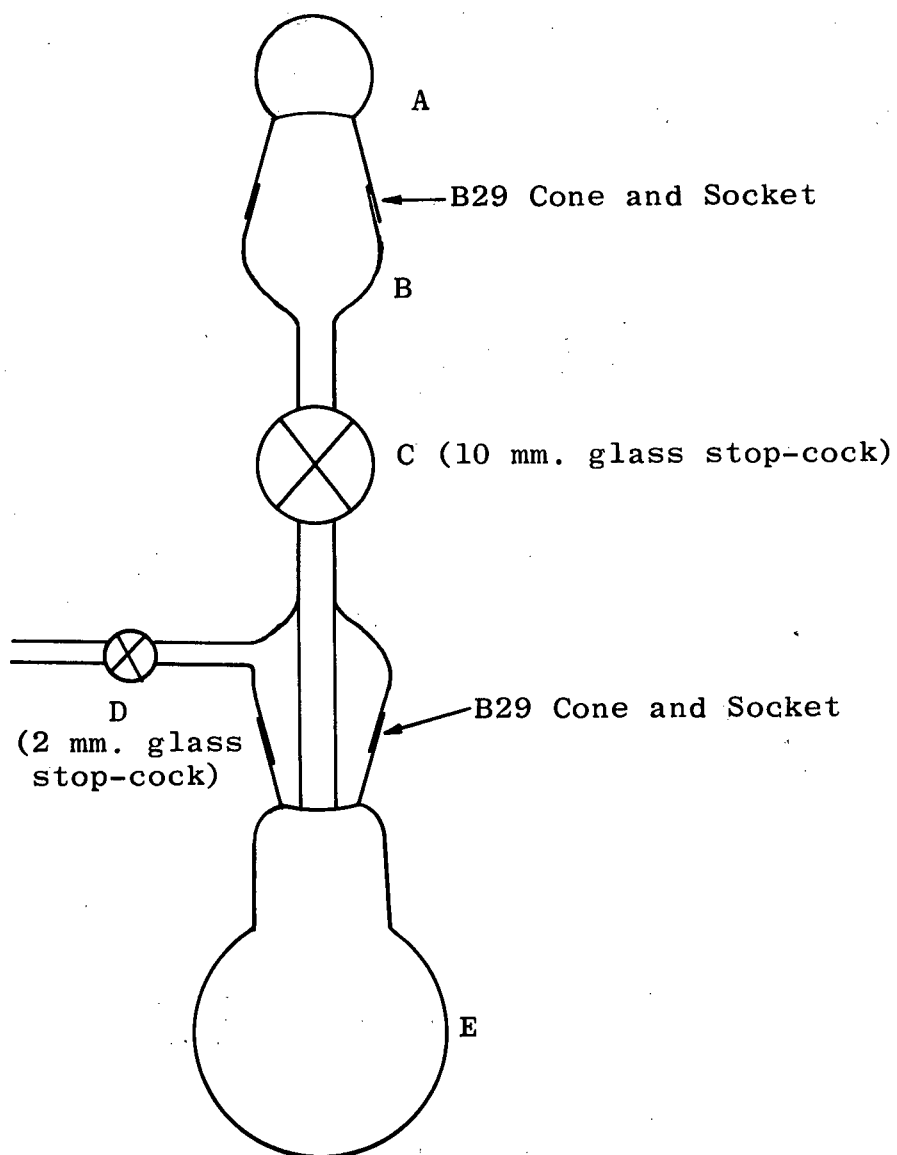


Figure 5. Apparatus for Hydrolysis of Osmium Compounds

In some of the osmium compounds it was found that some osmium dioxide was precipitated during the alkaline hydrolysis. Estimation of osmium in aliquots would not have been possible in such cases, so it was desirable to precipitate all of the osmium from solution at this stage. A glass bulb could not be used for a sample bulb because of the resulting admixture of osmium dioxide precipitate with broken glass pieces. In view of these difficulties the hydrolysis method was slightly modified. Some hydrazine hydrate was added to the alkaline solution in order to precipitate osmium. The small cap A was replaced by a second flask like E and the glass bulb was replaced by a small glass-stoppered weighing bottle. The apparatus was turned upside down so that the end B of the apparatus was down. 75 mls. of the alkaline solution containing hydrazine hydrate were taken in the flask A. Air was pumped out through tap D and tap C was closed. Subsequently air was admitted to flask E which was then opened for insertion of the weighing bottle containing the sample. Air was pumped from the recapped flask E, tap C was then opened to admit the alkaline solution. Care had to be taken to ensure that the alkaline solution had minimum contact with the tap grease. A voluminous precipitate of osmium dioxide formed in the apparatus. The suspension of this in the alkaline liquors was transferred to a beaker and the precipitation of osmium was completed as described below.

(iii) Estimation of osmium

Osmium in an aliquot of hydrolysed solution was estimated using hydrazine hydrate⁴³ to precipitate osmium

as a mixture of metal and hydrated dioxide. For complete precipitation, repeated boiling of the solution, with dropwise addition of hydrazine hydrate was necessary. A Munroe platinum crucible was used for the filtration of the mixture and the precipitate was ignited to metal in hydrogen following the procedure described by Gilchrist and Wichers.⁴⁴

(iv) Estimation of fluorine

Fluorine in solutions containing fluoride ion (such as the solutions obtained in pyrohydrolysis or the filtrate from precipitation of osmium) was estimated as lead chlorofluoride following a standard procedure.⁴⁵ The precipitate was filtered in a medium porosity sintered glass crucible and was heated to constant weight at 130-140°.

Estimation of fluorine in solutions containing complex fluoro-anions (as obtained in alkaline hydrolysis) was achieved by first distilling hydrogen fluoride from the solution and then estimating fluorine in the distillate as lead chlorofluoride. The distillation procedure was that given by Willard and Winter.⁴⁶ Aliquots of (50 ml.) solution containing complex fluoro-anions were placed in a two-necked distillation flask fitted with a side arm. One neck carried a thermometer, the other a dropping funnel, and the side arm carried a condenser. Ferrous sulphate (5 g.) was added to the solution (FeSO_4 prevented distilling of osmium tetroxide. Osmium was retained in the distillation flask as osmium dioxide). Concentrated H_2SO_4 (25 ml.) was added slowly through the dropping funnel and the mixture was heated. It was kept boiling at 130-135° by addition of water

from the dropping funnel; 250 mls. of distillate were collected. Fluorine in the distillate was precipitated as PbClF .

A check on the purity of lead chlorofluoride was routinely done but was particularly important following a sulphuric acid distillation when contamination with PbSO_4 was likely. This was done by dissolving the precipitate in cold dilute nitric acid, the chloride being precipitated from this solution as silver chloride.

(v) Estimation of nitrogen

The estimation of nitrogen in these compounds was done by the conventional Dumas method in the Micro-analytical Laboratory of the Chemistry Department of the University of British Columbia.

(vi) Estimation of Sulphur

Sulphur was estimated in the case of iridium and platinum compounds by a slight modification of the pyrohydrolysis method. During the pyrohydrolysis sulphur evolved as sulphurous acid along with hydrogen fluoride. The two acids were absorbed by bubbling through a standard alkaline solution. The titration of excess alkali gave the combined acid concentrations. The sulphite was oxidized to sulphate by the addition of hydrogen peroxide and sulphate was precipitated as barium sulphate. But prior to the precipitation of BaSO_4 it was necessary to remove fluoride ions from the solution which would precipitate as BaF_2 along with BaSO_4 . The removal of fluoride was achieved by volatilising hydrogen fluoride from the solution by repeated addition of concentrated HCl followed by evaporation in a teflon beaker.

The estimation of sulphur in osmium compounds was done in the filtrate after the precipitation of osmium. Aliquots of hydrolysed solution were treated as described above.

Sometimes individual compounds created problems in their analysis. Methods had to be modified for them and they are described in the appropriate sections.

2.1.4 Gauges for Vapour Pressure and Gas Pressure Measurements

Two types of gauges - a nickel bellows gauge used in conjunction with an optical lever and a diaphragm gauge with an electrical make and break - were used for vapour and gas pressure measurements.

(i) The Nickel bellows gauge

This consisted of a small nickel bellows which terminated one arm of a nickel U-trap; the bellows being silver-soldered to the trap. The other end of the trap was provided with a Hoke A431 valve which was connected to the vacuum manifold. The arm of the U-trap below the bellows was in the form of a cone on which a cylindrical metal tube, one end of which was in the form of a socket, was fitted, thus housing the bellows. The other end of the cylindrical tube was threaded inside and out. Another thin and small threaded cylinder carrying a circular plane mirror was fitted inside the main tube. The mirror was mounted on a metal plate which was attached to the smaller cylinder by means of two thick wires soldered at the ends. The metal plate on which the mirror was mounted was grooved at the back. A pin which was glued to the top of the bellows was situated to move in this groove. At the

top of the main cylinder a circular glass plate was fitted by means of neoprene O-rings and a metal screw cap having a circular window in its centre. The main cylinder was also connected through a side arm to a mercury manometer, vacuum manifold and an arrangement to admit dry air. The bellows was thus housed in a leak-tight cylinder. A light source, the plane mirror at the top of the bellows and a screen were used as the optical lever to magnify the movements of the bellows. The gauge was used as a null instrument, the pressure due to a gas inside the bellows being balanced by adjustment of the pressure in the bellows housing and the latter pressure being registered by a mercury manometer. An accuracy of better than 0.5 mm. of Hg was attainable with this arrangement.

(ii) The diaphragm gauge

This gauge was a slightly modified form of Cromer Electronic Pressure Transmitter.⁴⁷ A cross-sectional diagram of the gauge including the electrical circuit is shown in Figure 6. The main modification was in the insulation of the diaphragm housing from the adjustable electrical contact. In the present case the holder for the adjustable contact was made of nickel-plated brass and was insulated from the main body housing the diaphragm (nickel 0.003 in., 4 1/2 in. diam.) by a teflon ring and teflon sleeves for the screws. A small cylindrical monel reservoir to which two 1/4 in. O.D. monel tubes were welded, was joined by one arm to the gauge and by the other to a Hoke A431 valve which was connected to the vacuum manifold. The gauge was used as a null instrument, the sensing depending

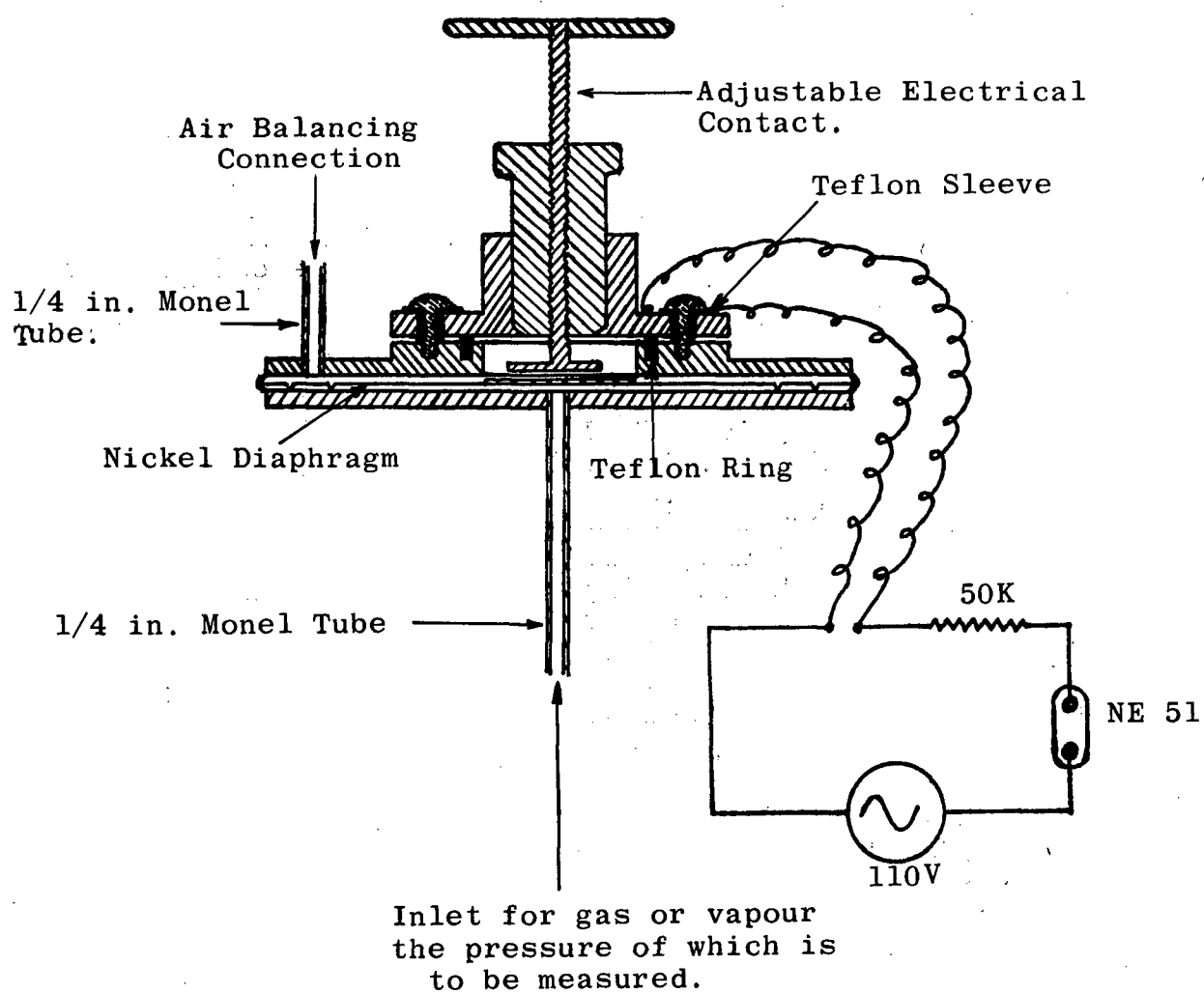


Figure 6. The Diaphragm Gauge.

upon the making or breaking of an electrical circuit. The null point of the gauge was determined with a high vacuum on both sides of the diaphragm. It was signalled by a small lamp incorporated in the electrical circuit. The electrical make and break was so adjusted that with high vacuum on both sides of the diaphragm, the diaphragm just closed the electrical circuit and the lamp glowed. In vapour pressure or gas pressure measurement the diaphragm was brought back to the zero position with a controlled admission of dry air to the outside housing of the diaphragm. The pressure was read directly from a manometer registering the pressure of the admitted air. The gauge was very sensitive, even a difference of pressure of 50 microns being detectable but the accuracy in this work was limited by the cathetometer which was accurate only to $\pm .01$ mm.

The nickel bellows gauge had the advantage of being thermostated easily because of its compactness; the diaphragm gauge, on account of its large size, was inconvenient in this respect. However, the former was found to suffer from mechanical hysteresis, its null point changing after relatively few readings. Both the gauges were susceptible to damage by large pressure differences.

2.1.5 Tensimetric Titrations

During this work reactions of some of the volatile hexafluorides with gaseous reactants were followed tensimetrically. The reactants were measured out by pressure and volume at a fixed temperature. Sometimes the measured reactants were mixed as gases; these reactions will be referred

to as gas-gas reactions. At other times one of the reactants present as a gas, reacted with the other, present as solid and as vapour; these reactions will be referred to as solid-gas reactions. The apparatus used for these titrations is shown in Figure 7. All pressure measurements were carried out using one of the gauges described in Section 2.1.4.

(i) Solid-gas reaction

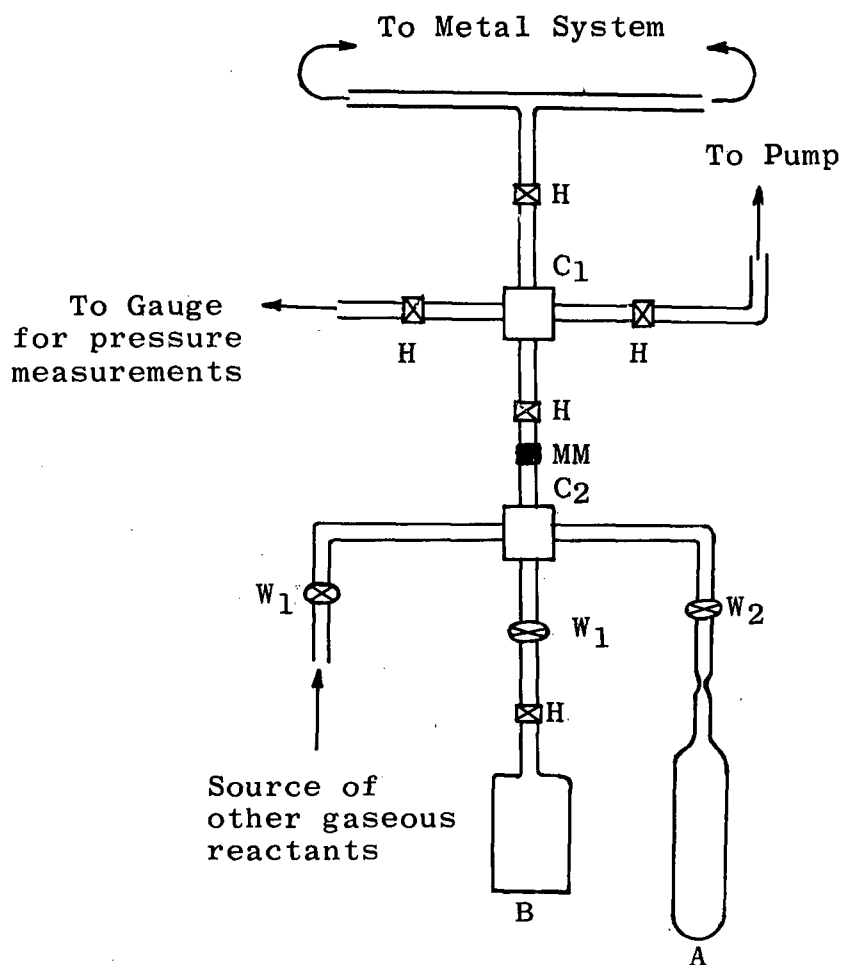
A known pressure of hexafluoride was taken in a fixed volume containing the gauge and the two crosses C_1 and C_2 . It was condensed in the reaction bulb A with liquid nitrogen. A known pressure of the other gaseous reagent was also taken in the same volume and was also condensed in bulb A. The bulb was then warmed to room temperature. The hexafluoride reacted with the other gas, both as solid and vapour. The residual gas was condensed in the reservoir of the gauge where its pressure, in the fixed volume at room temperature was measured.

(ii) Gas-gas reactions

A known quantity of hexafluoride was measured out and transferred to the reaction bulb as described above. It was vaporized in the bulb by warming to room temperature. A similar volume of the other reactant at a higher known pressure was then admitted to the reaction bulb. After the reaction the pressure of the residual gas was measured in the usual way.

(iii) Titration with a reactant gas having an appreciable vapour pressure at liquid nitrogen temperature.

In such cases the ratio of the volume of



- H Hoke A431 Valves
- W₁ Whitey Valve
- W₂ Whitey Valve designed to join glass or silica to metal.
- MM Swaglok Compression Fitting Straight Union (Metal to Metal).
- A Glass or Silica Reaction Bulb.
- B Storage Vessel for MF₆

Figure 7. Apparatus for Tensimetric Titrations.

the system containing the gauge, the crosses and the reaction bulb to that of the gauge and two crosses was determined beforehand with the aid of a condensible inert gas. The reaction was carried out as in the gas-gas case but the pressure of the residual gas was measured in the system containing the gauge, two crosses and the reaction bulb. This pressure was converted to the equivalent pressure in the system containing the gauge and two crosses only.

In most cases the identity of the residual gas was established by its infrared spectrum. Sometimes the reaction bulb was replaced by an infrared cell provided with a reservoir and reactions were carried out in the cell, the infrared spectrum being recorded before and after reaction.

2.1.6 Magnetic Measurements

The magnetic susceptibility measurements of the compounds were made by the Guoy technique. The samples were enclosed in thin walled quartz or Pyrex tubes of 3 to 5 mm. O.D. The sample tubes were loaded in a dry box and were sealed under vacuum. However, in some cases it was desirable to avoid manipulation in a dry box. This was accomplished by sealing off the compound with nickel shot in a quartz or Pyrex bulb with a side arm terminating in a Guoy tube. The sample was powdered inside the bulb by the nickel shot and transferred to the Guoy tube which was then sealed off at a proper length.

To prepare Guoy samples of volatile fluorides the latter method was used. The fluoride was condensed in a quartz tube containing nickel shot, the Guoy tube being a

side arm. The sample was powdered by alternate cooling in liquid nitrogen and pounding with nickel shot. After transferring the sample to the Guoy tube, both the main bulb and the Guoy tube were kept cool in liquid nitrogen while the Guoy tube was drawn off.

Magnetic measurements were done using the same Guoy balance described in detail by Clark and O'Brien.⁴⁸ Essentially it consisted of an electromagnet, a microbalance and a cryostat. The electromagnet produced a field of approximately 15 kilogauss with a current of 2 amp. The microbalance had a sensitivity of $\pm .01$ mg. The arrangement was similar to that described by Figgis and Nyholm.⁴⁹ The temperature of the sample was kept constant at any point to within $\pm 0.1^\circ$ over the range 77° - 300° K by use of liquid nitrogen, an electrical heater and air pressure adjustment within the inner Dewar vessel. Temperatures were obtained using a copper constantan thermocouple and a potentiometer.

The sample tube was suspended from the balance pan by means of a brass chain and a brass cap. All the sample tubes used were of the same length (11.4 mm. in the present case) to ensure that the bottom of the sample tube was always at the centre of the pole caps. The length of the sample column inside the tube was usually 8-9 cm. The Guoy tube containing the sample was weighed with the field on and the field off at each temperature. Mercury cobalt tetrathio-cyanate was used as the magnetic standard⁵⁰ for paramagnetic materials. Whenever possible, the same tube was used for the

sample and the standard. Alternatively the tubes were from the same length of tubing. A diamagnetic correction for the container was obtained by weighing the container in and out of the field over the temperature range used for the sample.

Whenever possible uniform packing of the sample or standard was ensured by using a mechanical vibrator.

The gram susceptibility, χ_g , was calculated from the equation:

$$\chi_g(s) = \chi_g(st) \times \frac{\Delta W(s) + dm.}{W(s)} \times \frac{W(st)}{\Delta W(st) + dm.}$$

where $\chi_g(s)$ is the g. susceptibility of sample, $\chi_g(st)$ the g. susceptibility of standard ($= 16.44 \times 10^{-6}$ c.g.s. units for HgCo(CNS)_4 at 20°),⁵⁰ $\Delta W(s)$ and $\Delta W(st)$ are the changes in weights for the sample and standard respectively, $W(s)$ and $W(st)$ are the weights of the sample and standard respectively, and $dm.$ is the diamagnetic correction due to container.

The molar susceptibility, χ_M , was corrected for the diamagnetic susceptibility of ligands with Pascal's constants,⁵¹ to give the Gram atomic susceptibility χ_A . μ_{eff} is given by $\mu_{\text{eff}} = 2.839\sqrt{\chi_A \times T}$, where T is the temperature in $^\circ\text{K}$.

In the cases where the plot of $\frac{1}{\chi_A}$ vs. T indicated obedience to the Curie-Weiss law, the best straight line was obtained by a least squares approximation, using program No.1 (Appendix 1) on an IBM 7040 Computer.

2.1.7 X-Ray Powder Photographs

Quartz or Pyrex capillaries (0.3 or 0.5 mm.

diam⁸) were used for the X-ray powder samples. As all of the compounds studied were moisture-sensitive, the capillaries were loaded in a dry box.

Sometimes, for a very reactive material, the sample was made without exposure in a dry box. The sample along with some nickel shot was sealed off under vacuum in a quartz or Pyrex bulb fitted with an arm carrying a drip cone with a capillary protected by an outer jacket. The compound was powdered with the nickel shot by careful shaking of the apparatus and a sample was transferred to the capillary, which was then drawn off.

The capillaries were sealed with a small hot flame and the newly sealed ends were dipped into molten wax to ensure a perfect seal.

X-ray powder photographs were taken using a camera with Straumanis loading having a diameter of 14.32 cm. A general Electric Model XRD-5F11 X-ray diffraction unit was used. The usual radiation was $\text{CuK}\alpha$ with Ni filter to reduce the β radiation ($K\alpha = 1/2 (2K\alpha_1 + K\alpha_2) = 1.5418\text{\AA}$. $K\alpha_1 = 1.5443\text{\AA}$, $K\alpha_2 = 1.5405\text{\AA}$). For a quick exposure for identification purposes a slit collimator was used but for the films to be measured and indexed a pinhole collimator was preferred. The exposure time required with slit collimator was 2-4 hours and with pinhole collimator 10-16 hours.

The positions of the arcs on the X-ray powder patterns were measured on a light box provided with an accurate scale and vernier. Readings were obtained with an accuracy of $\pm .005$ cm. Bragg angles, interplaning spacings,

$1/d^2$ values and Nelson Riley extrapolation function⁵² were obtained from the arc measurements by use of program No.2 (Appendix II), the computer being the IBM 7040. To assist in indexing a complex pattern the calculated $1/d^2$ values for an assumed set of parameters of the unit cell were obtained by using program No.3 (Appendix III). Whenever possible the parameters were corrected for absorption by a Nelson Riley plot.

2.1.8 Infrared, Visible and UV Spectroscopy

Because of the reactivity of the fluorides of the noble metals the body of the 10 cm.infrared gas cell was made of nickel or monel, and was provided with Hoke A431 valves. The material for the windows of the cell was silver chloride which had the advantage of being transparent in the region 400-4000 cm.^{-1} and being less reactive towards these fluorides. The windows were from silver chloride sheets 1 mm. thick (supplied by the Harshaw Chemicals, Elysia, Ohio). The cell ends were provided with heavy gauge brass flanges each of which was cut to hold a teflon ring. The windows were held under compression between these rings and end caps with six steel bolts. The silver chloride windows were protected from light by means of black tape.

A monel reservoir was attached to the cell by way of a Hoke A431 valve by the use of which the pressure of the sample inside the cell could be varied while recording the IR spectrum. The reservoir also helped in carrying out some reactions in the infrared cell and in studying the nature of the products by infrared. The inside of the cell body and

the reservoir could be cleaned and windows could be replaced whenever required.

The infrared spectra were recorded using various Perkin Elmer infrared spectrophotometers.

The visible and UV gas cells were made of quartz and were provided with Whitey valves (drilled on one side to take 7 mm. quartz tube). The spectra were recorded using a Cary 14 spectrophotometer.

2.1.9 Reagents

(i) The following were used as supplied.

Fluorine, Nitric oxide, Nitrosyl chloride, Bromine trifluoride, and Iodine pentafluoride were obtained from the Matheson Co., Inc., East Rutherford, N.J. Sulphur tetrafluoride was obtained in cylinders from E. I. Dupont De Nemours & Co., Wilmington, Delaware. Tungsten hexafluoride was obtained in cylinders from Allied Chemical, General Chemical Division, Beaton Rouge, Louisiana. Xenon and Krypton were Airco reagent grade supplied in 1-1 Pyrex flasks by Matheson of Canada, Ltd., Whitby, Ontario. Osmium and Iridium were obtained in powder form (spectroscopically pure grade) from Johnson, Matthey & Co. Ltd., London and from A. D. Mackay Inc., New York. Rhodium and Pt wires of 0.03 in. diam. were obtained from Johnson, Matthey & Co. Ltd., London.

(ii) Cesium fluoride

It was prepared by the action of 48% hydrofluoric acid on cesium carbonate in a platinum crucible. The solution was evaporated to dryness. The solid was then

melted to drive off all hydrogen fluoride and was resolidified. It was kept in a vacuum desiccator until use.

(iii) Osmium tetroxide

It was prepared by igniting osmium powder in a stream of dry oxygen. It was collected in glass traps provided with break-seals which were cooled in liquid oxygen. The tetroxide collected was then sealed off in the break-seal bottles.

(iv) Anhydrous osmium dioxide.

It was prepared by reduction of osmium tetroxide with absolute alcohol. Osmium tetroxide was dissolved in a solution of potassium hydroxide to which requisite amount of absolute alcohol was added. The solution was then neutralised to litmus with dilute H_2SO_4 when precipitation of black $\text{OsO}_2 \cdot 2\text{H}_2\text{O}$ occurred. The mixture was boiled and filtered off. The precipitate was washed with very dilute NH_4Cl solution. It was first dried in an oven at low temperature to drive off moisture. The anhydrous material was obtained by heating this hydrated product in vacuum for a few hours at 500° . Usually the hydrated material was put into a monel reaction bottle and heated under vacuum at 500° . The anhydrous dioxide produced was directly fluorinated in the monel can.

(v) OsF_6 and IrF_6

These hexafluorides were prepared by heating the respective metals in powder form in a monel can at 300° - 400° , with excess fluorine for about two hours. The can was cooled in acetone-dry ice bath and excess fluorine was pumped out. The hexafluorides were then stored in monel storage bottles

containing dry sodium fluoride (to absorb any hydrogen fluoride present).

(vi) PtF₆ and RhF₆

These hexafluorides were prepared by electrical heating of the metal wire in an atmosphere of fluorine by an adaptation⁵³ of the method of Weinstock and his coworkers.^{23(b)} The yield of platinum hexafluoride was approximately 60% whereas the yield of rhodium hexafluoride was only 8%.

2.2. THE FLUORIDES AND OXYFLUORIDES OF OSMIUM

2.2.1 Search for Higher Binary Fluorides of Osmium

Metallic osmium powder (lg.) was taken in a high pressure monel reaction vessel which had been preconditioned to fluorine, the reaction vessel was then filled with fluorine at 180 p.s.i. The vessel was heated in a furnace at 400-500° for several hours, then it was quenched in cold water.

The reaction product was condensed in the reservoir of a monel infrared gas cell which had been pretreated with fluorine. The product was expanded into the gas cell, the infrared spectrum recorded, the vapour pumped out and the process repeated exhaustively. The infrared spectrum of the product was found to be identical with that of osmium hexafluoride.¹³

2.2.2 Osmium Oxide Pentafluoride

(i) Preparation

Several preparative routes to osmium oxide pentafluoride were tried.

(a) Osmium metal was treated with a mixture of oxygen and fluorine (1:2 volume) in a flow system (See Section 2.1.2). The reaction, which was carried out in a quartz tube with the osmium in a nickel boat, was initiated by the heat from a small flame. Once started, the reaction continued to completion. The product was a mixture of an emerald green solid and a pale yellow, more volatile solid. The difference in volatility of the components of the mixture permitted their separation by trap to trap fractional distillation under reduced pressure, from a

trap held at -16° to receivers cooled with liquid nitrogen. The emerald green solid remained behind in the trap at -16° . The more volatile yellow component from its infrared spectrum proved to be osmium hexafluoride. Freedom of the emerald green solid from OsF_6 was established by infrared spectroscopy. The yield of this material was 50%. It melted sharply at 59.2° .

(b) A variation of the above method was the fluorination of anhydrous osmium dioxide. (See Section 2.1.9). Fluorine diluted with nitrogen was passed over the dioxide. The products were again the hexafluoride and oxide pentafluoride of osmium, the yield of the latter being 50%.

(c) Oxyfluorination of osmium metal in a closed monel can (See Section 2.1.2) provided with a Hoke A431 valve using a fluorine-oxygen mixture (2.5:1) by volume at 300° for a period of two hours, also yielded the oxide pentafluoride and hexafluoride but the yield of the former was less than 50%.

(d) The best preparation of osmium oxide pentafluoride proved to be the fluorination at 250° of anhydrous osmium dioxide in a similar system to the last, the fluorine being in slight excess of that required by the equation $\text{OsO}_2 + 2\frac{1}{2} \text{F}_2 = \text{OsOF}_5 + \frac{1}{2} \text{O}_2$. The oxide pentafluoride was recovered from the admixture with OsF_6 in the usual way. The yield of OsOF_5 under these conditions was above 90%.

(ii) Analysis

The analysis was done by alkaline hydrolysis of osmium oxide pentafluoride followed by estimation of osmium and fluorine in the hydrolysed solution. The hydrolysis was

done by breaking a sealed capsule, containing the sample, in a closed system containing an aqueous alkali (See Section 2.1.3). Osmium was determined by the hydrazine hydrate method and fluorine was estimated by Willard and Winter distillation followed by precipitation of fluoride as PbClF . Fluorine was also determined in the filtrate after osmium precipitation. (Found: F, 31.1; Os, 61.9%. OsOF_5 requires F, 31.5; Os, 63.1% .)

(iii) The Vapour pressure-temperature behaviour of OsOF_5

A diaphragm gauge (See Section 2.1.4) was used for the vapour pressure measurements. The monel reservoir of the gauge was treated with fluorine and was then conditioned to OsOF_5 . A sample of OsOF_5 was then condensed in the reservoir. It was kept at the temperature of acetone-dry ice and pumped for a few hours to remove any traces of hydrogen fluoride or silicon tetrafluoride. The sample was then isolated from the vacuum manifold. The entire gauge was immersed in silicone oil contained in a 5l-Dewar vessel which served as the thermostat bath. Temperatures were measured with a precision of $\pm 0.1^\circ$. The gauge was used as a null instrument (See Section 2.1.4). The pressure of dry air required to balance the vapour pressure of the sample at certain temperature was read directly from the manometer with a cathetometer with an accuracy of ± 0.01 mm.

After each run, an infrared spectrum of the sample from the gauge was recorded. This showed that negligible production of volatile products (e.g. CF_4 , SiF_4) had taken place in the gauge during the run.

The vapour pressure data are summarized by

the equations:

Solid OsOF_5 (32° - 59°).

$$\log P_{\text{mm.}} = \frac{-2266}{T} + 9.064.$$

Liquid OsOF_5 (59° - 105°)

$$\log P_{\text{mm.}} = \frac{-1911}{T} + 7.994$$

The equations were derived from the vapour pressure data, the curve for each phase being considered to be a straight line. The plot of $\log P_{\text{mm.}}$ vs. $1/T$ is shown in Figure 8. The observed and calculated vapour pressures and their differences are listed in Table IV. The melting point obtained from the vapour pressure data was $58.8^\circ \pm 0.2^\circ$ whereas that observed directly using a sample in a thin walled quartz capillary was 59.2° . The boiling point and some thermodynamic data were derived from the vapour pressure equations and they are tabulated in Table V.

The existence of a phase transition in the solid was indicated by the vapour pressure data to be between 32° and room temperature. Since the change in slope of the $\log P_{\text{mm.}}$ vs. $1/T$ plot at the solid-solid transition was small, it was not possible to precisely locate the transition point from this data. It was determined accurately with the aid of a polarizing microscope and X-ray powder photographs.

(iv) The solid-solid phase transition

(a) X-ray powder photographs

X-ray powder samples were prepared in 0.3 mm. quartz capillaries in the usual way for the volatile products

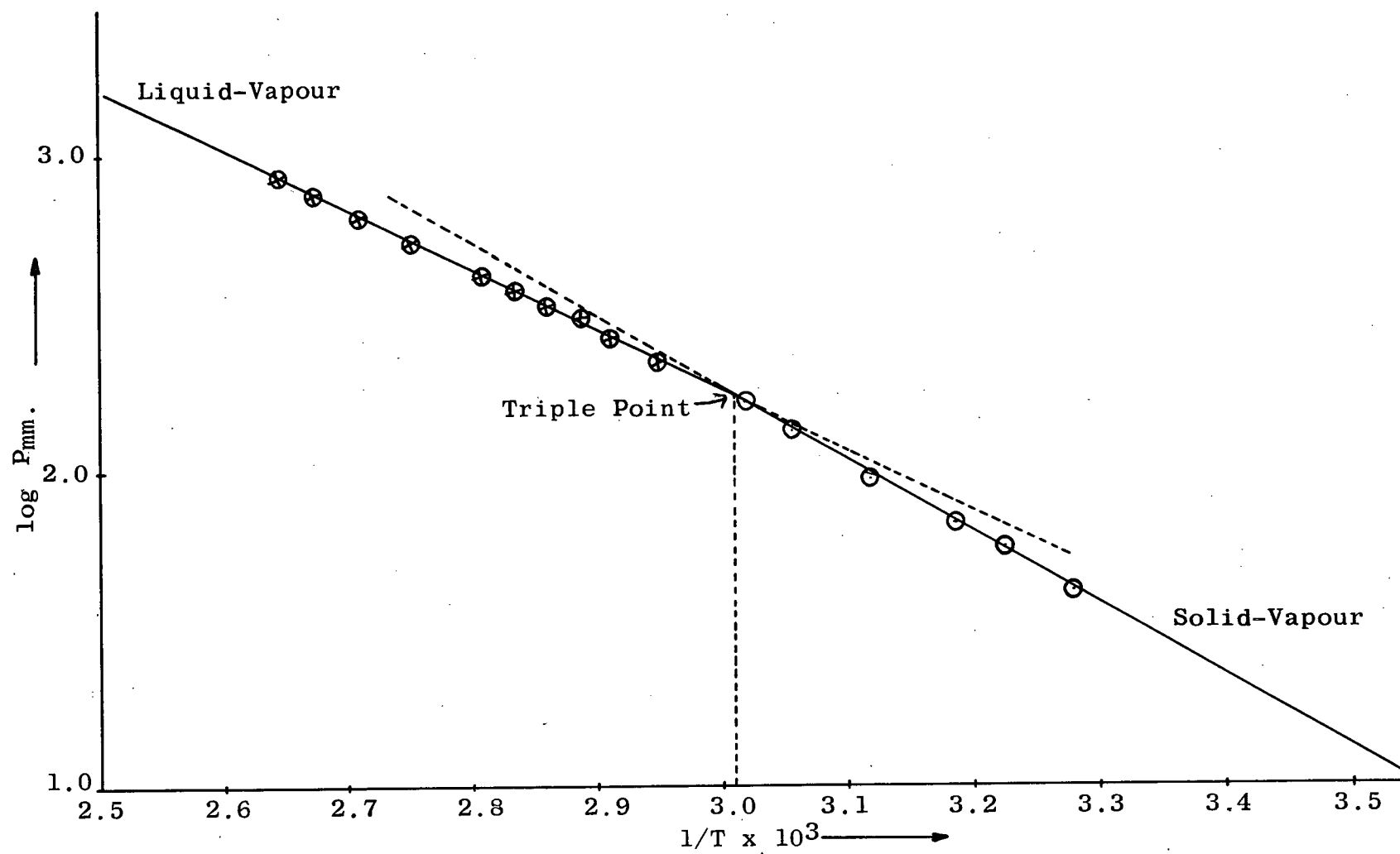


Figure 8. Plot of $\log P_{\text{mm.}}$ vs. $1/T$ for OsOF_5 .

Table IV

Vapour Pressure Data for OsOF₅

	Temp ^o K	P _{obs.} (mm)	P _{calc.} (mm)	P _{calc.} - P _{obs.} (mm.)
Solid	304.8	41.1	42.6	+1.5
	310.0	58.0	56.8	-1.2
	313.8	68.6	69.6	+1.0
	320.5	95.3	98.6	+3.3
	326.7	136.7	134.3	-2.4
	328.4	147.7	145.9	-1.8
	330.9	169.4	164.4	-5.0
Liquid	332.8	176.4	178.6	+2.2
	334.2	189.5	188.8	-0.7
	336.1	205.4	202.8	-2.6
	338.8	227.3	225.9	-1.4
	343.3	267.5	267.9	+0.4
	346.0	307.7	295.8	-11.9
	349.4	341.6	335.0	-6.6
	352.4	376.5	372.4	-4.1
	356.0	416.8	422.7	+5.9
	363.5	542.9	545.8	+2.9
	368.7	640.1	647.1	+7.0
	374.0	763.4	767.4	+4.0
	378.1	877.4	871.0	-6.4

TABLE VSome Thermodynamic Data for OsOF₅

Triple point °C	B.P. mm.	Latent heat of vap. of liquid. °C (cal/mole).	Latent heat of sublima- tion (above transition point). (cal/mole).
58.8	173.0	100.6	8,745
			10,368
Entropy of vap. of liquid (cal/mole/deg.)	Heat of fusion (cal/mole)	Entropy of fusion (cal/mole/deg.)	
23.4	1,623	5.29	

(Section 2.1.7) and X-ray powder photographs were taken at various temperatures. Higher temperatures were achieved by blowing hot air over the capillary, the temperature being controllable to $\pm 1^\circ$.

The diffraction pattern of powder photographs taken at room temperature was indexed on the basis of an orthorhombic unit cell, as shown in Table VI, with $a = 9.540$, $b = 8.668$, $c = 5.019\text{\AA}$, $U = 415.0\text{\AA}^3$ and $Z = 4$.

X-ray powder photographs of the sample at temperatures above 35° were indexed on the basis of a cubic unit cell as shown in Table VII with $a = 6.143\text{\AA}$, $U = 231.8\text{\AA}^3$ and $Z = 2$.

From the X-ray examination the transition point from orthorhombic to cubic form was found to lie between 31° and 35° . That the cubic form changed back to the orthorhombic on cooling was also established.

TABLE VI

X-Ray Powder Data for OsOF₅ (Orthorhombic)*

<u>1/d²</u>			<u>1/d²</u>		
hkl	Calc.	Obs.	hkl	Calc.	Obs.
011	0.0530		203	0.4012	0.4021
020	0.0532	0.0527			
210	0.0572	0.0577	531	0.4342	
111	0.0644	0.0645	601	0.4353	0.4365
201	0.0837	0.0859			
121	0.1039	0.1042	611	0.4486	
301	0.1386	0.1390	620	0.4488	0.4488
311	0.1519	0.1525	432	0.4544	
112	0.1831	0.1840	223	0.4545	0.4561
321	0.1918	0.1925	303	0.4562	
202	0.2027	0.2027	152	0.5024	
231	0.2034		450	0.5085	0.5057
401	0.2155	0.2162	161	0.5298	0.5305
212	0.2160		710	0.5518	0.5513
411	0.2288		612	0.5667	0.5689
420	0.2290	0.2285	243	0.6141	
302	0.2577		361	0.6178	0.6158
331	0.2584	0.5297	641	0.6482	
312	0.2710	0.2721	162	0.6489	0.6510
510	0.2880	0.2899	433	0.6529	
132	0.2895		603	0.7529	
322	0.3109		811	0.7564	0.7547
501	0.3144	0.3124	820	0.7566	
232	0.3225	0.3247	134	0.7659	
402	0.3346		552	0.7662	0.7663
431	0.3353	0.3368	613	0.7662	
			371	0.7908	
			741	0.7911	0.7908

(cont'd)

* Since the photograph was spotty intensity estimates were impossible.

TABLE VI (cont'd)

hkl	Calc.	$\frac{1}{d^2}$ Obs.
623	0.8061	
404	0.8110	0.8083
562	0.9127	
661	0.9145	0.9140
822	0.9154	
860	1.1826	
415	1.1816	1.1838
473	1.1853	

TABLE VIIX-Ray Powder Data for OsOF₅ (cubic)

hkl	Calc.	Obs.	Relative Intensity
110	0.0530	0.0543	10
200	0.1060	0.1069	5
211	0.1590	0.1603	8
220	0.2120	0.2122	4
310	0.2650	0.2646	7
321	0.3710	0.3712	5
411,330	0.4770	0.4770	4

(b) Polarization microscopy

In order to determine the transition point with greater accuracy, a polarizing microscope provided with a hot stage (Leitz Model 350, Ernst Leitz GMBH Wetzlar, Germany) was used. A single crystal of osmium oxide pentafluoride which had developed from a powder specimen in a capillary over a period

of days, was used. The crystal could be seen with the polarizer and the analyzer crossed. The stage of the microscope was then gradually heated and at 32.5° the crystal disappeared from view. This indicated the solid-solid transition temperature.

(v) Magnetic properties

A sample for magnetic measurement was prepared in a thin walled quartz tube of 4 mm. diameter. The magnetic susceptibility was measured between 77° and 295°K . One set of readings was taken while cooling the sample and the other set while warming up. The molar susceptibilities were corrected for diamagnetic contributions from the ligands in the molecule (See Section 2.1.6). The susceptibility was found to obey the Curie-Weiss law throughout the temperature range, the molecular field constant being $+6^{\circ}$. The observed atomic susceptibilities and the deviations from the ideal susceptibilities (for Curie-Weiss law obedience) at various temperatures are shown in Table VIII. The plot of $1/\chi_A$ vs T is shown in Figure 9. The value of μ_{eff} (1.47 B.M.) was found to be nearly constant throughout the temperature range as shown in Table VIII.

A separate set of measurements on another sample gave similar results.

(vi) Infrared spectrum

The infrared spectrum of OsOF_5 was recorded at room temperature using a monel infrared cell. Because OsOF_5 had an absorption in the region of 960 cm.^{-1} where OsO_4 has strong absorption,⁵⁴ the spectrum of OsOF_5 was also recorded with OsO_4 kept in the reference beam. The pressure of the OsO_4

vapour was adjusted to cancel the absorption by the OsO_4 impurity in the OsOF_5 . This established the authenticity of the 960 cm^{-1} OsOF_5 peak.

TABLE VIII

Magnetic Data for OsOF_5

a) Increasing temperature

Temp. $^{\circ}\text{K}$	$\chi_A(\text{obs.}) \times 10^6$ c.g.s. units	$[\chi_A(\text{obs.}) - \chi_A(\text{ideal})^*] \times 10^6$ c.g.s. units	$\mu_{\text{eff}}(\text{B.M.})$
78.1	3,521	195	1.49
84.8	3,068	-6	1.45
91.5	2,828	-30	1.44
102.5	2,477	-85	1.43
112.7	2,262	-76	1.47
127.1	2,002	-79	1.43
146.9	1,848	39	1.48
164.5	1,632	12	1.47
181.1	1,498	23	1.48
198.4	1,387	38	1.49
215.4	1,267	23	1.48
232.9	1,161	9	1.48
249.7	1,065	-10	1.46
263.9	1,008	-10	1.46
279.0	966	2	1.47
293.8	917	1	1.47

(cont'd)

* Curie-Weiss law obedience, $\Theta = 6^{\circ}$.

TABLE VIII (cont'd)

b) Decreasing temperature

Temp. °K	$\chi_A(\text{obs.}) \times 10^6$	$[\chi_A(\text{obs.}) - \chi_A(\text{ideal})] \times 10^6$	$\mu_{\text{eff}}(\text{B.M.})$
	c.g.s. units	c.g.s. units	
295.6	913	2	1.48
280.2	948	-12	1.44
267.6	994	-10	1.43
250.7	1,058	-13	1.43
235.5	1,136	-3	1.43
216.3	1,255	16	1.46
199.4	1,352	10	1.48
182.1	1,473	6	1.48
165.1	1,634	20	1.47
151.2	1,792	33	1.47
138.5	1,958	42	1.47
123.9	2,146	12	1.48
114.4	2,208	-97	1.47
102.7	2,459	-99	1.46
93.4	2,718	-84	1.46
84.5	3,052	-32	1.46
77.1	3,553	186	1.47

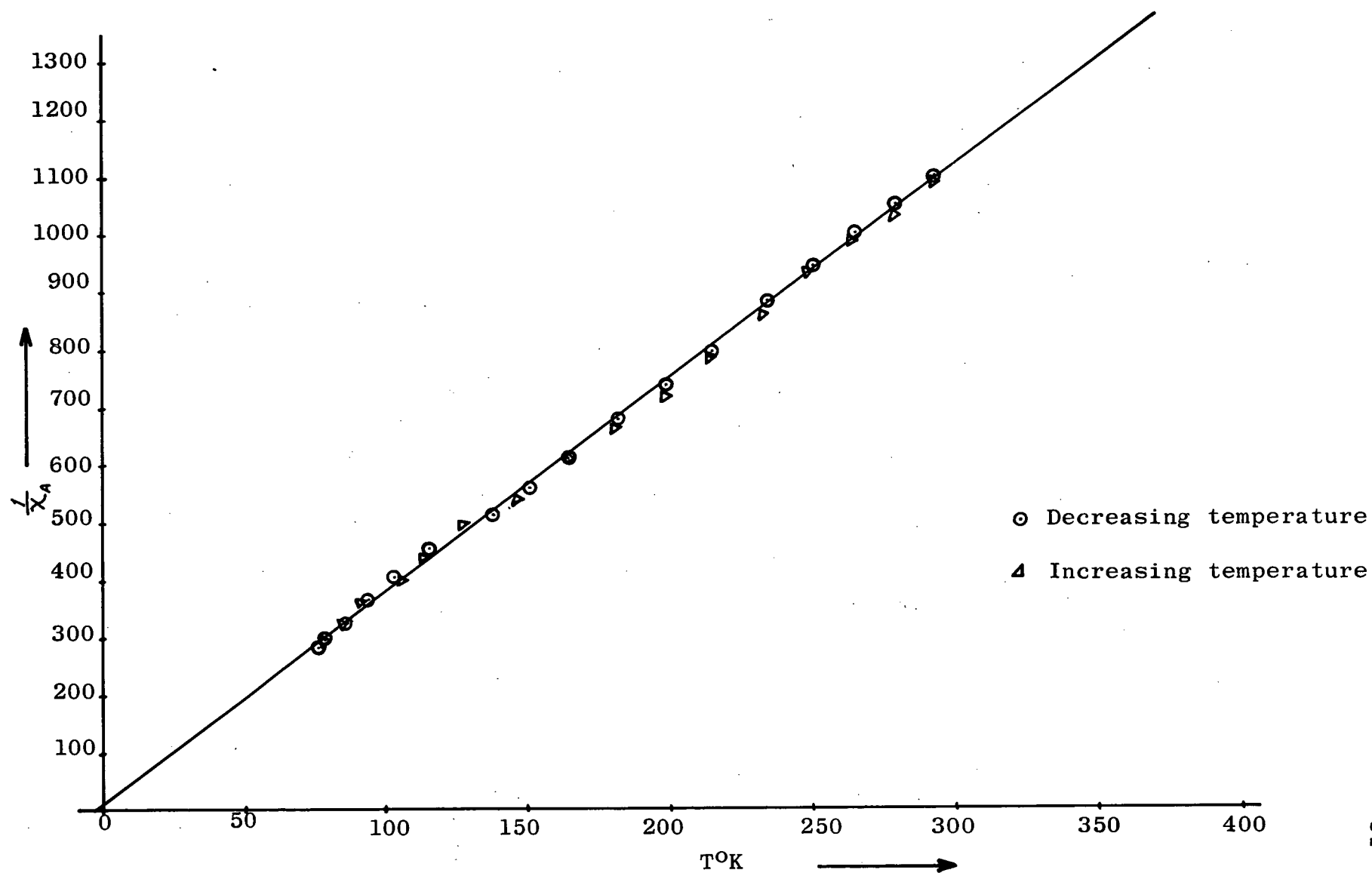


Figure 9. Plot of $1/\chi_A$ vs. T for OsOF_5

The vapour pressure of OsOF_5 is only about 22 mm. at room temperature; hence it was desirable to record the IR spectrum at higher temperatures where the vapour pressure is much greater. This was achieved by placing the IR cell in a small electrically heated box fitted with silver chloride windows.

The observed absorptions are listed in Table IX and the IR spectra at different pressures are shown in Figures 10 and 11.

TABLE IX

Infrared Data for OsOF_5

Cm^{-1}	Intensity	
440	w	
535	vw	
640	s	(shoulder at 650 cm^{-1})
700	vs	(shoulder at 710 cm^{-1})
800	w	
960	s	
1337	w	
1405	w	
1915	w	

(vii) UV, visible and near infrared spectra

The spectra in UV, visible and near infrared regions were recorded using a quartz cell provided with a Whitey valve.

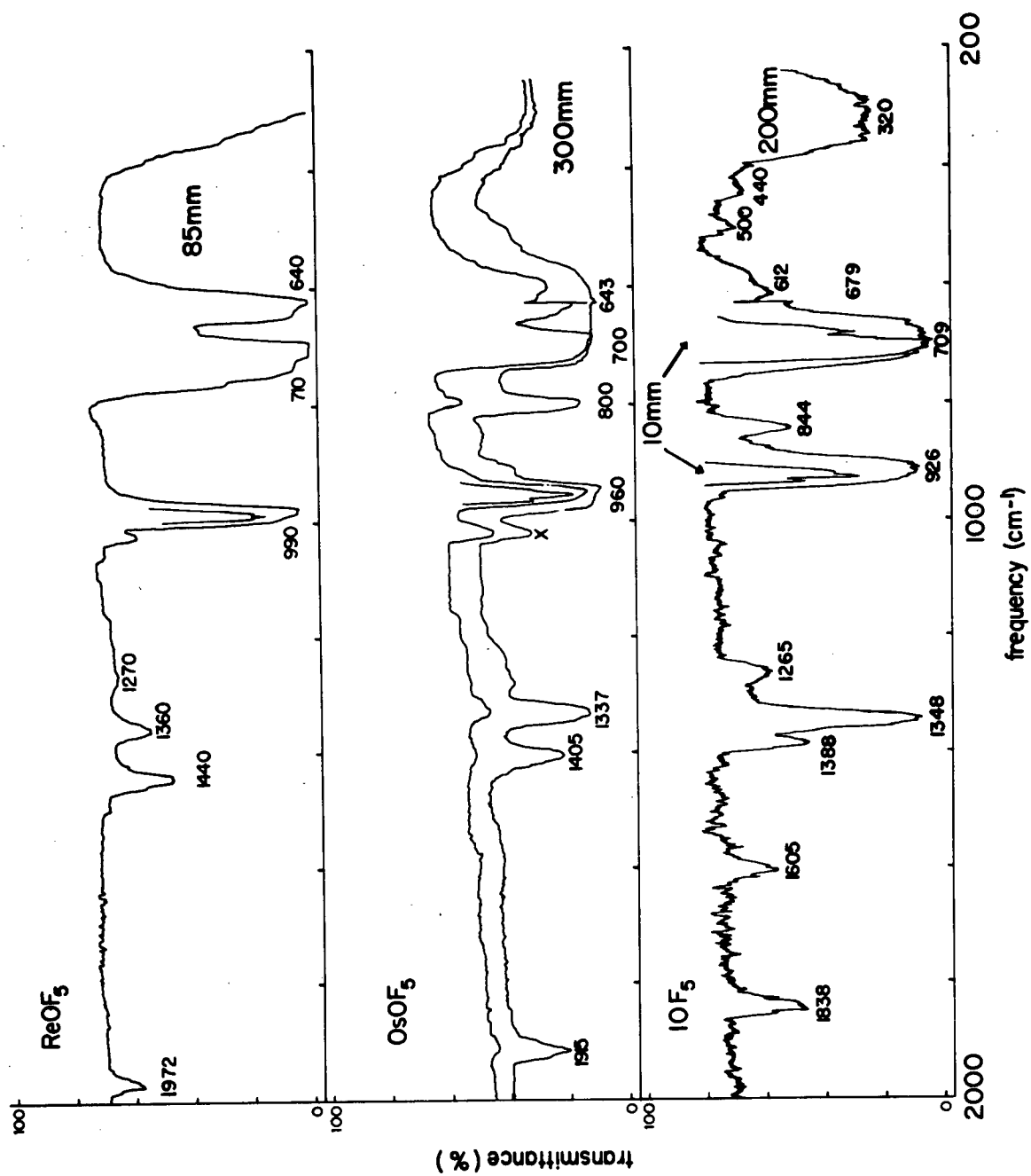


Figure 10. Infrared Spectra of ReOF_5 , OsOF_5 and IOF_5 .

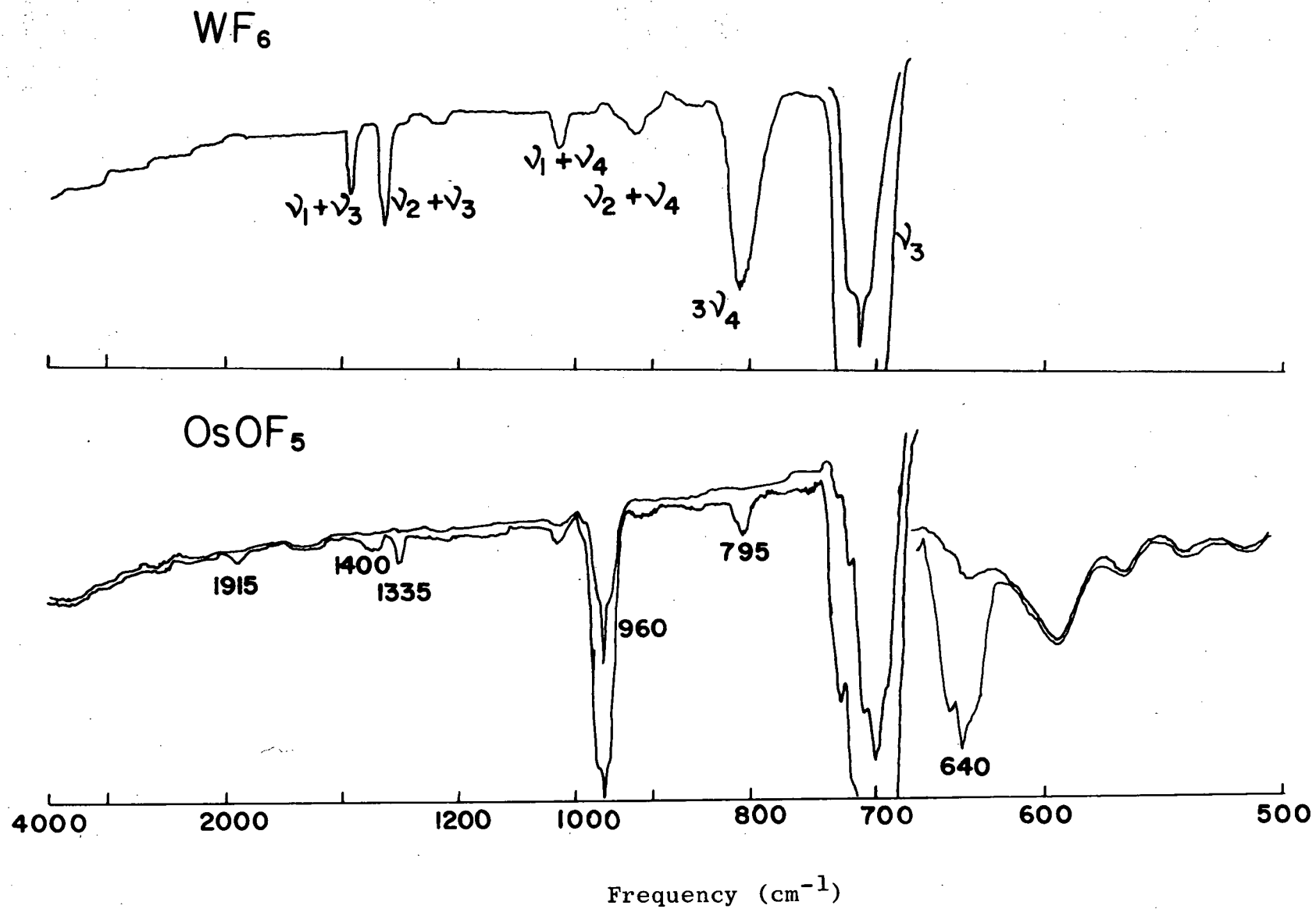


Figure 11. Infrared Spectra of WF₆ and OsOF₅.

In the near infrared region peaks were observed at 8,080 (w), 8,300 (w), 8,450 (w), 8,700 (w), 8,950 (w), 10,800 (w), 11,200 (w), 11,450 (w), 11,925 (w), and 12,380 (w) Å.

In the visible region the sample started to absorb at 4600Å and showed a maximum at 3500Å.

In the ultraviolet region from 3500Å to 2600Å the absorption was very high.

(viii) N.M.R. and e.s.r. spectra

A solution of OsOF₅ in WF₆ (1:3) prepared in a 4 mm. diameter quartz tube was used as the sample for recording the ¹⁹F n.m.r. spectrum of OsOF₅. A single broad low intensity peak with chemical shift at -215 p.p.m. from the internal SiF₄ standard was observed.

A 1% solution of OsOF₅ in WF₆ prepared in a quartz tube was used as a sample for recording the e.s.r. spectrum of OsOF₅. The spectrum consisted of a single broad signal centred around g~2 and about 200 gauss wide. No fine structure was observed.

(ix) Reaction of OsOF₅ with NO

(a) Tensimetric titration

A solid-gas reaction of OsOF₅ with NO was followed tensimetrically in the usual way (See Section 2.1.5). A dirty white product was formed in the reaction bulb. The result of the tensimetric titrations are shown below. The residual gas was condensible at -196°.

The X-ray powder photograph of the product showed a more complex diffraction pattern than NOOsF₆ and it was not indexed.

OsOF ₅ pressure, mm.	40.1
Initial NO pressure, mm.	98.0
Residual pressure, mm.	62.3
Combining ratio, NO/OsOF ₅	0.89:1

(b) Reaction in tungsten hexafluoride solution

An apparatus was set up as shown in Figure 12. The small monel can M contained purified nitric oxide at ~ 150 p.s.i. The storage can of OsOF₅ and the cylinder of WF₆ were attached to the main vacuum manifold.

Approximately 1 g. of OsOF₅ was condensed in the Kel-F reaction trap D from the OsOF₅ storage bottle. Tungsten hexafluoride was then condensed in the same trap, enough being taken to half fill the Kel-F trap. The mixture in the trap was warmed to $\sim 10^{\circ}$, whereupon the OsOF₅ dissolved in the liquid WF₆ to give a light green solution. The Kel-F trap was kept at $7-10^{\circ}\text{C}$. The apparatus was then filled with dry nitrogen through Pyrex traps A and B cooled in liquid oxygen. A sulphuric acid bubbler in the nitrogen line served as a blow off to maintain the internal pressure of the apparatus close to one atmosphere. With the apparatus filled with dry nitrogen, traps A and B were drawn off. The remaining apparatus was opened to the atmosphere at the end K through Pyrex traps E and F cooled in liquid oxygen. With Kel-F trap D maintained at $7-10^{\circ}$ nitric oxide was bubbled into the WF₆ solution. A white precipitate formed initially but subsequently the whole mixture turned brown. When the reaction was judged to be complete, excess WF₆ was pumped off. A pale lilac solid

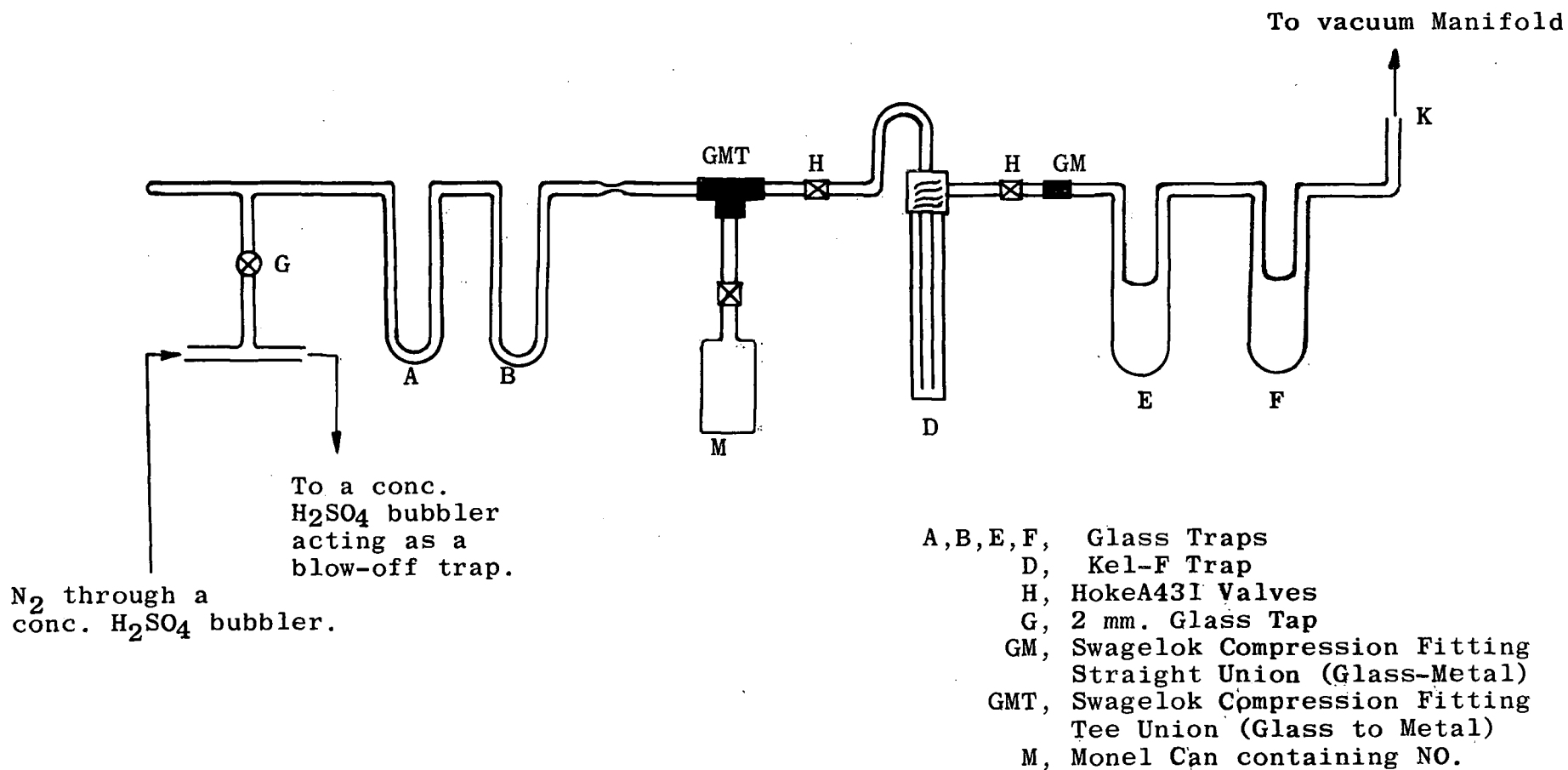


Figure 12. Apparatus for the Reaction of $OsOF_5$ with NO in WF_6 Solution.

remained in the trap.

The X-ray powder photograph of the product was similar to that of the product formed in the tensimetric titration of NO and OsOF₅.

Analysis of the product was done by alkaline hydrolysis. Osmium was estimated by the hydrazine hydrate method. Difficulty was experienced in obtaining complete precipitation of the osmium and it is probable that some remained in solution as evidenced by the light yellow colour of the filtrate. Fluorine was estimated in the filtrate from the osmium precipitation. Nitrogen was estimated on a separate sample by the conventional Dumas method (Found: N, 3.25; F, 29.3; Os, 50.1%. NOOsOF₅ requires N, 4.23; F, 28.68; Os, 57.42%. (NO)₂ OsOF₅ requires N, 7.75; F, 26.30; Os, 52.65%).

Magnetic susceptibility measurements done at room temperature gave the value $\chi_g = 0.788 \times 10^6$ c.g.s. units, with $\mu_{\text{eff}} = 0.78$ B.M. (using NOOsOF₅ as the molecular formula of the product).

In one of the reactions of NO with OsOF₅ in WF₆, the reaction product was red. A preliminary analysis showed that it contained tungsten. It was assumed that WF₆ was still adsorbed in the product so it was heated to 100° in vacuum for two hours. The colour of the product changed from red to grey but no WF₆ was obtained in the cold traps in the vacuum line.

The X-ray powder photograph of the grey product was identical with that of the red one. The pattern was similar to that of NOOsF₆ and was indexed on the basis of cubic

unit cell with $a = 10.152 \pm .003\text{\AA}$.

The product was analysed for fluorine, osmium and tungsten. The last mentioned element was estimated as its trioxide. (Found: F, 29.3; W, 23.9; Os 30.2%. NOOsF_6 , NOWOF_5 requires F, 31.7; W, 27.9; Os, 28.9%).

The magnetic susceptibility was measured over a temperature range 77° to 297°K . Molar susceptibilities were calculated by taking the molecular formula, NOOsF_6 , NOWOF_5 . They were corrected for diamagnetic contributions from the ligands in the molecule in the usual way. The susceptibility was found to obey the Curie-Weisslaw throughout the temperature range, θ being 24° , with $\mu_{\text{eff}} = 3.15$ B.M. at 297°K . The observed values of the atomic susceptibilities and their deviations from the ideal values (for Curie-Weiss law obedience) at various temperatures are shown in Table X. The plot of $1/\chi_A$ vs T is shown in Figure 13.

TABLE X

Magnetic Data for the Mixture NOOsF_6 , NOWOF_5

$T^\circ\text{K}$	$\chi_A \times 10^6$ c.g.s. units	$[\chi_A(\text{obs.}) - \chi_A(\text{ideal})^*] \times 10^6$ c.g.s. units
295.7	4,159	19
274.3	4,443	6
253.2	4,733	-40
233.7	5,227	92
213.7	5,609	42
193.3	6,051	-38
173.5	6,631	-68

* Curie-Weiss law obedience, $\theta = 24^\circ$

(cont'd)

TABLE X (cont'd)

T°K	$\chi_A \times 10^6$ c.g.s. units	$[\chi_A(\text{obs.}) - \chi_A(\text{ideal})] \times 10^6$ c.g.s. units
153.5	7,329	-125
139.2	7,995	-112
121.9	8,858	-210
107.3	9,847	-228
95.0	11,112	-4
84.6	12,542	361
77.1	13,946	862

2.2.3 Osmium Trioxide Difluoride

(i) Preparation

Osmium trioxide difluoride was prepared as described by Hepworth and Robinson,³⁰ by the reaction of bromine trifluoride with osmium tetroxide. The apparatus and method used were similar to those outlined in Section 2.1.2 for fluorination with BrF₃. The reaction took place on warming the mixture of OsO₄ and BrF₃ to room temperature. Large amounts of bromine and oxygen were evolved. A dark red liquid with some solid in it was first formed. This mixture was warmed gently to complete the reaction, then excess bromine trifluoride was removed under vacuum. Complete removal of BrF₃ was accomplished by heating the product to 60° under vacuum for a few hours. The product was an orange yellow powder.

(ii) Analysis

The product was analysed for fluorine following alkaline hydrolysis (Found: F, 13.46%. OsO₃F₂

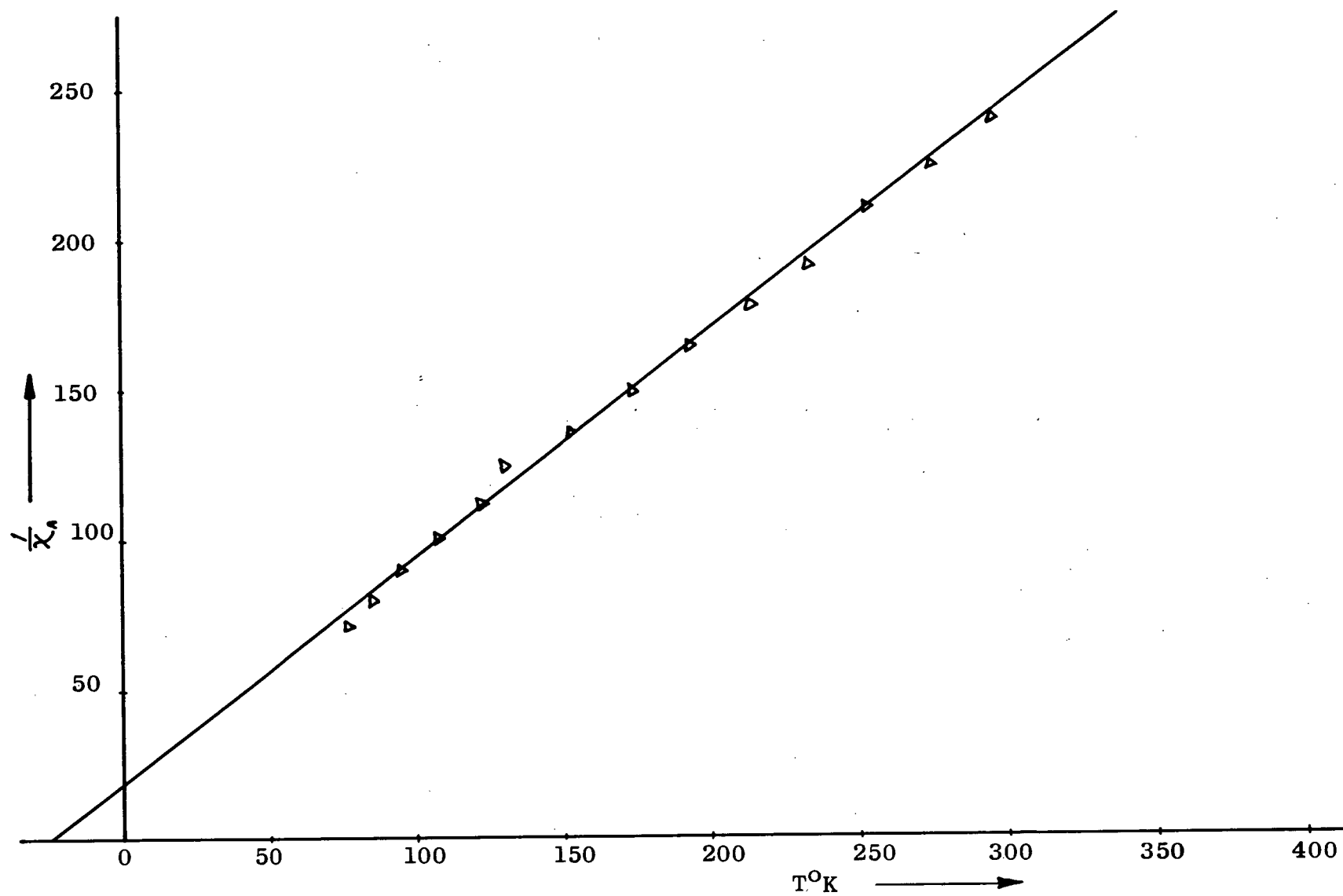


Figure 13. Plot of $1/\chi_A$ vs. T for the 1:1 Mixture NOOsf_6 , NOWOF_5

requires F, 13.75%).

(iii) Phase transition in the solid

When freshly prepared osmium trioxide difluoride was orange-yellow. The colour of the sample changed to red slowly at room temperature. The red form on heating changed to the orange-yellow form at $\sim 90^\circ$.

(iv) X-Ray powder photograph

The X-ray diffraction pattern of the orange-yellow form was indexed on the basis of a monoclinic unit cell as shown in Table XI with $a = c = 5.571\text{\AA}$, $b = 5.555\text{\AA}$, $\beta = 93^\circ$, $U = 171.9\text{\AA}^3$ and $Z = 2$.

The X-ray powder photograph of the red form was more complex than that of the yellow form and was not indexed. A superficial similarity of this pattern was found to the patterns of the pentafluorides, RuF_5 ,⁵⁵ RhF_5 ,⁵⁶ IrF_5 ,⁵⁷ and PtF_5 .⁵⁸

(v) Magnetic properties

The magnetic susceptibilities of both the yellow and red forms of osmium trioxide difluoride were measured at room temperature. Both were found to be diamagnetic. The value of the susceptibility was based on benzene as standard. The magnetic susceptibility of benzene saturated with air was taken as -0.720×10^{-6} c.g.s. units.⁵⁹ The results are shown below:

$$\begin{aligned}\chi_M \text{ for yellow form} &= -24.9 \times 10^{-6} \text{ c.g.s. units} \\ \chi_M \text{ for red form} &= -26.0 \times 10^{-6} \text{ c.g.s. units}\end{aligned}$$

TABLE XI

X-Ray Powder Data for OsO_3F_2 (orange-yellow form)

hkl	Calc.	$\frac{1}{d^2}$	Obs.	Relative Intensities
100	0.0324		0.0334	6
10 $\bar{1}$	0.0603		0.0618	7
110	0.0648		0.0653	10
101	0.0693		0.0707	5
111	0.1017		0.1032	5
200	0.1296		0.1313	7
210	0.1620		0.1634	6
201	0.1710		0.1727	5
11 $\bar{2}$	0.1854		0.1872	7
112	0.2034		0.2033	3
+ ---	-----		0.2160	1
202	0.2412		0.2428	4
220	0.2592		0.2612	5
300	0.2916		0.2928	6
221	0.3006		0.3026	6
30 $\bar{1}$	0.3105		0.3117	7
310	0.3240		0.3254	6
31 $\bar{1}$	0.3429		0.3444	6
311	0.3699		0.3718	7
22 $\bar{2}$	0.3708			
222	0.4068		0.4057	vw
320	0.4212		0.4238	7
302	0.4482		0.4473	5

(cont'd)

+ These superlattice lines are accounted for by a unit cell of double cell edge.

TABLE XI (cont'd)

	hkl	Calc.	$\frac{1}{d^2}$	Obs.	Relative Intensities
+	---	---		0.4944	w
	400	0.5184		0.5192	1
	40 $\bar{1}$, 23 $\bar{2}$	0.5328		0.5322	2
	410	0.5508		0.5513	6
	41 $\bar{1}$	0.5652		0.5677	4
	401, 232	0.5688			
	322	0.5778		0.5795	4
	14 $\bar{1}$	0.5787			
	411	0.6012		0.6029	2
	33 $\bar{1}$	0.6021			
	331	0.6291		0.6293	2
	41 $\bar{2}$	0.6444		0.6463	1
	420	0.6480			
	313	0.6561		0.6599	1
	42 $\bar{1}$	0.6624			
	402	0.6840		0.6856	2
	33 $\bar{2}$	0.6858			
	421	0.6984		0.6972	1
	412	0.7164		0.7162	1
+	---	---		0.7863	vw
	500, 430	0.8100		0.8096	6
	43 $\bar{1}$	0.8244		0.8267	vw
	34 $\bar{1}$	0.8289			
	403	0.8640		0.8645	vw
	501	0.8649			
	50 $\bar{2}$	0.8946		0.8956	3
	413	0.8964			
	511	0.8973			

(cont'd)

TABLE XI (cont'd)

hkl	$\frac{1}{d^2}$		Relative Intensities
	Calc.	Obs.	
34 $\bar{2}$ 333	0.9124 0.9153	0.9136	vw
520	0.9394	0.9386	3
25 $\bar{1}$ 404 342	0.9630 0.9648 0.9664	0.9659	2
+ ---	---	0.9907	1
512	1.0170	1.0158	1
43 $\bar{3}$	1.0476	1.0477	1
441, 252	1.0872	1.0847	2
404	1.1088	1.1076	1
351	1.1475	1.1494	1
600	1.1664	1.1667	1
513 442	1.2015 1.2024	1.2018	3
+ ---	---	1.2532	vw
51 $\bar{4}$	1.2708	1.2708	1
620	1.2960	1.2943	2

2.2.4 Nitrosyl Trioxytrifluoroosmate (VIII)

(i) Preparation

The salt nitrosyl trioxytrifluoroosmate (VIII) was prepared by the reaction of BrF_3 and NOCl with OsO_4 . The apparatus was similar to that used for the preparation of OsO_3F_2 , the only difference being the inclusion of a cylinder of NOCl in the apparatus. The reactants OsO_4 , NOCl and BrF_3 were condensed in the reaction bulb one after another. A vigorous reaction with evolution of large amounts of gas took place on warming the reaction mixture to room temperature. On pumping out excess BrF_3 a yellow powder was left in the reaction bulb along with some white solid. The latter was assumed to be NOBrF_4 (formed by the reaction of NOCl with BrF_3). This was completely removed from the product by heating under vacuum at 100° for several hours.

(ii) Analysis

The sample was analysed for osmium and fluorine after dissolution in aqueous alkali. Nitrogen was estimated by the Dumas method. (Found: N, 3.38; F, 16.72; Os, 57.9%. NOOsO_3F_3 requires N, 4.30; F, 17.53; Os 58.48%).

The X-ray diffraction pattern of the compound was complex and was not indexed.

The compound was found to be diamagnetic.

2.2.5 The search for OsO_2F_4

During the investigation of the osmium-oxygen-fluorine system (Section 2.2.2) the reaction conditions were varied in order to obtain other oxyfluorides in addition

to OsOF_5 . Larger ratios of oxygen to fluorine than 1:2 were tried but no products other than OsOF_5 and OsF_6 were observed; finally with a 2:1 ratio of oxygen and fluorine the orange-yellow solid, OsO_3F_2 was formed.

It was assumed that if any OsO_2F_4 was formed it might be colourless and hence difficult to detect visually in the admixture with OsOF_5 . However, the infrared spectra of osmium oxide pentafluoride prepared under various conditions were identical with one another. Two independent magnetic measurements on samples of OsOF_5 prepared in different batches gave magnetic susceptibility values equal within the experimental uncertainty. Furthermore the magnitude of the susceptibility was consistent with pure OsOF_5 .

2.3 OXIDIZING PROPERTIES OF THE NOBLE METAL HEXAFLUORIDES

2.3.1 Platinum Hexafluoride and Oxygen

(i) Infrared, visible and UV spectra

A 10 cm. monel infrared cell provided with a monel reservoir was attached to a vacuum manifold and evacuated. A known pressure of platinum hexafluoride vapour was admitted to the cell body. A known quantity of dry oxygen was taken in the monel reservoir at a pressure in excess of that of the PtF_6 vapour in the body of the cell. The infrared spectrum of the PtF_6 vapour was recorded. Oxygen from the reservoir was admitted to the cell which resulted in the instantaneous disappearance of the deep red PtF_6 vapour and the appearance of a yellowish powder on the cell windows. A layer of O_2PtF_6 was thus deposited on the windows. The spectrum showed peaks at 631 cm^{-1} (vs) and 545 cm^{-1} (s).

In a similar way a layer of O_2PtF_6 was deposited on the windows of a quartz gas cell and visible and UV spectra were recorded. Only one intense absorption was observed with a maximum in the neighbourhood of 3500\AA .

These values are similar to those reported by Bartlett and Lohmann.³⁴

(ii) Solid-gas reaction

Platinum hexafluoride was condensed in a silica bulb and excess oxygen was introduced into the bulb. The bulb was then warmed to room temperature. When the dark red colour of PtF_6 vapour vanished, the reaction was assumed to be complete. When excess oxygen had been removed, however, some PtF_6 vapour was subsequently removed from the bulb. Evidently

the platinum hexafluoride and oxygen had not reacted completely presumably because of the formation of an impervious layer of O_2PtF_6 on solid PtF_6 .

This preliminary reaction showed that this method could not be used for large scale preparation of O_2PtF_6 without higher reaction temperatures - an undesirable condition in quartz or glass apparatus.

(iii) Synthesis of O_2PtF_6 on a large scale

A flow method was used for large scale preparation of O_2PtF_6 by a gas-gas reaction. The apparatus was set up as shown in Figure 14. The monel storage bottle B contained a known amount (~ 4 g.) of PtF_6 . The apparatus was evacuated and flamed out thoroughly. Platinum hexafluoride was condensed in trap C from bottle B. Trap C was kept cool in liquid oxygen and all the other traps (except D) in the system were also cooled in liquid oxygen. The apparatus was then filled with nitrogen which had been dried by passing through concentrated sulphuric acid bubblers (one bubbler acting as blow off valve) and through trap A cooled in liquid oxygen. The blow off valve bubbler was disconnected from the system and nitrogen was kept passing through the apparatus at a slow rate. Oxygen dried by passing through trap I cooled in liquid oxygen was also passed through the apparatus. Streams of oxygen and nitrogen thus passed through the apparatus and escaped through the small mercury head in the manometer M.

Liquid oxygen around the trap C containing PtF_6 was replaced by an ice-water mixture. Platinum hexafluoride vapour was carried into the reaction trap D by the stream of

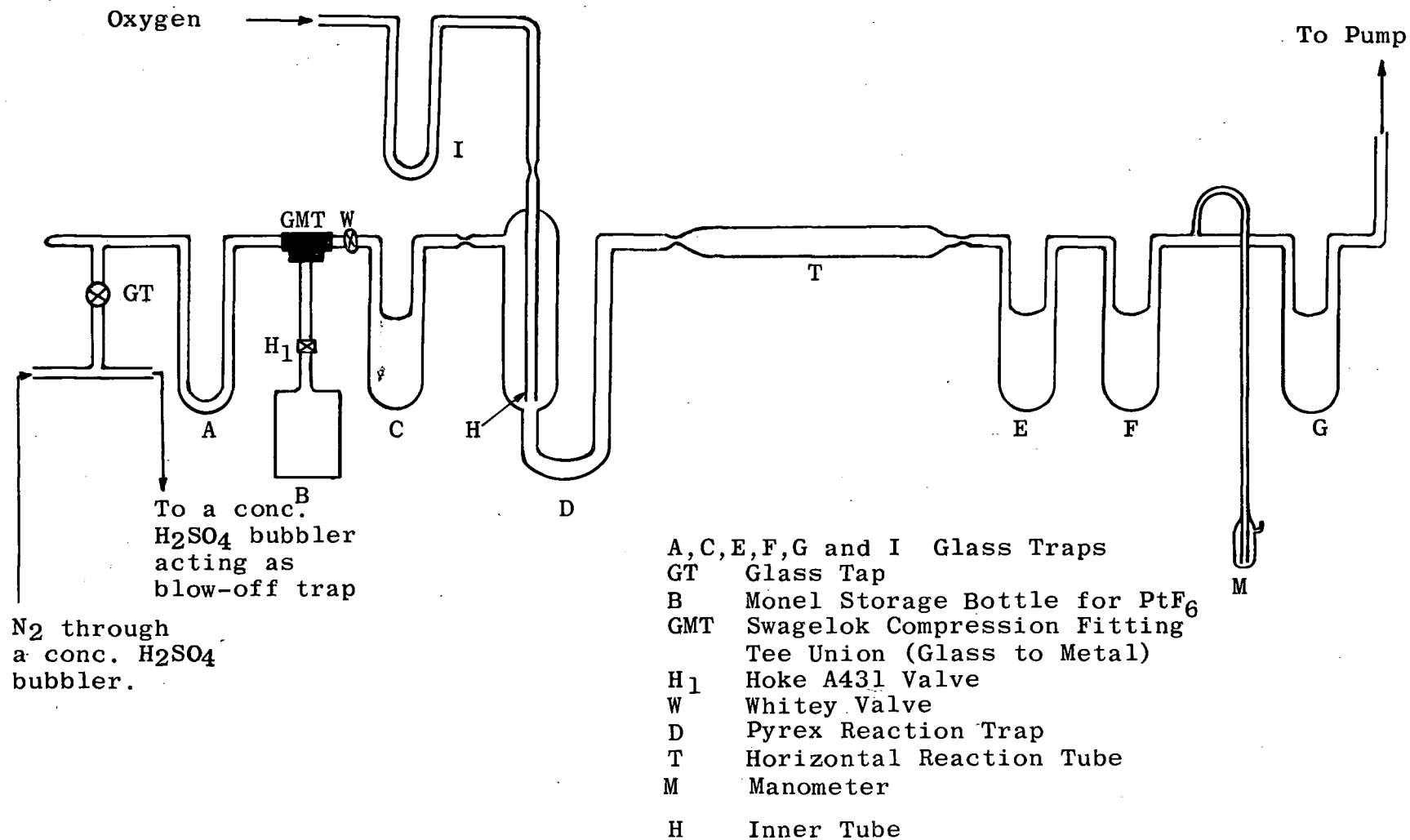


Figure 12. Apparatus for Large Scale Synthesis of O_2PtF_6

nitrogen where it came into contact with oxygen coming out of tube H. At the opening of tube H an orange cloud formed and the particles collected, for the most part, at the bottom of D. Some material was also carried by the gas stream to the horizontal tube T and trap E. Frequent adjustment in the rates of flow of nitrogen and oxygen was necessary in order to keep the reaction zone always around the opening of H. The reaction was continued until all of the PtF_6 had been consumed, when the nitrogen and oxygen streams were stopped and the apparatus was evacuated. Trap D and tube T containing O_2PtF_6 were drawn off under vacuum.

The X-ray powder photograph of the product was identical with that of O_2PtF_6 reported by Bartlett and Lohmann.³⁴ The product was heated in vacuum at 70° for some time to convert any of the rhombohedral form³⁴ into the cubic form. The sample was then packed in a dry box into a thin walled aluminum cylinder of $\frac{1}{4}$ in. O.D. x $3\frac{1}{4}$ in. long which was closed by a screw cap sealed with a teflon gasket.

This sample and a duplicate can were dispatched to the Brookhaven National Laboratory, Upton, N.Y. for structural analysis by neutron diffraction spectroscopy.

2.3.2 Platinum Hexafluoride and Xenon

(i) Gas-gas reaction in glass apparatus

A Pyrex glass break-seal bulb, the seal of which was bypassed by a small bore tube was joined to a metal manifold by way of a metal valve. The bulb was evacuated by way of a glass side arm to avoid introducing moisture to the

metal system. The glass was flamed out under vacuum, and the side arm drawn off. Platinum hexafluoride of known volume, temperature and pressure was condensed from the metal system into the glass tube. The break-seal bypass was sealed to isolate the fluoride, which was allowed to vaporize. Xenon, also measured out in the metal system, was admitted by breaking the glass seal. The colour of PtF_6 vanished and yellow powder was produced. The residual gas was colourless and condensible at -196° . The results for the reactions are shown below.

Experiment No.	1	2
PtF_6 pressure, mm.	95.0	70.0
Initial Xe pressure, mm.	156.6	72.0
Residual Xe pressure, mm.	82.0	23.0
Combining ratio Xe/ PtF_6	1:1.27	1:1.42

(ii) Solid-gas reaction in quartz apparatus

Solid-gas reactions of PtF_6 with Xe were carried out in a quartz bulb as described in Section 2.1.5. The results of the tensimetric titrations are shown below.

Experiment No.	1	2	3
Initial PtF_6 pressure, mm.	93.0	117.5	56.0
Residual PtF_6 pressure, mm.	0	0	12.0
Initial Xe pressure, mm.	108.0	117.5	27.5
Residual Xe pressure, mm.	17.0	59.0	0
Combining ratio Xe/ PtF_6	1:1.02	1:2.0	1:1.6

(iii) Solid-gas reactions in nickel apparatus

A series of reactions were carried out using a nickel weighing can with a capacity of approximately 113 ml., weight 174.5 g. This bottle was fitted with a Hoke A431 valve and was joined to the vacuum system by a compression fitting. The can was conditioned by exposure to platinum hexafluoride gas for several hours. In each experiment tensimetrically measured platinum hexafluoride was condensed in the can, which was then weighed. Next a tensimetered sample of xenon was condensed in the can, which was then warmed to room temperature. Gaseous residues were transferred to the gauge for measurement, and the can was reweighed. The results for a sequence of solid-gas reaction in the nickel can are summarized below.

Experiment No.	1	2	3	4	5	6
PtF ₆ , pr., mm.	-	97.0	73.0	90.0	96.0	95.0
PtF ₆ , wt., g.	0.1117	0.0829	0.0714	0.0828	0.0897	0.0893
Initial Xe, pr., mm.	-	58.0	46.0	53.0	59.0	74.0
Residual Xe, pr., mm.	-	6.0	7.0	3.0	5.0	23.0
Xe, wt., g.	0.0175	0.0212	0.0144	0.0188	0.0255	0.0212
Temperature °C	20.8	22.2	23.6	23.6	23.6	23.6
Combining ratio:						
Tensimetric		1:1.87	1:1.87	1:1.80	1:1.78	1:1.86
Gravimetric	1:2.3	1:1.66	1:2.1	1:1.87	1:1.49	1:1.78

The over-all combining ratio:

Tensimetric 1:1.83

Gravimetric 1:1.89

(iv) The reaction of Xe (PtF₆)_{1.89} with xenon gas

Sufficient xenon (311 mm.) was added to the weighing can containing 0.6464 g. of adduct of composition Xe(PtF₆)_{1.89} to bring the composition to XePtF₆, and the can was heated to 130° for one hour. Most of the xenon was consumed (residual pressure 128 mm.) and amounted to 0.0621 g., this representing a change in composition to Xe(PtF₆)_{1.24}. Prolonged heating with excess xenon did not change this composition significantly.

(v) Gas-gas reaction in a nickel apparatus

The procedure was similar to that described for the gas-gas reaction in a quartz bulb. The results for the reactions are shown below.

Experiment No.	1	2	3	4
PtF ₆ pressure, mm.	86.0	76.5	88.5	88.5
Initial Xe pressure, mm.	112.0	94.5	154	146.0
Residual Xe pressure, mm.	12.0	53.0	114	95.5
Combining ratio Xe/PtF ₆	1:0.86	1:1.84	1:2.2	1:1.75

(vi) Spectra of Xe-PtF₆ adduct

The infrared spectrum of material deposited on silver chloride windows in the nickel-bodied gas cell was recorded. The composition of the adduct was Xe(PtF₆)_{1.72}. Only two peaks in the region 400-4000 cm⁻¹ were assignable to the adduct: 625 cm⁻¹ (vs), 550 cm⁻¹ (s). The visible and ultraviolet spectrum of material deposited on the windows of a silica gas cell was recorded. A single peak at 3825⁰Å was observed. No

differences in the absorption spectra were noted for several separate adduct samples.

(vii) Physical properties of the Xe-PtF₆ adduct

The adduct is yellow when deposited in thin films but in bulk is deep red. The solid becomes glassy in appearance when heated to 115⁰, but does not melt below 165⁰, when it decomposes to produce xenon tetrafluoride, X-Ray powder photographs of the adduct of composition XePtF₆ show no diffraction pattern. Complex patterns were observed with samples of material richer in platinum. The plasticity of the material made the preparation of good powder samples difficult. Even well-cooled samples did not grind well.

(viii) The thermal decomposition of the Xe-PtF₆ adduct

A sample of material of composition Xe(PtF₆)_{1.8} contained in a quartz bottle was heated under an atmosphere of nitrogen. No change was observed up to 115⁰, when the red solid deepened in colour and became glassy. There was no further change up to 165⁰, when the solid fell to a brick-red powder and a deposit of colourless crystals collected on the colourless silica. The temperature was maintained close to 165⁰ until decomposition appeared to be complete (~1hr).

An infrared spectrum of the white solid over the range 400-4000 cm⁻¹ showed peaks at 595 cm⁻¹ (vs) and 589 cm⁻¹ (vs), values in close agreement with those given by Claassen, Chernick and Malm⁶⁰ for the strong doublet of xenon tetrafluoride.

The residual platinum compound was analysed for platinum and fluorine by pyrohydrolysis (Found: F, 27.0,

26.4; Pt, 54.5; Xe, 14.7, 14.7%. $\text{XePt}_2\text{F}_{10}$ requires F, 26.7, Pt, 54.8; Xe, 18.5%).

The decomposition product, $\text{XePt}_2\text{F}_{10}$ was found to be diamagnetic. Its interaction with cesium fluoride in iodine pentafluoride gave a yellow product, X-ray powder photographs of which indicated the presence of cesium hexafluoroplatinate (IV).

(ix) The preparation of RbPtF_6 from XePtF_6 in iodine pentafluoride

Platinum hexafluoride (total pressure in the known volume at 21.3° of 186 mm.) was condensed, followed by xenon (pressure 216 mm.) on rubidium fluoride (0.10 g.) in a quartz bulb. The quantities of PtF_6 and RbF were arranged to be equimolar. The mixture was warmed slowly until the platinum hexafluoride was seen to react with the xenon. The reaction was moderated by judicious cooling. A residual pressure of xenon of 34 mm. indicated a composition $\text{Xe}(\text{PtF}_6)_{1.02}$ for the adduct. Iodine pentafluoride was distilled onto the rubidium fluoride-xenon fluoroplatinate mixture and the solids dissolved, some gas (probably xenon) being evolved. An orange-yellow solution formed. Removal of the iodine pentafluoride under vacuum left an orange-yellow solid. X-ray powder photographs of this material revealed a strong pattern of lines which were indexed on the basis of a rhombohedral unit cell, $a = 5.08\text{\AA}$; $\alpha = 96^\circ 58'$, indicative of RbPtF_6 . Subsequently reported rubidium hexafluoro-iridate (V) and hexafluoroosmate (V) have been found to have unit cells of similar dimensions⁸ as this compound.

(x) The preparation of CsPtF_6 from $\text{Xe}(\text{PtF}_6)_2$ in iodine pentafluoride

An experiment similar to the above, involving interaction of material which proved to have the composition $\text{Xe}(\text{PtF}_6)_2$ and cesium fluoride in iodine pentafluoride, produced an orange-yellow solid. The amounts of PtF_6 and CsF had been set to be in an equimolar ratio. X-Ray powder photographs of the solid identified it as cesium hexafluoroplatinate (V). No other lines were present on the photographs other than those attributable to the rhombohedral unit cell, $a = 5.27\text{\AA}$, $\alpha = 96^\circ 25'$. This cell is very similar in dimensions to that reported for cesium hexafluoroiridate(V) and osmate(V).⁶¹

(xi) Xenon tetrafluoride with platinum tetrafluoride in iodine pentafluoride solution

Although xenon tetrafluoride dissolved in iodine pentafluoride without reaction, no adduct could be isolated. Furthermore, this solution failed to react with platinum tetrafluoride even on prolonged reflux at $\sim 100^\circ$.

(xii) The gas-gas reaction of Xe and PtF_6 on a large scale

An apparatus similar to that used for the related reaction of oxygen and platinum hexafluoride was used here. The oxygen supply section of that apparatus was replaced by a xenon supply. Xenon was taken in a monel can at high pressure. The reactant gases were carried in streams of nitrogen. The two streams met in the reaction trap D where a yellow cloud was produced. Brown particles deposited in the apparatus. Unreacted xenon was transferred back from the traps to the storage

bottle and was reacted with PtF_6 again in the same way. The product in thin layers seemed to be a yellowish powder but in bulk it was a dark red sticky material.

An X-ray powder photograph of the friable material showed a complex pattern and the pattern was weak even after long exposures.

Only one very small sample could be prepared for magnetic measurements. It was packed in a Pyrex tube of 2 mm. diameter. Because of the small length of the sample the magnetic balance described in Section 2.1.6 could not be used. Instead a permanent magnet of field strength 8000 gauss (Arnold Engineering Corporation, Illinois) was used along with a microbalance. The magnetic susceptibility at room temperature was found by the usual mercury II cobalt tetrathiocyanate standard. It was found to be 9.89×10^{-6} c.g.s. units at room temperature. Assigning the formula $\text{Xe}(\text{PtF}_6)_2$ to the product, the magnetic moment is calculated to be 4 B.M.

The sample from the magnetic measurements was pyrohydrolysed for platinum and fluorine analysis. (Found: F, 32.2; Pt, 51.7%. $\text{Xe}(\text{PtF}_6)_2$ requires F, 30.4; Pt, 52.1%).

2.3.3 Reactions of PtF_6 with (i) Kr, (ii) NF_3 , (iii) CO, (iv) C_6F_6 and (v) Cl_2

(i) Krypton

Platinum hexafluoride and a large excess of krypton were separately condensed in a silica bulb. The red vapour of PtF_6 was observed on warm up and was still observable at 50° .

A certain pressure of platinum hexafluoride was taken in the infrared cell and a higher pressure of krypton was taken in the reservoir of the cell. The IR spectrum of PtF_6 was recorded and krypton was admitted to the cell. The red colour of PtF_6 vapour was still visible. That the platinum hexafluoride was not consumed at all was shown by the IR spectrum of the reaction mixture.

(ii) Nitrogen trifluoride

Nitrogen trifluoride was treated with platinum hexafluoride in the same way as krypton and the results obtained were similar, i.e., platinum hexafluoride did not react with nitrogen trifluoride.

(iii) Carbon monoxide

The gas-gas reaction of PtF_6 with CO was highly exothermic as evidenced by the production of a flame in the reaction bulb. A brilliant red coloured solid was initially produced which turned red-brown and finally grey on pumping off the residual gases. The result of the tensimetric titration is shown below.

	Initial PtF_6	Initial CO	Residual gases (PtF_6 absent)
Pressure, mm.	59.8	159.1	146.5

An infrared spectrum of the residual gases showed the presence of COF_2 and CO only. The X-ray powder photograph of the solid product showed lines attributable to PtF_4 and, in addition, there was a cubic pattern which was proved to be that of platinum metal.

(iv) Hexafluorobenzene

The gas-gas reaction of C_6F_6 with PtF_6 was very violent and a light brown solid was produced. The result of the titration is shown below. About 1 mm. of the residual gases was incondensable at -196° , possibly indicating the presence of fluorine.

	Initial PtF_6	Initial C_6F_6	Residual gases (PtF_6 absent)
Pressure, mm.	29.7	60.2	65.2

The infrared spectrum of the residual gases showed the presence of C_6F_6 and further peaks at 1200, 1260, 1280 and 1300 cm^{-1} attributable to CF_4 and other fluorocarbons. The X-ray powder photograph showed the solid product to be amorphous.

(v) Chlorine

The gas-gas reaction of PtF_6 with Cl_2 was exothermic but was not accompanied by a flame. The product was a pale yellow powder. The results of the tensimetric titrations are shown below.

	Initial PtF_6 Pressure, (mm.)	Initial Cl_2 Pressure, (mm.)	Residual gases Pressure, (mm.) PtF_6 absent)
Experiment I	41.0	132.8	115.8
Experiment II	49.0	100.9	85.8

The residual gases were condensable at -196° and their infrared spectra showed ClF , ClF_3 , or ClF_5 to be absent. The X-ray powder photograph of the solid product showed that it

was amorphous.

2.3.4 Reactions of Rhodium Hexafluoride with (i) Xe and

(ii) Kr

(i) Xenon

Since rhodium hexafluoride was reduced in the gauge and main line so rapidly that tensimetric measurements of the quantity of hexafluoride were unreliable, the stoichiometry of the reaction with xenon was determined from the weight of adduct formed in the consumption of a tensimetrically measured quantity of xenon. Rhodium hexafluoride was roughly measured out tensimetrically and quickly condensed in a nickel weighing-can at -196° . Xenon, in roughly twofold molar excess of the rhodium fluoride, was accurately measured tensimetrically and also condensed in the can, which was subsequently warmed to room temperature. Residual xenon was transferred from the can to the gauge by cooling the well of the gauge to -196° . The weight of xenon consumed was computed from the tensimetric measurements, the volume of the line and gauge being accurately known.

Results:	(1)	Wt. of xenon consumed	0.0050 g.
		Wt. of adduct formed	0.0139 g.
		Combining ratio, Xe/RhF ₆	1:1.05
	(2)	Wt. of xenon consumed	0.0120 g.
		Wt. of adduct formed	0.0337 g.
		Combining ratio, Xe/RhF ₆	1:1.0

Samples prepared in quartz and of uncertain composition were deep red. X-Ray powder photographs of this material showed only a faint, sharp pattern, perhaps belonging to a minor phase.

(ii) Krypton

When a mixture of RhF_6 and large excess of krypton was warmed to room temperature in a quartz bulb, the deep red vapour of RhF_6 persisted. It persisted even on heating up to 50° . This established that RhF_6 does not react with krypton.

2.3.5 Iridium Hexafluoride and Chlorine

When a known excess of chlorine was admitted to a reaction bulb containing IrF_6 vapour at lower pressure, no reaction seemed to occur. The reaction mixture was then condensed and slowly warmed to room temperature. Reaction occurred readily when the reactants became liquid and a pale yellow solid was formed. After a few minutes this solid transformed to darker yellow liquid droplets. The results of the titrations are shown below.

	Initial IrF_6 Pressure (mm.)	Initial Cl_2 Pressure (mm.)	Residual gases Pressure (mm.)
Experiment I	77.0	185.5	130.5
Experiment II	33.0	98.5	66.5

The residual gases were condensible at -196° and their infrared spectra indicated absence of ClF , ClF_3 or ClF_5 . Only small peaks were observed at 1300, 1280, 1240 and 1150 cm^{-1} .

The reaction bulb with the liquid droplets was sealed off. After a few weeks the liquid droplets had disappeared and a bright yellow solid had formed. An X-ray powder photograph of this showed it to be identical with iridium pentafluoride.⁵⁷

2.3.6 Reactions of the Hexafluorides of Osmium Iridium and Platinum with Nitric Oxide

(i) General

The reaction of nitric oxide with the three hexafluorides was followed tensimetrically both in solid-gas and gas-gas phases. The identity of the residual gas in all these cases was established by its infrared spectrum. It was found to be nitric oxide only, in all cases. X-ray powder photographs were taken to characterize the solid products.

The gas-gas product in each case was heated with excess NO at 80° for two hours to check whether any more NO was consumed by the product to change to a 2:1 adduct.

The reaction of NO with these hexafluorides was also carried out in tungsten hexafluoride solutions, the procedure being similar to that described in the reaction of NO and OsOF₅ (Section 2.2.2). The product in each case was characterized by analysis, magnetic measurements and X-ray powder photographs.

(ii) Osmium hexafluoride and nitric oxide

(a) Tensimetric titrations

The tensimetric titrations of NO with OsF₆ gave a lilac tinted white product in all the cases. The results

of the titrations are shown below.

	solid-gas reaction		gas-gas reaction	
	I	II	I	II
OsF ₆ , pr., (mm.)	96.2	108.3	122.0	98.0
Initial NO, pr., (mm.)	103.0	160.5	178.0	142.0
Residual NO, pr., (mm.)	6.0	52.0	58.0	47.0
Combining ratio, NO/OsF ₆	1.00:1	1.00:1	0.98:1	0.97:1

To the adduct from gas-gas reaction I 82.0 mm. of NO was added and the mixture heated at 80° for 2 hours. 75 mm. of NO was left unreacted. The stoichiometry of the final adduct was thus 1.04:1 (NO: OsF₆). There was no change in the solid phase as shown by the identity of the X-ray powder photographs of the adduct before and after heating with excess NO.

(b) Preparation on a large scale.

The reactions of OsF₆ with NO were also done on a large scale in a glass apparatus. Osmium hexafluoride was condensed into a reaction bulb followed by the condensation of excess NO into the same bulb. The reaction bulb was then opened to the atmosphere through two glass traps cooled in liquid oxygen. The bulb was then warmed to room temperature when NO and OsF₆ reacted giving a lilac tinted white solid. The bulb containing the product was drawn off under vacuum.

(c) Reaction of NO with OsF₆ in WF₆.

The reaction of NO with OsF₆ in liquid tungsten hexafluoride gave a white solid product.

(d) Analysis.

The synthesis of the product from NO and OsF₆

in 1:1 ratio established the formula NOOsF_6 .

(e) X-ray data.

The X-ray powder photographs of the products of the reactions of NO and OsF_6 done in various conditions were identical with one another. The X-ray powder photograph was indexed on a cubic CsCl type unit cell as shown in Table XII
 $a = 10.126 \pm 0.002 \text{\AA}$, $U = 1038.3 \text{\AA}^3$ and $Z = 8$.

(f) Magnetic data

The magnetic susceptibility was found to obey the Curie-Weiss law with $\theta = 22^\circ$ in the range 77° to 300°K with $\mu_{\text{eff}} = 3.36 \text{ B.M.}$ at 297°K . The magnetic data are shown in Table XIII and the plot of $1/\chi_A$ versus T is shown in Figure 15.

TABLE XII

X-Ray Powder Data for NOOsF_6

hkl	Calc.	<u>$1/d^2$</u>	Obs.	Relative Intensity
200	0.0390		0.0401	8
220	0.0780		0.0797	10
222	0.1170		0.1192	5
321	0.1365		0.1391	1
400	0.1560		0.1584	4
411, 300	0.1755		0.1784	1
420	0.1950		0.1979	7
332	0.2145		0.2183	2
422	0.2340		0.2372	9
431, 510	0.2535		0.2570	1
440	0.3121		0.3150	6

(cont'd)

TABLE XII (cont'd)

hkl	Calc.	$\frac{1}{d^2}$	Obs.	Relative Intensity
442,600	0.3511		0.3542	8
620	0.3901		0.3931	7
622	0.4291		0.4323	7
444	0.4681		0.4712	4
640	0.5071		0.5100	7
642	0.5461		0.5491	8
651,732	0.6046		0.6074	1
800	0.6242		0.6260	2
820,644	0.6631		0.6658	7
822,600	0.7021		0.7055	6
662	0.7411		0.7431	5
840	0.7802		0.7835	6
842	0.8192		0.8221 α_1	7
			0.8215 α_2	3
664	0.8582		0.8602 α_1	5
844	0.9362		0.9396 α_1	4
860,10 0 0	0.9752		0.9773 α_1	5
862,10 2 0	1.0142		1.0171 α_1	7
			1.0166 α_2	3
666,10 2 2	1.0532		1.0558 α_1	5
			1.0551 α_2	2
864,10 4 0	1.1312		1.1330 α_1	7
			1.1339 α_2	3
10 4 2	1.1702		1.1722 α_1	6
			1.1717 α_2	
880	1.2482		1.2491 α_1	1

(cont'd)

TABLE XII (cont'd)

hkl	Calc.	$\frac{1}{d^2}$	Obs.	Relative Intensity
882, 10 4 4	1.2872		1.2885 α_1 1.2885 α_2	6 2
866, 10 6 0	1.3263		1.3281 α_1 1.3277 α_2	6 3
10 6 2	1.3653		1.3665 α_1 1.3661 α_2	6 3
844, 12 0 0	1.4043		1.4051 α_1 1.4046 α_2	5 2
12 2 0	1.4433		1.4436 α_1 1.4438 α_2	3 1
12 2 2, 10 6 4	1.4823		1.4832 α_1 1.4826 α_2	7 5
12 4 0	1.5603		1.5604 α_1 1.5599 α_2	3 1
12 4 2, 10 8 0 886	1.5993		1.5994 α_1 1.5992 α_2	7 6
10 8 2	1.6383		1.6383 α_1 1.6383 α_2	6 5

TABLE XIII

Magnetic Data[†] for NOOsF₆

(a) Increasing temperature			(b) Decreasing temperature		
T°K	$\chi_A(\text{obs.})$	$[\chi_A(\text{obs.}) - \chi_A(\text{ideal})^*]$	T°K	$\chi_A(\text{obs.})$	$[\chi_A(\text{obs.}) - \chi_A(\text{ideal})^*]$
77.1	16,213	458	296.3	4,717	-151
83.5	14,535	-255	273.0	5,078	-176
95.2	13,369	70	253.3	5,763	132
107.4	11,434	-601	233.2	6,057	-20
121.4	10,492	-359	213.6	6,635	51
139.5	9,643	17	193.6	7,343	145
156.4	8,864	155	174.2	7,998	84
173.2	8,119	164	154.5	8,944	141
192.8	7,347	122	137.0	9,870	91
213.4	6,695	105	121.6	10,461	-374
233.6	6,167	100	109.2	11,183	-685
253.4	5,763	134	95.7	12,948	-294
273.5	5,402	157	85.0	14,696	116
297.1	4,717	-139	77.1	16,300	545

* Curie-Weiss law obedience $\theta = 22^\circ$ † The data in columns for χ_A are 10^6 times the absolute values in c.g.s. units/mole.

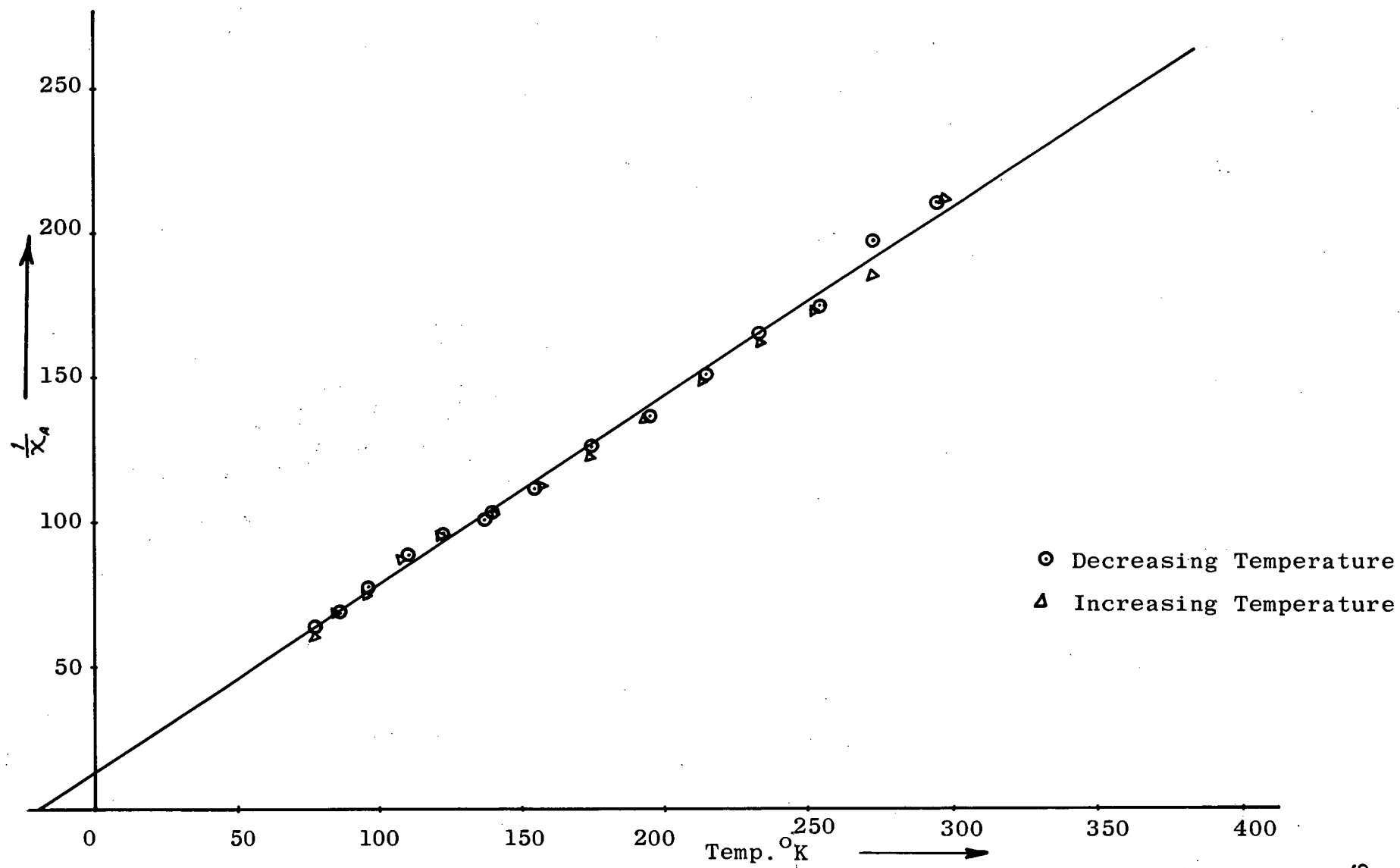


Figure 15. Plot of $1/\chi_A$ vs. T for NOOsF_6

(iii) Iridium hexafluoride and nitric oxide

(a) Tensimetric titrations.

The solid products from tensimetric titrations of NO and IrF_6 were white to light yellow in colour. The results of the titrations are summarized below. The identities of the residual gases were established by their infrared spectra.

	Solid-gas reaction		Gas-gas reaction	
	I	II	I	II
Initial IrF_6 pr., mm.	69.0	116.0	68.0	70.0
Initial NO pr., mm.	69.0	184.0	89.0	145.5
Residual IrF_6 pr., mm.	16.0	0	0	0
Residual NO pr., mm.	0	40.0	12.0	34.5
Combining ratio, NO/ IrF_6	1.30:1	1.24:1	1.13:1	1.58:1

To the adduct from gas-gas reaction I 95.0 mm. of NO was added and the mixture heated at 80° for two hours, 30 mm. of NO being consumed. It was further heated for two hours and another 22 mm. of NO was consumed. These consumptions of NO brought the ratio of NO: IrF_6 in the final adduct to 1.89:1.

The X-ray powder diffraction patterns of all the reaction products were complex but were similar to one another. In the complex pattern a cubic pattern similar to that of NOOsF_6 was readily detectable. The relative intensity of the cubic pattern as compared to that of another pattern present varied from product to product. The cubic pattern was very weak in the product of the composition $(\text{NO})_{1.9}\text{IrF}_6$. The strong pattern due to another phase resembled that of $(\text{NO})_2\text{PtF}_6$ (q.v.).

(b) Reactions of NO with IrF₆ in WF₆

The reaction of NO with IrF₆ in liquid tungsten hexafluoride gave a white solid, the characterization of which is given in following sections.

(c) Analysis

The compound was analysed by pyrohydrolysis. (Found: N, 4.15; F, 33.43; and Ir, 57.16%. NOIrF₆ requires N, 4.16, F, 33.91; Ir, 57.17%.

(d) X-Ray data

The powder photograph of the solid product from the WF₆ reaction was indexed on a cubic CsCl pattern as shown in Table XIV with unit cell size, $a = 10.114 \pm 0.002\text{\AA}$, $U = 1034.6$ and $Z = 8$. The pattern was identical with that present in the complex pattern of the NO- rich adducts formed in the tensimetric titrations.

TABLE XIV

hkl	Calc.	<u>1/d²</u>	Obs.	Relative Intensity
200	0.0391		0.0398	8
220	0.0782		0.0792	10
222	0.1173		0.1186	5
321	0.1368		0.1387	1
400	0.1564		0.1577	4
411,330	0.1759		0.1776	1
420	0.1955		0.1971	7
332	0.2150		0.2163	2
422	0.2346		0.2363	8

(cont'd)

TABLE XIV (cont'd)

hkl	Calc.	$\frac{1}{d^2}$	Obs.	Relative Intensity
431,510	0.2541		0.2562	1
440	0.3128		0.3149	6
442,600	0.3519		0.3540	8
620	0.3910		0.3929	7
622	0.4301		0.4322	7
444	0.4692		0.4700	4
640	0.5083		0.5093	7
642	0.5474		0.5495	8
800	0.6256		0.6275	1
644,820	0.6647		0.6662	7
822,660	0.7038		0.7059	6
662	0.7429		0.7441	5
840	0.7820		0.7831	6
842	0.8211		0.8222	7
664	0.8602		0.8608	5
844	0.9384		0.9395	4
860,10 0 0	0.9775		0.9778	5
862,10 2 0	1.0166		1.0168	6
666,10 2 2	1.0557		1.0555	5
864,10 4 0	1.1339		1.1349 α_1	7
10 4 2	1.1730		1.1725 α_1 1.1709 α_2	6 2
880	1.2512		1.2519 α_1	vw
882,10 4 4	1.2903		1.2907 α_1 1.2907 α_2	6 2

(cont'd)

TABLE XIV (cont'd)

hkl	Calc.	$\frac{1}{d^2}$	Obs.	Relative Intensity
866, 10 6 0	1.3294		1.3297 α_1 1.3279 α_2	6 2
10 6 2	1.3685		1.3699 α_1 1.3690 α_2	6 3
12 0 0	1.4076		1.4087 α_1 1.4077 α_2	5 2
12, 20	1.4467		1.4470 α_1 1.4452 α_2	3 1
10 6 4, 12 2 2	1.4858		1.4864 α_1 1.4850 α_2	7 5
12 4 0	1.5640		1.5639 α_1 1.5630 α_2	3 1
12 4 2 10 8 0, 866	1.6031		1.6033 α_1 1.6030 α_2	7 6
10 8 2	1.6422		1.6420 α_1 1.6424 α_2	6 5

(e) Magnetic properties

The magnetic susceptibility of the sample was measured over the temperature range 77°-298°K. It was found to show nearly temperature-independent paramagnetism as shown in Table XV with $\mu_{\text{eff}} = 1.23$ B.M. at 298°K.

TABLE XV

Magnetic Data for NOIrF₆

Temp. °K	$\chi_A(\text{obs.}) \times 10^6$ c.g.s. units	Temp. °K	$\chi_A(\text{obs.}) \times 10^6$ c.g.s. units
77.1	696	204.2	686
100.5	695	242.3	647
121.1	694	282.1	628
165.7	641	298.0	636

(iv) Platinum hexafluoride and nitric oxide

(a) Tensimetric titrations

The colour of the products of titrations of NO with PtF_6 varied from white to yellow. Usually a mixture of white and yellow materials was obtained in the solid-gas reaction. The identity of the residual gas was established by IR spectroscopy. The results of the titrations are tabulated below.

	Solid-gas reaction			Gas-gas reaction		
	I	II	III	I	II	III
PtF_6 pr., (mm.)	72.1	54.5	48.0	43.0	71.5	48.5
Initial NO pr., (mm.)	130.0	105.5	98.7	120.5	147.5	120.5
Residual NO pr., (mm.)	37.2	9.5	11.0	74.5	77.2	53.0
Combining ratio, NO/ PtF_6	1.28:1	1.76:1	1.83:1	1.07:1	0.98:1	1.39:1

The tensimetric titrations of NO and PtF_6 in the solid-gas reaction showed the combining ratio to vary from 1.3:1 to 1.8:1. X-ray powder photographs of the adducts from solid-gas reactions had a similar complex pattern to that of the $\text{NO}(\text{IrF}_6)_x$ adducts. A cubic pattern similar to that of NOOsF_6 was easily recognized, however, the cubic pattern was indexed on the basis of a cubic CsCl type unit cell with $a = 10.12 \pm 0.01 \text{ \AA}$.

In gas-gas reactions the ratio was found to vary from 1:1 to 1.4:1. The X-ray powder photograph of the 1:1 adduct was indexed on the basis of a rhombohedral unit cell as

shown in Table XVI with $a = 5.03\text{\AA}$, $\alpha = 97.6^\circ$ and $U = 123.5\text{\AA}^3$. The X-ray powder photograph of the adduct richer in NO was complex and contained the above rhombohedral pattern as well.

TABLE XVI

X-Ray Powder Data for NOPtF_6 (rhombohedral)

hkl	Calc. $\frac{1}{d^2}$	Obs.	Relative Intensity
100	0.0412	0.0414	10
10 $\bar{1}$	0.0698	0.0699	8
110	0.0950	0.0956	8
11 $\bar{1}$	0.1110	0.1111	6
200	0.1648	0.1644	5
20 $\bar{1}$	0.1808	0.1804	4
21 $\bar{1}$	0.2346	0.2349	9
20 $\bar{2}$	0.2792	0.2795	4
211	0.3092	0.3157	5
21 $\bar{2}$	0.3204		
300	0.3708	0.3689	5
310	0.4498	0.4491	5
31 $\bar{2}$	0.5138	0.5141	3
311	0.5414	0.5391	1
31 $\bar{3}$	0.6694	0.6691	1

The adduct from gas gas reaction II was heated with 100.6 mm. of NO at 80° for two hours in the reaction bulb. The pressure of residual NO was 31.6 mm. The consumption of NO indicated the stoichiometry of the final adduct to be 1.95:1 (NO:PtF₆). The X-ray powder pattern of this adduct was found to

be present in the complex pattern of the above mentioned NO-rich adducts from solid-gas and gas-gas reactions.

(b) Reaction of NO with PtF_6 in WF_6 .

The reaction of NO with PtF_6 in liquid tungsten hexafluoride was done in a slightly modified way as Kel-F traps were found to crack while handling solid PtF_6 . Platinum hexafluoride vapour carried in a stream of nitrogen, and a stream of NO, were bubbled simultaneously through liquid tungsten hexafluoride. The product was slightly yellow in colour. The characterization was done as follows.

(c) Analysis.

The compound was analysed by pyrohydrolysis. (Found: F, 30.72; Pt, 54.78%. NOPtF_6 requires F, 33.62; Pt, 57.53%. $(\text{NO})_2\text{PtF}_6$ requires F, 30.88; Pt, 52.86%).

(d) X-Ray data.

The X-ray powder pattern showed two mixed phases, a weak cubic pattern (identical to that found for the solid-gas reaction product) and another, a strong pattern which was indexed on the basis of a hexagonal unit cell, $a = 10.01\text{\AA}$, $c = 3.53$ and $U = 306.3\text{\AA}^3$, the data for which are given in Table XVII. This strong pattern was identical with that of the 1.95:1 adduct of NO and PtF_6 mentioned earlier. A remarkable feature of these photographs was that they contained sharp and diffuse lines.

(e) Magnetic data.

The g. susceptibility of the sample was found to be 0.747×10^{-6} c.g.s. units at room temperature (which gives

TABLE XVII

X-Ray Powder Data for $(\text{NO})_2\text{PtF}_6$

hkl	Calc.	$\frac{1}{d^2}$	Obs.	Relative Intensity	
110	0.0399		0.0399	10	S
200	0.0532		0.0539	6	D
210	0.0931		0.0942	4	D
101	0.0935				
300	0.1197		0.1193	8	S
111	0.1201				
201	0.1330		0.1344	6	D
220	0.1596		0.1599	4	S
301	0.1995		0.2011	6	D
400	0.2128		0.2150	4	D
311	0.2531		0.2548	3	D
320	0.2527				
410	0.2793		0.2801	5	S
401	0.2930		0.2915	3	D
002	0.3208		0.3204	1	D
330	0.3591		0.3580	4	S
112	0.3603				
411	0.3595				
202	0.3740		0.3735	1	D
420	0.3724				
302	0.4405		0.4406	2	D
331	0.4393				
421	0.4526		0.4557	2	D
520	0.5188		0.5172	2	D
402	0.5332		0.5335	4	S
610	0.5719		0.5754	4	S
322	0.5735				
431	0.5723				

(cont'd)

TABLE XVII (cont'd)

hkl	Calc.	$\frac{1}{d^2}$	Obs.	Relative Intensity	
--	--		.6123	2	
512	0.7349				
701	0.7319		0.7339	w	D
531	0.7319				
710	0.7581		0.7566	1	D
--	--		0.8343	vw	D
800	0.8512		0.8496	1	D

the values of $\mu = 0.73$ or 0.81 B.M. on the basis of a molecular formula NOPtF_6 or $(\text{NO})_2\text{PtF}_6$ respectively).

(f) Reaction with KF in water.

A small amount of the product from the tungsten hexafluoride reaction was poured into a saturated solution of potassium fluoride in water. The yellow solid which precipitated was filtered and washed. The X-ray powder photograph of the solid was identical with that of K_2PtF_6 .

(g) Preparation of pure NOPtF_6

The pure cubic form of NOPtF_6 was prepared by Mr. S. Beaton of these laboratories using the novel reaction: $\text{NOF} + \text{PtF}_6 = \text{NOPtF}_6 + 1/2 \text{F}_2$.⁶² The X-ray powder photograph of the bright yellow product was identical with the cubic pattern observed in the photograph of the $\text{NO} + \text{PtF}_6$ products. Mr. Beaton has indexed the powder photograph of the pure material on the basis of a CsCl type cubic unit cell, $a = 10.112 \pm .002 \text{\AA}$, $U = 1033.9 \text{\AA}^3$, $Z = 8$.

(h) Treatment of pure cubic NOPtF_6 with excess NO .

Some pure NOPtF_6 , kindly supplied by Mr. Beaton, was taken in a glass reaction bulb and treated with excess NO . The colour of the solid changed from yellow to brown. The X-ray powder photograph was identical with the photograph indexed on the hexagonal pattern mentioned earlier.

2.3.7 Reactions of the Hexafluorides of Osmium, Iridium and Platinum with Sulphur Tetrafluoride

The reactions of OsF_6 , IrF_6 and PtF_6 with SF_4 were followed tensimetrically in the usual way both in solid-gas and gas-gas reactions.

Large scale reactions of these hexafluorides with sulphur tetrafluoride were also carried out. They were done by condensing the hexafluoride in a glass bulb then condensing an excess of sulphur tetrafluoride in the same bulb. The bulb was then opened to the atmosphere through two glass traps cooled in liquid oxygen. The reaction bulb was warmed to room temperature and the reaction between hexafluoride and SF_4 took place. In some cases the bulb was slightly warmed with a hot air blower to complete the reaction. Excess SF_4 was pumped off and the bulb was drawn off.

(i) Osmium hexafluoride and sulphur tetrafluoride

(a) Solid-gas reaction.

A known pressure of OsF_6 vapour in a known volume was condensed in the reservoir of a monel infrared gas cell followed by the condensation of a known quantity of SF_4 . The reservoir was warmed to room temperature. The pressure of

residual gases was nearly the sum of the pressures of OsF_6 and SF_4 taken. The infrared spectrum of the residual gases showed the presence of OsF_6 and SF_4 .

(b) Gas-gas reaction.

A gas-gas reaction of OsF_6 and SF_4 was done in a glass bulb. No visible reaction seemed to occur and the IR spectrum of the residual gases again showed the presence of SF_4 and OsF_6 .

(c) OsF_6 and liquid SF_4 .

The reaction of solid OsF_6 with liquid SF_4 was exothermic, starting before the reaction mixture had attained room temperature. After the reaction was complete, the reaction bulb contained a white precipitate in a deep yellow orange liquid. The colour of the solution indicated that the product was possibly soluble in liquid SF_4 . On pumping out excess SF_4 a white solid remained.

(d) Analysis.

The analysis of the product was done by the closed system alkaline hydrolysis and osmium, sulphur and fluorine were estimated in the hydrolysed solution. Because of the presence of sulphite ions in the hydrolysed solution the method of analysis was slightly modified. Osmium forms a sulphite complex with sulphite ions and hence the destruction of sulphite ions was necessary in order to precipitate osmium completely. This was achieved by oxidizing sulphite to sulphate by addition of hydrogen peroxide solution in an aliquot of hydrolysed solution. Osmium was then precipitated as usual with hydrazine

hydrate.

Fluorine and sulphur were estimated in the filtrate from the estimation of osmium as described in Section 2.1.3. Fluorine was also estimated by the Willard and Winter distillation of an aliquot of hydrolysed solution followed by precipitation as PbClF . (Found: F, 42.00; S, 7.46; Os, 47.82%. $\text{SF}_4, \text{OsF}_5$ requires F, 43.48; S, 8.14; Os, 48.36%).

(e) Magnetic data

The magnetic susceptibility was measured at room temperature only. $\mu_{\text{eff}} = 3.46$ B.M. at 294°K .

(f) X-Ray data.

The X-ray powder pattern was similar to that of NOOsF_6 . Lines only up to $\theta = 40^\circ$ were observed on the pattern even with long exposures of the sample, hence the unit cell dimensions were not found with great accuracy. However, a crude Nelson Riley plot gave the unit cell size $a = 11.162 \pm 0.004 \text{ \AA}$, $U = 1390.6 \text{ \AA}^3$, $Z = 8$. The X-ray data are shown in Table XVIII.

(ii) Iridium hexafluoride and sulphur tetrafluoride

(a) Gas-gas reaction.

No visible reaction seemed to occur in the attempted gas-gas reaction of SF_4 and IrF_6 in a glass bulb. The infrared spectrum of the residual gases showed the presence of both SF_4 and IrF_6 .

(b) Solid-gas reaction

In the attempt of solid-gas reaction of SF_4 and IrF_6 some yellowish white solid was found to form at the

bottom of the reaction bulb. The infrared spectrum of the residual gases showed the presence of both SF_4 and IrF_6 . It seemed that a reaction had taken place where solid IrF_6 was in contact with excess of liquid SF_4 .

(c) IrF_6 and liquid SF_4

This reaction was more exothermic than the reaction of solid OsF_6 with liquid SF_4 as indicated by the reaction bulb becoming quite hot. After the completion of the reaction, the bulb contained a buff coloured solid in a pale pink solution. The colour of the solution indicated that the product was possibly soluble in liquid SF_4 . On pumping off excess SF_4 a pale yellow to buff solid was left.

(d) Analysis

The analysis was done by pyrohydrolysis. Sulphur and fluorine were estimated in the distillate as described in Section 2.1.3 (Found: F, 43.53; S, 7.46; Ir 47.86%. $\text{SF}_4, \text{IrF}_5$ requires F, 43.26, S, 8.11; Ir 48.62%).

(e) Magnetic data.

The magnetic susceptibility measurement at room temperature gave a value of $\mu_{\text{eff}} = 1.51$ B.M.

(f) X-Ray data.

The X-ray powder photograph was almost identical with that of $\text{SF}_4, \text{OsF}_5$. Lines only up to $\theta = 40^\circ$ were observed. In the visual comparison of the photographs of $\text{SF}_4, \text{OsF}_5$ and $\text{SF}_4, \text{IrF}_5$ a few (two or three) lines near $\theta = 40^\circ$ indicated that the unit cell size of the latter was smaller than that of the former. Because of the very low intensities of these lines, they could not be measured accurately. The unit cell was

cubic as shown in Table XVIII with $a = 11.162 \pm .004 \text{ \AA}$ $U = 1390 \text{ \AA}^3$, $Z = 8$.

(iii) Platinum hexafluoride with sulphur tetrafluoride

(a) Gas-gas reaction

Unlike OsF_6 and IrF_6 , PtF_6 reacted with SF_4 in a gas-gas reaction, producing a brown solid. The sample was poorly crystalline and very few lines were seen on the X-ray powder photograph which seemed to have some similarity to the pattern of $(\text{NO})_2\text{PtF}_6$.

(b) PtF_6 with liquid SF_4

Solid PtF_6 seemed to react with liquid SF_4 at very low temperature, in fact the reaction seemed to occur while SF_4 was being condensed on the solid PtF_6 . On warming to room temperature a chocolate coloured solid was seen in a colourless liquid. The colourless liquid indicated that the product was not soluble in liquid SF_4 . On pumping off excess SF_4 a buff solid remained.

(c) Analysis

The analysis was done by pyrohydrolysis. (Found: F, 35.48; S, 6.17; Pt, 52.54%. $\text{SF}_4, \text{PtF}_5$ requires F, 42.93; S, 8.05; Pt, 49.02%. $(\text{SF}_4)_2 \text{PtF}_4$ requires F, 46.78; S, 13.15; Pt, 40.06%).

(d) Magnetic data.

The magnetic susceptibility measurements were done only at room temperature. $\chi_g = 0.877 \times 10^{-6}$ c.g.s. units at 295°K . (This gives 1.00 B.M. for μ_{eff} using $\text{SF}_4, \text{PtF}_5$ as molecular formula).

(e) X-Ray photograph.

The product was amorphous. No lines were seen on the X-ray powder photograph.

2.3.8 Nitrosyl Hexafluoroniobate and -tantalate

NONbF_6 and NOTaF_6 were prepared by the reaction of Nb_2O_5 and Ta_2O_5 with NOCl and BrF_3 . The apparatus and methods used were similar to those given under the preparation of NOOsO_3F_3 . The only difference was that the oxides in this case were taken in the reaction bulb itself before joining it to the apparatus. Both NONbF_6 and NOTaF_6 were white solids.

(a) X-Ray data

The X-ray powder patterns of these two compounds were identical with each other and were similar to that of NOOsF_6 . They were indexed on the basis of cubic unit cells of CsCl type with $a = 10.22 \pm .004 \text{ \AA}$ and $Z = 8$ for both. The X-ray data powder are given in Table XIX.

2.3.9 Magnetic Properties of Platinum Hexafluoride

A sample of platinum hexafluoride was sealed in a 4 mm. diam. quartz tube and the magnetic susceptibility was measured over the temperature range 77° to 297°K . The molar susceptibility was found to be nearly temperature-independent. The magnetic data are given in Table XX. The value of μ_{eff} at 296°K was found to be 1.30 B.M.

TABLE XVIII

X-Ray Powder Data for SF_3OsF_6 and SF_3IrF_6

SF_3OsF_6				SF_3IrF_6		
hkl	$1/d^2(\text{Calc})$	$1/d^2(\text{Obs.})$	Relative Intensity	$1/d^2(\text{Obs.})$	Relative Intensity	
		0.0262	1	0.0263	1	β_{200}
200	0.0321	0.0323	8	0.0321	8	
		0.0419 *	1	0.0423*	1	
		0.0526	2	0.0532	2	β_{220}
220	0.0642	0.0646	10	0.0646	10	
		0.0744 *	1	0.0751 *	1	
222	0.0963	0.0974	6	0.0975	6	
				0.1039*	vw	
		0.1170*	vw	0.1174	vw	
400	0.1284	0.1293	5	0.1297	5	
420	0.1605	0.1618	6	0.1622	6	
422	0.1926	0.1935	7	0.1945	7	
		0.2268 *	vw	0.2309 *	vw	
521	0.2408	0.2418	1	0.2436	1	
440	0.2568	0.2575	5	0.2586	5	
442, 600	0.2889	0.2901	7	0.2906	7	
620	0.3210	0.3216	5	0.3232	5	
				0.3403*	vw	
622	0.3531	0.3545	4	0.3550	4	
				0.3777 *	w	
444	0.3852	0.3871	1	0.3884	1	
640	0.4173	0.4186	4	0.4200	4	(cont'd)

* The intensities of these lines vary between photographs of different specimens and hence are assumed to be lines due to some impurities.

TABLE XVIII (cont'd)

hkl	$1/d^2(\text{Calc})$	$1/d^2(\text{Obs})$	Relative Intensity	$1/d^2(\text{Obs})$	Relative Intensity
642	0.4494	0.4514	6	0.4517	6
				0.4889*	vw
644, 820	0.5458	0.5477	3	0.5472	3
660, 822	0.5779	0.5787	1	0.5774	1
662	0.6100	0.6112	vw		
840	0.6421	0.6422	1		
842	0.6742	0.6761	1	0.6746	1

TABLE XIXX-Ray Powder Data for NONbF_6 and NOTaF_6

hkl	Calc.	$\frac{1}{d^2}$	Obs.	Relative Intensity
200	0.0383		0.0391	8
211	0.0574		0.0589	vw
220	0.0766		0.0776	10
310	0.0957		0.0948	w
222	0.1149		0.1164	5
321	0.1340		0.1358	1
400	0.1532		0.1545	4
330, 411	0.1723		0.1732	1
420	0.1915		0.1933	7
332	0.2106		0.2120	2
422	0.2298		0.2313	8

(cont'd)

TABLE XIX (cont'd)

hkl	Calc.	$\frac{1}{d^2}$	Obs.	Relative Intensity
431,510	0.2489		0.2506	1
440	0.3064		0.3081	6
442,600	0.3446		0.3464	8
620	0.3829		0.3851	7
622	0.4212		0.4230	7
631	0.4404		0.4389	w
444	0.4595		0.4615	4
640	0.4978		0.5003	7
642	0.5361		0.5385	8
732,651	0.5935		0.5937	w
800	0.6127		0.6146	1
644,820	0.6893		0.6915	7
660,822	0.6893		0.6915	6
662	0.7276		0.7304	5
840	0.7659		0.7676	6
842	0.8042		0.8058	7
664	0.8425		0.8429	5
844	0.9191		0.9206	4
860,10 0 0	0.9574		0.9589	5
862,10 2 0	0.9957		0.9964	6
666,10 2 2	1.0340		1.0325	4
864,10 4 0	1.1106		1.1124 *	6
10 4 2	1.1489		1.1505 *	6
880	1.2255		1.2259 *	w (cont'd)

*These lines are due to $\text{CuK}\alpha_1$. The corresponding α_2 lines were weak and hence could not be measured accurately.

TABLE XIX (cont'd)

hkl	Calc.	$\frac{1}{d^2}$	Obs.	Relative Intensity
882, 10 4 4	1.2637		1.2639*	6
866, 10 6 0	1.3021		1.3032*	6
10 6 2	1.3404		1.3409*	6
12 0 0	1.3786		1.3788*	5
12 2 0	1.4169		1.4171*	3
12 2 2, 10 6 4	1.4552		1.4563*	7
12 4 0	1.5318		1.5338*	3
12 4 2, 10 8 0, 886	1.5701		1.5707*	7
10 8 2	1.6084		1.6093*	5

TABLE XX

Magnetic Data for PtF_6

Set I		Set II	
Temp. °K	$\chi_A \times 10^6$ (c.g.s. units)	Temp. °K	$\chi_A \times 10^6$ (c.g.s. units)
77.1	740	77.1	721
92.8	702	92.2	707
107.6	698	107.1	697
122.3	706	122.8	697
138.9	702	140.6	702
156.1	708	157.2	701
171.3	714	173.1	707
191.2	714	191.2	708
208.0	715	209.2	715

(cont'd)

TABLE XX (cont'd)

Temp. °K	$\chi_A \times 10^6$ (c.g.s.units)	Temp. °K	$\chi_A \times 10^6$ (c.g.s.units)
225.9	714	227.4	701
242.9	713	243.7	714
261.0	720	259.9	713
278.0	721	277.8	711
296.2	711		

Chapter III

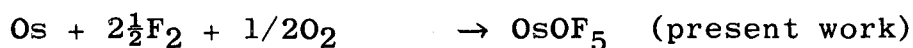
DISCUSSION

3.1 THE FLUORIDES AND OXYFLUORIDES OF OSMIUM3.1.1 Higher Oxidation States of Osmium

As expected of a transition metal, osmium shows a wide range of oxidation states in its compounds. Its electronic configuration is $(\text{Xe})5d^6 6s^2$ and all of the extra-xenon electrons can be involved in bonding as evidenced by the compounds OsO_4 and OsO_3F_2 .

Attempts to prepare higher simple fluorides of osmium than the hexafluoride have failed (though recently a very unstable heptafluoride of osmium has been reported⁶³). This instability, or absence, of higher simple fluorides than the hexafluoride, in spite of the existence of oxides and oxyfluorides which show oxidation states higher than 6 (e.g. OsO_4 , OsOF_5 and OsO_3F_2) is at first sight puzzling. This is particularly so in view of the fact that both oxygen and fluorine are usually able to excite the highest oxidation state of an element. A study of the osmium-oxygen-fluorine system has, however, better defined the attainable oxidation states and the factors which control them.

The nature of the compounds produced with varying proportions of oxygen and fluorine is shown below.



The above reactions show that the attainable formal oxidation state of osmium decreases as the proportion of fluorine in the oxidizing gases increases. It is seen that the maximum number of ligands around osmium is six; moreover, there is no other known example of osmium in an oxygen or fluorine environment having a coordination number greater than 6, so the oxidation limit for a fluoride may be supposed to have been imposed by a maximum coordination number of six for osmium. However, this could not exclude the possibility of OsO_2F_4 for which a very careful search was made in this work, but of which no trace was found. So the coordination limit does not seem to be the sole factor controlling the attainable oxidation states of osmium with oxygen and fluorine.

This behaviour can be rationalized if a distinction between real and formal oxidation states of a metal is made. The electron withdrawing power of an oxygen atom is supposed to be twice that of a fluorine in assigning the formal oxidation state. This seems unlikely in view of the low electron affinity of oxygen compared to fluorine. On the other hand if the electron withdrawing power of oxygen is taken to be only 1.5 times that of fluorine then the real oxidation state of osmium in OsO_4 is equated with that in OsF_6 . On this basis OsOF_5 and OsO_3F_2 would be equivalent to $\text{OsF}_{6.5}$. Also OsO_2F_4 would be equivalent to OsF_7 , both of which are unknown. In view of the instability of OsF_7 and the presumed instability of OsO_2F_4 it can be taken that OsF_8 will be extremely unstable.

3.1.2 Osmium Oxide Pentafluoride

Osmium oxide pentafluoride is of special interest in that it is the first simple compound of osmium to show a formal oxidation state of +7. It has only one non-bonding electron. As such it is electronically related to rhenium hexafluoride, although in its molecular symmetry it more closely resembles the only previously known MOF₅ compound, ReOF₅.⁶⁵

Since the oxygen atom is similar in size to fluorine and since the non-bonding d-electron should not show any steric activity, the molecule OsOF₅ is expected to be similar in size and shape to OsF₆. A complete crystal structure analysis of the orthorhombic form (stable below 32.5°) has been done by Bartlett and Trotter⁶⁶ and has been described in detail. It shows that the structure consists of discrete, approximately octahedral OsOF₅ molecules (Table XXI and Figure 16). It has not been possible to distinguish between oxygen and fluorine atoms on the basis of the electron density distribution alone because of the high scattering factor of the osmium atoms.

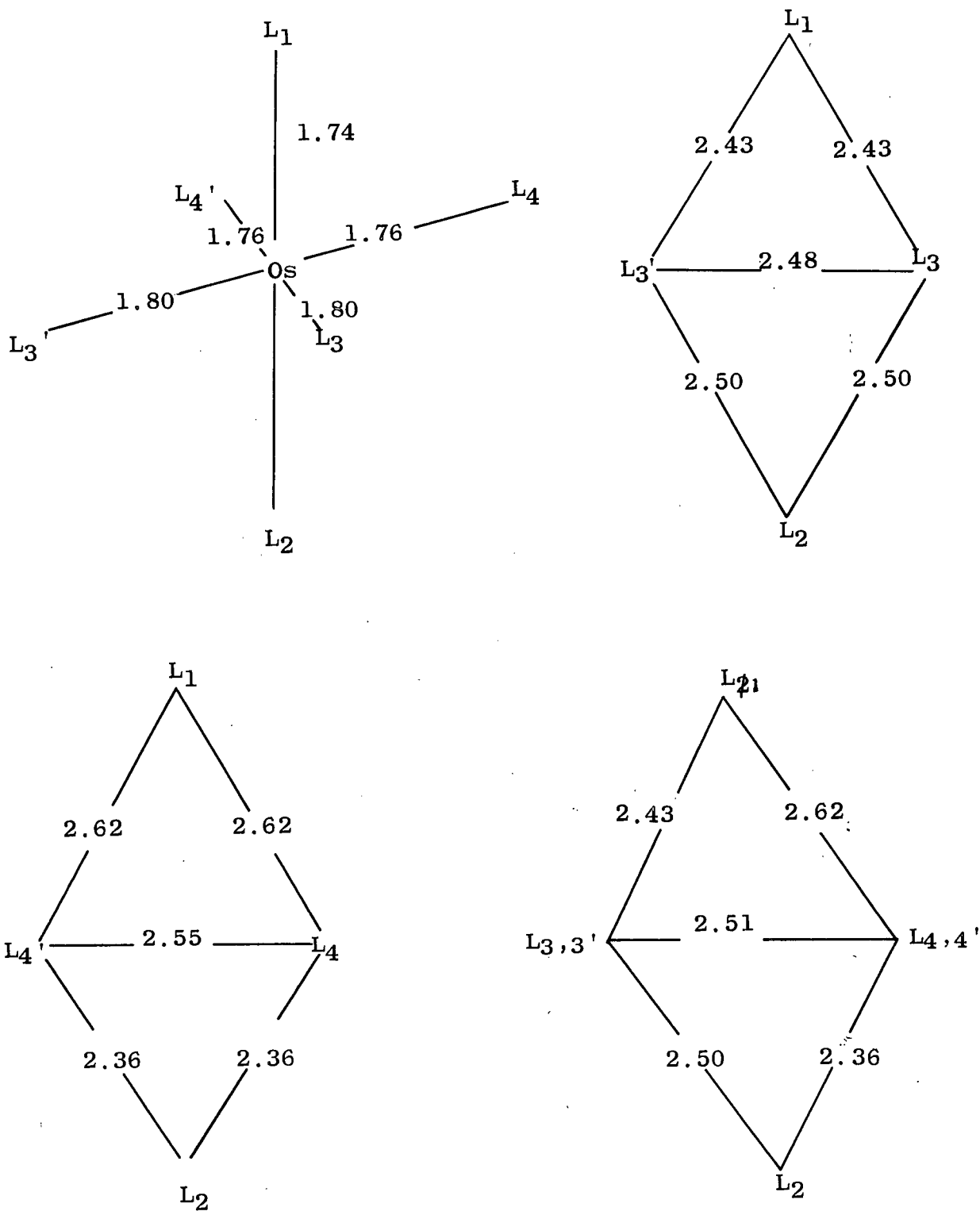
A non-centrosymmetric structural unit is indicated by the inequality of the diametrically opposed triangular faces of the approximately octahedral molecular unit of OsOF₅ which is represented in Figure 16. In particular the sides of face 2,3,3' are 2.50, 2.50 and 2.48⁰Å and of face 1,4,4' are 2.62, 2.62 and 2.55⁰Å.

TABLE XXI

Intramolecular Distances with Standard Deviations (\AA)
and Valency Angles (degrees) for OsOF₅ Molecule.

Os - 1	1.74 ± 0.03	1 - Os - 2	176
Os - 2	1.71 ± 0.03	1 - Os - 3	87
Os - 3	1.80 ± 0.03	1 - Os - 4	97
Os - 4	1.75 ± 0.03	2 - Os - 3	91
		2 - Os - 4	86
1 - 3	2.43 ± 0.04	3 - Os - 4	90
1 - 4	2.62 ± 0.04	3 - Os - 3'	87
2 - 3	2.50 ± 0.04	3 - Os - 4'	175
2 - 4	2.36 ± 0.04	4 - Os - 4'	93
3 - 4	2.51 ± 0.04	1 - 3 - 2	89
3 - 3'	2.48 ± 0.04	1 - 4 - 2	88
4 - 4'	2.55 ± 0.04	3 - 4 - 4'	89
		4 - 3 - 3'	91

Position 1 has been assigned to the oxygen ligand on the basis of this asymmetry. Since oxygen has a greater van der Waals radius than fluorine as a consequence of its lower nuclear charge, the oxygen-fluorine distances are anticipated to be greater than the corresponding fluorine-fluorine distances. The ligand in position 1 is generally further from its immediate ligand neighbours than the ligands in positions 2,3,3',4 and 4' and so ligand 1 is considered most likely to be oxygen.

Figure 16. The Molecular Structure of OsOF_5

It is significant that all the Os-ligand distances are shorter than the Os-F distance of $1.831\overset{\text{O}}{\text{\AA}}$ given⁵ for the gas phase OsF_6 molecule. This indicates that the polarizing power of the osmium in OsOF_5 is greater than in OsF_6 . The shorter bond distances in OsOF_5 will in part be responsible for the smaller volume of the orthorhombic oxyfluoride ($\text{U}_{\text{obs.}}/\text{Z} = 103.8\overset{\text{O3}}{\text{\AA}^3}$) compared with the orthorhombic hexafluoride³² ($\text{U}_{\text{obs.}}/\text{Z} = 105.7\overset{\text{O3}}{\text{\AA}^3}$). The greater density of the oxide pentafluoride, however, will also be due in part to the dipolar interactions of the molecules.

The single, unpaired, valence electron of the OsOF_5 molecule is presumably non-bonding, and its most probable location, because of the greater polarizability of the oxygen compared with the fluorine ligands, is in the plane normal to Os-O axis. With the oxygen ligand in position 1 (Figure 16) the lowest energy orbital available for the electron is the atomic d-orbital which has its nodes approximately coincident with the 3, 3', 4 and 4' locations of the fluorine ligands. A consequence of this assignment would be a weakening of the $p_{\pi} - d_{\pi}$ bonding in the plane, because of the anti-bonding influence of the electron. Therefore the Os-F bonds normal to the Os-O axis in OsOF_5 are anticipated to be longer than the unique Os-F bond. The atomic assignments give bond lengths in accord with this.

Osmium oxide pentafluoride resembles the related rhenium compound, ReOF_5 ^{65,67} in various properties. The oxide pentafluoride would also be expected to resemble the corresponding hexafluoride on account of the similarity in size of

oxygen and fluorine. In Table XXII some thermodynamic data for ReF_6 ,¹⁶ ReOF_5 ,⁶⁷ and OsF_6 ,¹⁶ derived from vapour pressure temperature studies, are compared with the data derived for OsOF_5 in this work.

TABLE XXII

Comparison of Some Thermodynamic Data for ReF_6 ,

	ReOF_5 , OsF_6 and OsOF_5			
	ReF_6 ¹⁶	ReOF_5 ⁶⁷	OsF_6 ¹⁶	OsOF_5 *
M.P. (°C)	18.7	40.8	33.4	59.2
B.P. (°C)	33.8	73.0	47.5	100.5
Transition pt. (°C)	-1.9	30.0	-0.4	32.5
Heat of fusion (cal./mole)	940	1220	1760	1623
Entropy of fusion ((cal./mole/deg.))	3.21	3.88	5.72	5.29
Latent heat of vap. of liquid ((cal./mole))	6,860	7,720	6,720	8,745
Latent heat of sublimation (above transition pt., ((cal./mole))	7,800	8,940	8,480	10,368
Entropy of vap. of liquid ((cal./mole/deg.))	22.3	22.3	21.0	23.4

*Present work.

As with the hexafluorides and ReOF_5 , OsOF_5 is not associated in the liquid phase, as is indicated by a value of 23.4 for Trouton's constant. The low value for the entropy of fusion of OsOF_5 is similar to the values of the hexafluorides of the 4d and 5d series^{16,23(b)} and ReOF_5 ,⁶⁷ which undergo transformation from the orthorhombic form to cubic form at higher

temperatures.^{29,23(b),6} The molecules in this form are presumed to have some rotational freedom.^{23(b),5,6}

The entropy of fusion of 5f-hexafluorides which do not undergo such a transformation is higher (~ 13 cal/mole/deg.)^{5,6} than that of 4d- and 5d- hexafluorides (~ 3 to 5 cal/mole/deg.).^{5,6}

Although the vapour pressure-temperature studies indicated that a solid-solid phase transition occurred in the neighbourhood of 30° and the entropy of fusion data indicated the existence of a cubic phase above this temperature, this remained to be established. Accordingly, X-ray powder photographs were taken above the microscopically observed transition point of 32.5° . The photographs established the higher temperature solid phase to be cubic.

The molecular volume of OsOF_5 in the cubic form is less than that of the cubic form of OsF_6 , just as the molecular volume of orthorhombic form of OsOF_5 is less than that of the orthorhombic OsF_6 . The volumes of the orthorhombic and cubic forms of OsOF_5 and some hexafluorides are shown in Table XXIII.

TABLE XXIII

Comparison of the Molecular Volumes of Orthorhombic and Cubic forms of PtF_6 , OsF_6 , IrF_6 and OsOF_5 .

Compound	PtF_6	OsF_6	IrF_6	OsOF_5
Cubic, \AA^3	119.7 ^{23(b)}	121.5 ²⁹	120.5 ³²	115.9
Orthorhombic, \AA^3	104.6 ³²	105.7 ³²	105.4 ³²	103.8
Difference, \AA^3	15.1	15.8	15.1	12.1

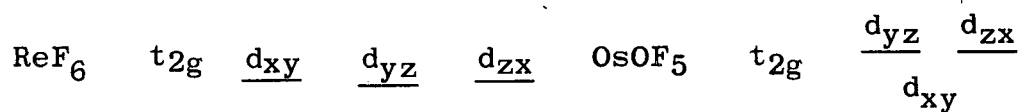
The osmium of OsOF_5 possesses one formally non-bonding d electron. For a d^1 system, the spin only value of the magnetic moment should be 1.73 B.M. However, the spin-orbit coupling constant, for Os (VII) should be large,⁶⁸ and with O_h symmetry the moment for a t_{2g}^1 system would be less than the spin only value.¹⁰ This situation is observed in the ReF_6 molecule, the low value of 0.51 B.M.⁶⁹ for the magnetic moment being attributed to the considerable spin-orbit coupling (4000 cm^{-1}). The susceptibility of OsOF_5 obeys the Curie-Weiss law and since the Weiss constant is small, $\theta = 6^\circ$, the magnetic moment is almost temperature-independent with $\mu_{\text{eff}} = 1.47$ B.M. This compares closely with the value for $[\text{ReOF}_5]^-$ salts and indeed with the moments for $[\text{WOX}_5]^{2-}$ salts as shown in Table XXIV.

TABLE XXIV

Magnetic Properties of Some d^1 Complexes

Complex	μ_{eff}	θ	Reference
$\text{Rb}_2[\text{WOCl}_5]$	1.55	18	70
$\text{Cs}_2[\text{WOCl}_5]$	1.49	12	70
$[(\text{CH}_3)_3\text{N}]_2[\text{WOCl}_5]$	1.35	6	70
$\text{Rb}_2[\text{WOBr}_5]$	1.37	-	71
$\text{Cs}_2[\text{WOBr}_5]$	1.55	20°	71
$\text{M}[\text{ReOF}_5]$	1.4	-	72
(M = K, Rb, Cs)			
OsOF_5	1.47	6	Present work

The higher value of the moment in these compounds compared with ReF_6 must be attributed to the non- O_h symmetry of the field about the transition metal, the energy splitting by the asymmetric field being at least comparable with the spin-orbit coupling. The highest symmetry permitted the osmium in OsOF_5 is C_{4v} . In a field of this symmetry the degeneracy of the t_{2g} orbitals would be removed. Since the oxygen ligand, by virtue of its smaller nuclear charge, is more polarizable than the fluorine ligands, it is presumed that the orbital in the plane normal to Os-O axis will be lowest in energy and the degenerate pair of orbitals in the planes containing the Os-O axis will be higher in energy. The d-orbital splitting accompanying the change from ReF_6 to OsOF_5 can be represented thus, as follows:



The location of the single non-bonding electron of OsOF_5 in the non-degenerate orbital is presumably responsible for the greater moment than observed for ReF_6 .

From the structure of OsOF_5 one would expect two fluorine resonances in the ^{19}F n.m.r., one due to the axial fluorine which would be a quintet and other due to equatorial fluorines, which would be a doublet. But the n.m.r. spectrum of OsOF_5 dissolved in WF_6 ²⁰ shows only one broad resonance to high field. The related diamagnetic compound, ReOF_5 ²⁰ shows the expected quintet and doublet. The resonance in OsOF_5 is in the region where, by analogy with ReOF_5 , the quintet of the

axial ^{19}F resonance should be observed. This peak is therefore presumed to be a smeared quintet. The anticipated stronger equatorial resonance is not observed, presumably because it is broadened by interaction of the ^{19}F equatorial nuclei with the unpaired electron localized in that plane. Assuming that the oxygen dominates as a π -bond donor and hence monopolizes the d_{yz} and d_{zx} orbitals (the Os-O axis being taken as z axis), the non-bonding unpaired electron will be confined to the d_{xy} orbital.

The broad, asymmetric e.s.r. absorption centred around $g \sim 2$ observed for a solution of OsOF_5 in tungsten hexafluoride was of no diagnostic value.

Due to the near octahedral symmetry of the OsOF_5 molecule, some similarity between the infrared spectrum of OsOF_5 and the spectra of related hexafluorides is expected. Indeed, as may be seen by reference to Figure 11, this is so. Of course, the spectra of the MOF_5 molecules are markedly similar as may be seen by reference to Figure 10.

Unambiguous assignment of C_{4v} fundamentals has not been made. The green colour of the compound renders the securing of a Raman spectrum impossible with the instruments presently available. However, some assignments have been made on the basis of pseudo octahedral symmetry. In O_h symmetry there are six fundamentals. Each of the O_h fundamental modes, except ν_1 , is resolved into two modes with the transition to C_{4v} symmetry. Thus $\nu_1(O_h) \rightarrow \nu_1(C_{4v})$; $\nu_2(O_h) \rightarrow \nu_2', \nu_2''(C_{4v})$; $\nu_3(O_h) \rightarrow \nu_3', \nu_3''(C_{4v})$ etc. Table XXV gives assignments made for OsOF_5 on this basis and compares the O_h fundamentals for OsF_6 and ReF_6 .

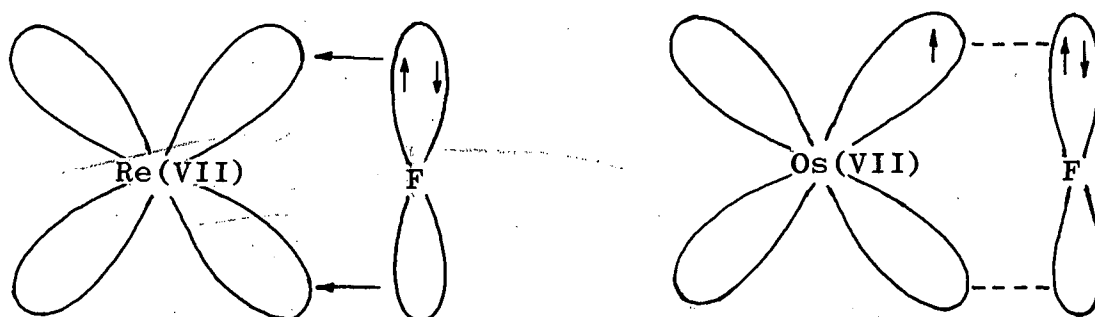
TABLE XXV

Infrared Data for OsOF₅ compared with
those for ReF₆¹⁵ and OsF₆.¹³

<u>OsF₆</u>		<u>ReF₆</u>		<u>OsOF₅</u>		Assignment Pseudo O _h
Peaks cm ⁻¹	Assign- ment, O _h	Peaks cm ⁻¹	Assign- ment, O _h	Obs.	Calc.	
230*	ν_6	170*	ν_6			
252 R	ν_5	246 R	ν_5			
268 IR	ν_4	257 IR	ν_4	440 IR		ν_4' ν_4''
364 IR	$\nu_2-\nu_4$			535 IR	520	$\nu_1'-\nu_4'$
402 IR	$\nu_2-\nu_6$	403 IR	$\nu_2-\nu_6$			
632 R	ν_2	596 R	ν_2	640 IR		ν_2'
				650 IR		ν_2''
720 IR	ν_3	715 IR	ν_3	700 IR		ν_3'
				710 IR		ν_3''
733 R	ν_1	755 R	ν_1	960 IR		ν_1'
				800 IR		?
894 IR	$\nu_2+\nu_4$					
969 IR	$\nu_3+\nu_5$	952 IR	$\nu_3+\nu_5$			
1268 IR	$2\nu_4+\nu_3$					
1352 IR	$\nu_2+\nu_3$	1302 IR	$\nu_2+\nu_3$	1337 IR	1340	$\nu_2'+\nu_3'$
1453 IR	$\nu_1+\nu_3$	1468 IR	$\nu_1+\nu_3$			
				1405 IR	1400	$\nu_1'+\nu_4'$
				1915 IR	1920	$2\nu_1'$

* Inactive, R, Raman active; IR, infrared active.

It is of interest that the totally symmetric fundamental vibrational mode for OsOF_5 ($\nu_1 = 960 \text{ cm}^{-1}$) is of lower frequency than for the corresponding ReOF_5 molecule ($\nu_1 = 989 \text{ cm}^{-1}$ ⁶²). This may be a consequence of the antibonding effect of the single unpaired electron of OsOF_5 . Although formally non-bonding, this electron will have anti-bonding influence in $d\pi-p\pi$ bonding with the fluorine ligands as represented below.



The comparison of the visible and UV spectra of OsOF_5 with those of ReF_6 , also a d^1 system would seem profitable. There are three regions of absorption in OsOF_5 , one centred around $11,700 \text{ cm}^{-1}$, another around $8,700 \text{ cm}^{-1}$; these two are of low intensity, and the third is a very broad and intense maximum extending from $28,500 \text{ cm}^{-1}$ to $38,500 \text{ cm}^{-1}$. The absorption spectrum of ReF_6 which show peaks around 5200 cm^{-1} and $24,000 \text{ cm}^{-1}$ and $32,500 \text{ cm}^{-1}$ have been interpreted by Moffitt and his co-workers¹¹ according to ligand field theory with proper regard to the high spin-orbit coupling common to the heavy metals. On the basis of their interpretation for ReF_6 the broad absorption at $28,500 \text{ cm}^{-1}$ for OsOF_5 is assigned to

the electronic transitions from the pseudo t_{2g} orbitals to pseudo e_g orbitals thus giving $10Dq$ a value of $33,500\text{ cm}^{-1}$. The spectra of ReF_6 and OsOF_5 are different in detail. The absence of an absorption at 5000 cm^{-1} as seen in ReF_6 and attributed by Moffitt et al. to a $t_{3/2} \rightarrow t_{1/2}$ electron transition must be attributed to the non- O_h symmetry of OsOF_5 .

Osmium oxide pentafluoride is expected to show some similarity in its chemical properties to OsF_6 and related hexafluorides. Although the formal valence of the osmium in this compound is seven, the greater polarizability of the oxygen ligand compared with fluorine as a ligand was expected to lead to a greater similarity of OsF_6 and OsOF_5 than provided for on a formal basis. The oxidative similarity of OsF_6 is demonstrated by the reactions of the compounds with nitric oxide. The reaction of OsOF_5 with nitric oxide under a variety of conditions gives rise to $\text{NO}^+[\text{OsOF}_5]^-$ and OsF_6 gives, under similar conditions $\text{NO}^+[\text{OsF}_6]^-$. The behaviour of OsOF_5 is therefore much closer to OsF_6 than it is to IrF_6 . The latter combines with nitric oxide to give mixtures of the compounds NOIrF_6 and $(\text{NO})_2\text{IrF}_6$, excess nitric oxide ensuring the formation of the quadrivalent iridium complex.

It appears therefore that the representation given earlier of OsOF_5 as $\text{OsF}_{6.5}$ is a better approximation than OsF_7 . The latter would surely be more like IrF_6 in its oxidative power.

The formal oxidation state of Os in NOOsOF_5 is +6 and hence it would be interesting to compare its magnetic

properties with other compounds of Os in which Os has both the coordination number and oxidation state of 6. The magnetic moment of the compound is 0.78 B.M. at room temperature. Some examples of the above mentioned compounds are collected in Table XXVI.

TABLE XXVI

Magnetic Properties of Some d^2 Complexes of Osmium

Compound	Magnetic moment	Reference
$\text{Cs}_2\text{OsO}_2\text{Cl}_4$	diamagnetic	30
K_2OsNCl_5	diamagnetic	73
OsF_6	1.50 B.M.	74

The magnetic behaviour of OsF_6 is in keeping with a d^2 system in an octahedral ligand field.¹⁰ The diamagnetism of $\text{Cs}_2\text{OsO}_2\text{Cl}_4$ and K_2OsNCl_5 is explained by the assumption that the ligand field departs markedly from octahedral symmetry, a single d orbital lying lowest or by the assumption that there is a strong magnetic exchange.¹⁰ The low value of 0.78 BM in the case of NOOsF_5 can be attributed to partial spin pairing due to departure from an octahedral ligand field, the departure not being as great as that in the case of $\text{Cs}_2\text{OsO}_2\text{Cl}_4$ and K_2OsNCl_5 .

The reaction of OsOF_5 in WF_6 solution with nitric oxide gas proved to be unexpected and remarkable. Previous experiments had established that nitric oxide reacted with OsOF_5 to give non-cubic solid $\text{NO}^+[\text{OsOF}_5]^-$, and that WF_6 and NO did not interact. When nitric oxide was passed into a solution of OsOF_5 in WF_6 , however, a cubic phase strikingly similar to $\text{NO}^+[\text{OsF}_6]^-$ was obtained. This proved to be $(\text{NO})_2\text{OsWOF}_{11}$ and all

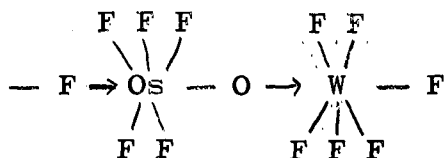
of the experimental evidence suggests that it is a solid solution of an equimolar mixture of $\text{NO}^+[\text{OsF}_6]^-$ and $\text{NO}^+[\text{WOF}_5]^-$.

The magnetic properties of this solid solution were exactly as expected for such an equimolar mixture. NOWF_7 ⁷⁵ is not cubic and NOOsOF_4 is unlikely to be cubic.

The formation of the equimolar mixture, NOOsF_6 , NOWOF_5 can be explained by the reactions given below:



It is possible that the exchange of oxygen occurs by way of an oxygen- and fluorine-bridged intermediate as indicated below:



If this is so, it may be possible that some $[\text{OsOF}_5]^-$ salts can react with tungsten hexafluoride to yield osmium hexafluoride.

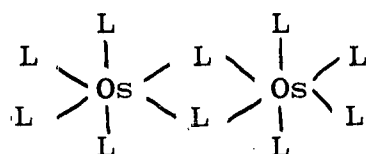
3.1.3 Osmium Trioxide Difluoride

Other fluorides of osmium were suspected of wrongful characterization after the identification of 'osmium octafluoride' as osmium hexafluoride. The reinvestigation of lower fluorides of osmium by Hargreaves and Peacock³¹ showed that 'osmium hexafluoride' reported by Ruff and Tschirch²⁸ is, in fact, osmium pentafluoride. The former workers also prepared osmium tetrafluoride which has quite different properties

from the substance of the same composition reported by Ruff.

The reinvestigation of the oxyfluoride, OsO_3F_2 done during the present work confirms the formulation OsO_3F_2 . Furthermore it has been found to exist in two modifications, a low temperature red form and a high temperature yellow form.

The unusually low volatility of OsO_3F_2 compared with OsO_4 can be explained if it is supposed to exist in a polymeric form with fluorine or oxygen bridging in which osmium is six-coordinated. Some evidence to this effect is provided by the scanty structural data obtained. Unfortunately detailed structural information could not be obtained because of the failure of the attempts to prepare single crystal of this compound. The X-ray powder photography shows that the high temperature form of OsO_3F_2 has a monoclinic unit cell in which $a \neq b$. The pseudo unit cell has, as indicated by its volume, two molecules in it. The X-ray powder pattern of the low temperature form is more complex than that of the high temperature form. It could not be indexed but it is akin to the powder photographs of the pentafluorides of the noble metals e.g. RuF_5 ,⁵⁵ RhF_5 ,⁵⁶ IrF_5 ,⁵⁷ PtF_5 .⁵⁸ This similarity suggests that the low temperature form may contain six-coordinated metals in tetrameric units as in those pentafluorides.⁹ The high temperature form of OsO_3F_2 is probably a dimer with two ligand-bridging of the osmium atoms with a total of six coordination of each osmium as indicated below:



(where L = O or F)

As expected, since all osmium electrons are involved in bonding, this compound is diamagnetic and its molar susceptibility is -25×10^{-6} c.g.s. units.

3.1.4 Nitrosyl Trioxytrifluoroosmate (VIII)

The nitrosyl derivative of OsO_3F_2 , NOOsO_3F_3 is similar in its properties to the other derivatives, MOsO_3F_3 ($\text{M}=\text{K}, \text{Rb}, \text{Cs}, \text{Ag}$).³⁰ It reacts with cold water giving nitric oxide, osmium tetroxide and hydrofluoric acid. It is therefore formulated as $\text{NO}^+ [\text{OsO}_3\text{F}_3]^-$. It is diamagnetic as expected for an Os(VIII) compound.

3.1.5 Interrelationships of Osmium Fluorides

The interrelationships of the osmium fluorides, oxyfluorides and their complexes are shown in Figure 17.

3.2 THE OXIDIZING PROPERTIES OF THE NOBLE METAL HEXAFLUORIDES

3.2.1 Dioxygenyl Hexafluoroplatinate (V)

Since it was clear that single crystals of dioxygenyl hexafluoroplatinate (V), $O_2^+[PtF_6]^-$ would be both difficult to prepare and manipulate for X-ray single crystal work, a large polycrystalline sample was prepared for a neutron diffraction study. Such a study held high promise of yielding the oxygen-oxygen distance in the O_2^+ cation with significant accuracy.

In the experiments preliminary to the necessary large scale preparation, it was found that reaction of oxygen gas with a solid-vapour equilibrium mixture of the hexafluoride led to product containing occluded hexafluoride. In order, therefore, to produce pure O_2PtF_6 it was necessary to carry out the $O_2 + PtF_6$ reaction in the gas phase by a flow method. Several gram lots of O_2PtF_6 were prepared in high purity by this technique.

The neutron diffraction study was carried out by Drs. J. A. Ibers and W. C. Hamilton⁸⁰ of the Brookhaven National Laboratory. They concluded from analysis of their data that the space group and unit cell atomic positions were as given by Bartlett and Lohmann³⁴ on the basis of the X-ray data. The parameters obtained from the neutron data, however, are slightly different and much more precisely defined than those arrived at from the X-ray data.

Ibers and Hamilton find⁸⁰ that the O-O bond length in the O_2^+ cation is $0.91 \pm 0.03 \text{ \AA}$ and that the PtF_6 group is approximately a regular octahedron with a Pt-F bond length of $1.83 \pm 0.02 \text{ \AA}$. Their parameters show that the shortest O-F

distance (that from one end of the O_2^+ cation to the three closest fluorine ligands of one PtF_6 group) is $2.56\overset{O}{\text{\AA}}$. The salt like character of O_2PtF_6 is therefore confirmed but the extreme shortness of the O-O distance in the cation O_2^+ is unexpected and there is no ready explanation for it.

To appreciate the significance of the observation it is first necessary to review the available internuclear distances reported for gaseous O_2^+ and related species. These data are derived from emission spectra. Table XXVIII gives the internuclear separations reported for various ground state diatomics. The O-O distance in the dioxygenyl salt cation is seen to be $0.21\overset{O}{\text{\AA}}$ shorter than that given for the gaseous ion and is seen to be shorter than the distance reported for the O_2^{2+} ion⁸¹ also. At first sight then it appears that formulation of the cation as O_2^{2+} or O_2^{3+} would be more appropriate than O_2^+ .

Formulations $O_2^{2+}[PtF_6]^{2-}$ and $O_2^{3+}[PtF_6]^{3-}$ may be disposed of on thermodynamic grounds alone, although they are also inconsistent with the magnetic and chemical properties of the compound. It is seen from Table XXVII that if the salt were $O_2^{2+}[PtF_6]^{2-}$ the combined electron affinities for the formation of $[PtF_6]^{2-}$ would need to be greater than 653 kcal/mole (see Appendix IV).

Since the first electron affinity is always more exothermic than the second, the first electron affinity of PtF_6 should be greater than 326 kcal/mole. This value is greater than that needed for the formation of $N_2^+[PtF_6]^-$ (233 kcal/mole) but nitrogen and PtF_6 do not react. On the same grounds $O_2^{3+}[PtF_6]^{3-}$ is seen to be even less probable.

TABLE XXVII

Alternative Formulations for O_2PtF_6 and the Lattice Energy,
Ionization potential and Electron affinity Data.

Formulation	U (kcal/mole)	ΣI (kcal/mole)	Minimum ΣE for Exothermic ΔH_f (kcal/mole)	
			$[PtF_6]^-$	$[PtF_6]^{2-}$
$O_2^+[PtF_6]^-$	-125	281	-156	
$O_2^{2+}[PtF_6]^{2-}$	-500	1153		-653

The magnitude and temperature behaviour of the magnetic susceptibility of O_2PtF_6 have been well accounted for by Bartlett and Lohmann³⁴ on the basis of the formulation $O_2^+[PtF_6]^-$. If the salt had the formulation $O_2^{2+}[PtF_6]^{2-}$ it would be diamagnetic, since $[PtF_6]^{2-}$ is known to be diamagnetic in other compounds¹⁰ and O_2^{2+} being isoelectronic with nitrogen, is also expected to be diamagnetic, the ion being formed by the removal of two antibonding electrons from O_2 .

It is significant that the Pt-F distance, $1.83 \pm 0.02 \text{ \AA}$, observed in the PtF_6 species is the distance expected for a $[PtF_6]^-$ ion. The Pt-F distance observed by Mellor and Stephenson⁸² in the salt K_2PtF_6 is 1.91 \AA , this being consistent with Pt(IV). In $KOsF_6$ Hepworth, Jack and Westland⁶¹ noted an Os-F distance of 1.82 \AA . The only satisfactory formulation for O_2PtF_6 , therefore, is as the $O_2^+[PtF_6]^-$ salt.

An explanation of the short internuclear distance has been given by Bartlett.⁸³ He suggests a novel arrangement

of the electrons for the O_2^+ salt ion, the new arrangement being attributed to the high ligand field about the cation.

TABLE XXVIII

Internuclear Distances and Molecular Orbital Electron
Configurations of some Diatomic species.^{81,84,85}

r_N^*	1.098	1.116		1.150	1.062	1.082	1.207	1.123	1.010
$\sigma_g 3s$	—	—	$\sigma_g 3s$	—	—	—	—	—	—
$\sigma_u 2p$	—	—	$\sigma_u 2p$	—	—	—	—	—	—
$\pi_g 2p$	— —	— —	$\pi_g 2p$	\uparrow —	— —	— —	$\uparrow \uparrow$	\uparrow —	— —
$\sigma_g 2p$	$\uparrow \downarrow$	\uparrow	$\pi_u 2p$	$\uparrow \downarrow \uparrow \downarrow$	$\uparrow \downarrow \uparrow \downarrow$	$\uparrow \downarrow \uparrow$	$\uparrow \downarrow \uparrow \downarrow$	$\uparrow \downarrow \uparrow \downarrow$	$\uparrow \downarrow \uparrow \downarrow$
$\pi_u 2p$	$\uparrow \downarrow \uparrow \downarrow$	$\uparrow \downarrow \uparrow \downarrow$	$\sigma_g 2p$	$\uparrow \downarrow$	$\uparrow \downarrow$	$\uparrow \downarrow$	$\uparrow \downarrow$	$\uparrow \downarrow$	$\uparrow \downarrow$
$\sigma_u 2s$	$\uparrow \downarrow$	$\uparrow \downarrow$	$\sigma_u 2s$	$\uparrow \downarrow$	$\uparrow \downarrow$	$\uparrow \downarrow$	$\uparrow \downarrow$	$\uparrow \downarrow$	$\uparrow \downarrow$
$\sigma_g 2s$	$\uparrow \downarrow$	$\uparrow \downarrow$	$\sigma_g 2s$	$\uparrow \downarrow$	$\uparrow \downarrow$	$\uparrow \downarrow$	$\uparrow \downarrow$	$\uparrow \downarrow$	$\uparrow \downarrow$
	N_2	N_2^+		NO	NO^+	NO_2^+	O_2	O_2^+	O_2^{2+}

* Internuclear distance, in Å.

Bartlett points out that the observed internuclear separation in O_2^+ (salt) can be satisfactorily accounted for if seven electrons are permitted in the internuclear region. It is noteworthy in Table XXVIII that a diminution occurs in the internuclear separation with increase in the total nuclear charge for the isonuclear pairs NO and NO^+ (g) and O_2 (g) and O_2^+ (g). Similarly the O_2^{2+} (g) internuclear separation is less than in O_2^+ (g). The contraction with removal of an antibonding electron is seen from Table XXVIII to be about 0.08 to 0.1 Å. Therefore, if the O_2^+ salt ion is permitted seven bonding electrons, such as would be the case if the antibonding $\pi_g 2p$ and $\sigma_u 2p$ orbitals were

higher in energy than certain 3σ or 3π bonding orbitals a contraction somewhat greater than 0.08\AA would be expected. If the shortening in the internuclear separation by the addition of an extra bonding electron is equivalent to the shortening due to the removal of an antibonding electron then the contraction from the O-O distance of the gaseous O_2^+ ion would be 0.16 to 0.2\AA . Thus an internuclear separation of 0.96 to 0.92\AA in O_2^+ (salt) could be accounted for.

It is not unreasonable, as pointed out by Bartlett, that the antibonding orbitals should be high in the O_2^+ salt since the cation is closely surrounded by twelve electron rich ligands. Presumably this high field renders the internuclear region energetically preferable, for electrons, to the peripheral antibonding regions.

It should incidentally also be appreciated that the removal of a bonding electron, such as would occur for $\text{O}_2^{2+} \rightarrow \text{O}_2^{3+}$, should lead to an increase in the internuclear separation, such as occurs for $\text{N}_2(\text{g}) \rightarrow \text{N}_2^+(\text{g})$. And on this ground O_2^{3+} will not account for the short O-O distance in O_2PtF_6 .

Of course the change in the order of molecular orbitals required for O_2^+ in $\text{O}_2^+[\text{PtF}_6]^-$ probably occurs in NO^+ also when that cation is surrounded by $[\text{PtF}_6]^-$ groups. However, this change will not affect the number of bonding electrons since the antibonding $\pi_g 2p$ and $\sigma_u^* 2p$ orbitals are empty in NO^+ . Hence the internuclear separation in NO^+ in its salts should be akin to that in the gaseous NO^+ and as a consequence the internuclear separation in NO^+ salt ion should be greater than

in the O_2^+ salt ion.

Unfortunately, although sample of $NOIrF_6$ and $NOPtF_6$ have been submitted for neutron diffraction study, results are not yet available. However, the unit cell dimensions of the rhombohedral form of $NOPtF_6$ reported in this work and the accurate cubic dimensions for $NOPtF_6$ (cubic) obtained in these laboratories by Beaton⁶², show that the nitrosyl salt is more voluminous than the dioxygenyl salt. The molecular volume differences within the pairs of $NOPtF_6$ (rhomb.) and O_2PtF_6 (rhomb.) and $NOPtF_6$ (cub.) and O_2PtF_6 (cub.) may be assumed to be due to the difference in the effective molecular volumes of NO^+ and O_2^+ cations. The volumes are compared in Table XXIX.

TABLE XXIX

Comparison of $NOPtF_6$ (rhomb.) and O_2PtF_6 (rhomb.) and $NOPtF_6$ (cub.) and O_2PtF_6 (cub.) Molecular Volumes (in \AA^3).

Compound	Rhomb.	Cubic
$NOPtF_6$	123.5 *	129.2 ⁶²
O_2PtF_6	119.9 ³⁴	126.2 ³⁴
Difference	3.6	3.0

* Present work

The data show that NO^+ is approximately 3\AA^3 larger in its effective size than O_2^+ . In part this may be attributed to a shorter internuclear separation in O_2^+ than in NO^+ (the reverse of the gaseous ion situation) but will also be a consequence of the greater nuclear charge in the O_2^+ species, although the latter effect would have been appreciably offset by

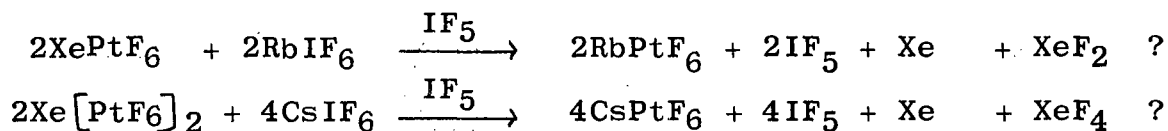
the presence of an antibonding electron. To pursue the latter point it is worth noting that the effective volume of the fluorine molecules in its β -form is 37.1\AA^3 ⁸⁶ compared with that of the oxygen molecule in the isomorphous γ -form which is 39.8\AA^3 . The contraction of 2.7\AA^3 is associated with an increase in nuclear charge of two units and increase of two in the number of antibonding electrons. It is possible then that the contraction associated with unit change in nuclear charge and the number of antibonding electrons would only be $\sim 1.5\text{\AA}^3$.

3.2.2. Xenon - Noble Metal Hexafluorides Adducts

In his initial work³⁵ on the xenon-platinum hexafluoride reaction Bartlett obtained tensimetric data which indicated a combining ratio close to 1:1, and by analogy with the salt $\text{O}_2^+[\text{PtF}_6]^-$ he formulated it as $\text{Xe}^+[\text{PtF}_6]^-$.

Further investigation of xenon-platinum hexafluoride has shown, however that the reaction is more complex than was first supposed. A large number of titrations have been carried out and the ratio of the Xe to PtF_6 in the solid product is seen to vary between 1:1 and 1:2. Indeed the variation in the nature of the product parallels the behaviour of nitric oxide in its reaction with iridium hexafluoride (q.v) in which varying proportions of the adducts NOIrF_6 and $(\text{NO})_2\text{IrF}_6$ have been detected. Unfortunately, the absence of reliable X-ray powder data has prevented the establishment of the existence of two compounds in the $\text{Xe} + \text{PtF}_6$ products, although the stoichiometry limits suggest XePtF_6 and $\text{Xe}(\text{PtF}_6)_2$ to be present in varying proportions.

The derivation of hexafluoroplatinates (V) both from material of composition XePtF_6 and from material of composition $\text{Xe}(\text{PtF}_6)_2$ has established the quinquevalence of the platinum in the adducts:



The iodine pentafluoride solvent was shown to be incapable of oxidizing Pt(IV) to Pt(V) even in the presence of xenon tetrafluoride.

Further support for the quinquevalence of the platinum in the adducts is given by the similarity of the infrared spectra with those of potassium and dioxygenyl hexafluoroplatinates (V). The data are compared in Table XXX. The spectra of the adducts of various composition show no recognizable change. The strong absorption at $\sim 640 \text{ cm}^{-1}$ is attributable to the octahedral $[\text{PtF}_6]^- \nu_3$ fundamental mode. For PtF_6 , $\nu_3 = 705 \text{ cm}^{-1}$ ¹³ and for $[\text{PtF}_6]^{2-}$, $\nu_3 = 583 \text{ cm}^{-1}$.⁸⁸

TABLE XXX

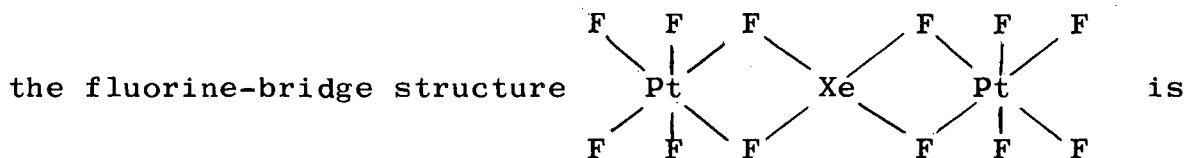
Comparison of the Infrared Data for $\text{Xe}[\text{PtF}_6]_x$,
 KPtF_6 and O_2PtF_6

	$\text{Xe}[\text{PtF}_6]_{1.7}$	KPtF_6 ⁸⁷	O_2PtF_6
IR (cm^{-1})	625(vs); 550(s)	649(vs); 590(s)	631(vs); 545(s)
Visible & U.V.(Å)	3825	---	3500

Although the $\text{Xe}[\text{PtF}_6]_x$ material has the colour and plastic consistency of platinum pentafluoride it is unlikely that it is merely a mixture of xenon difluoride and platinum

pentafluoride. Material of composition XePtF_6 could not be accounted for on this basis and although XeF_2 , 2PtF_5 represents $\text{Xe}(\text{PtF}_6)_2$ it is unlikely that the two fluorides could maintain their separate identities in close mixture. Xenon difluoride has been shown by Edwards, Holloway and Peacock⁸⁹ to form distinct compounds with antimony pentafluoride and tantalum pentafluoride. Furthermore, platinum pentafluoride usually gives a distinctive X-ray powder diffraction pattern and this pattern has at no time been observed in photographs of $\text{Xe}(\text{PtF}_6)_x$.

A sample prepared in a large scale gas-gas reaction of Xe and PtF_6 had the empirical formula $\text{Xe}(\text{PtF}_6)_2$ based on analysis. The magnetic moment of this material proved to be 4 B.M. at 298°K. This is best accounted for on the basis of the formulation $\text{Xe}^{2+}[\text{PtF}_6^-]_2$. It is necessary to postulate that the Xe^{2+} ions would have a high spin configuration. The moment calculated from the combination of the spin only value for Xe^{2+} with a p-orbital configuration $\uparrow\downarrow, \uparrow, \uparrow$ and the observed moment for $[\text{PtF}_6^-]$,⁶² yields a value of 3.75 B.M. A mixture of the diamagnetic XeF_2 ⁹⁰ and 2PtF_5 would have a moment of 2.70 B.M. on basis of the known moment of 1.9 B.M. for PtF_5 .⁵⁸ Although



attractive, it is less likely that xenon in such a bonding situation would be paramagnetic. The near degeneracy of the p-orbitals, required for paramagnetism of the $\text{Xe}(\text{II})$ would be most likely with a cationic xenon in a near octahedral or

tetrahedral ligand environment.

Combustion of a platinum wire in a xenon-fluorine atmosphere had been reported to result in XePtF_6 .⁹¹ Subsequently the product was given the formulation $\text{Xe}(\text{PtF}_6)_2$.⁹² With these products however, there was no indication of the valence of the platinum. The product could be the diamagnetic $\text{XePt}_2\text{F}_{10}$ material observed in this work.

Compounds of constitution $\text{XeF}_2 \cdot 2\text{MF}_5$ ($\text{M}=\text{Sb}$ and Ta) have been reported⁸⁹ which have been prepared by the reaction of XeF_4 or XeF_2 with corresponding pentafluorides. A bridged structure with xenon joining two hexafluoroantimonate octahedrons has been suggested for the antimony compound i.e. $\text{F}_5\text{SbFXeFSbF}_5$. It has also been suggested⁸⁹ that $\text{Xe}(\text{PtF}_6)_2$ might be of similar constitution. However, the weak X-ray powder patterns attributable to $\text{Xe}(\text{PtF}_6)_2$ are not similar to that of $\text{XeF}_2 \cdot 2\text{SbF}_5$. The photograph of the latter was kindly made available by Professor R. D. Peacock.

The formulation $\text{Xe}^+[\text{PtF}_6]^-$ requires the minimum electron affinity of PtF_6 to be 160 kcal/mole and the formulation $\text{Xe}^{2+}[\text{PtF}_6^-]_2$ requires this value to be 172 kcal/mole (Appendix IV).

It is clear that the constitution of the $\text{Xe}(\text{PtF}_6)_x$ adducts will only be settled when single crystals of the adducts have been obtained. Unfortunately, attempts to grow more crystalline material by the slow formation of adduct by reaction of xenon and PtF_6 in tungsten hexafluoride solution failed. The usual sticky material was obtained. It is possible that more crystalline material may be produced from an ionizing

solvent such as anhydrous hydrogen fluoride.

Material of composition XePtF_6 was never obtained in sufficient quantity for magnetic susceptibility measurement. Since the platinum is quinquevalent, however, the xenon is required to be monovalent. As such it is an exception to the normal even numbered valence of xenon.

The diamagnetic brick-red solid of composition $\text{XePt}_2\text{F}_{10}$, formed along with xenon tetrafluoride in the pyrolysis of $\text{Xe}(\text{PtF}_6)_{1.8}$ [and other adducts of different composition, $\text{Xe}(\text{PtF}_6)_x$], contains quadrivalent platinum. This is indicated by the diamagnetism of the material and its interaction with cesium fluoride in iodine pentafluoride. The X-ray powder photographs of the product of interaction of $\text{XePt}_2\text{F}_{10}$ material with CsF in IF_5 point out the presence of cesium hexafluoroplatinate (IV), Cs_2PtF_6 . The powder photographs show the pentapositive salt, CsPtF_6 to be absent. Although the X-ray powder pattern of $\text{XePt}_2\text{F}_{10}$ is complex, it does not contain lines attributable to platinum tetrafluoride. Formulation of this material as the mixture $\text{PtF}_4 + \text{XePtF}_6$ is therefore inadmissible.

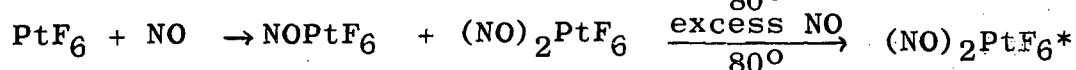
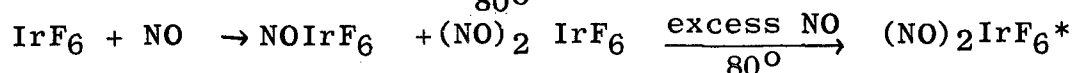
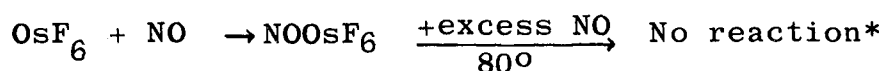
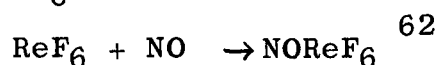
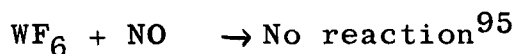
As pointed out earlier rhodium and ruthenium hexafluorides are normally less stable than platinum hexafluoride^{5,6} and hence are expected to have oxidizing powers greater than that of platinum hexafluoride. However, rhodium hexafluoride is clearly not powerful enough as an oxidizer to react with krypton. It does react with xenon, however, and the departure from the 1:1 reaction stoichiometry in this case is less than for the platinum system. This is surprising. In view of the

greater instability and chemical reactivity of the rhodium hexafluoride the adduct $\text{Xe}[\text{RhF}_6]_2$ might also have been expected. Ruthenium hexafluoride has been reported⁹⁴ to combine non-stoichiometrically with xenon in ratios greater than 2:1. It has been suggested that some reduction of ruthenium occurs in this reaction. However, the reaction product has not been characterized. The 1:1 addition in the case of Xe and RhF_6 may well have been favoured by the excess xenon and the use of small concentrations of the reactants. It may be that the 1:2 adduct would result from the interaction of higher partial pressures of the reactants. The 1:1 adduct has not been characterized but $\text{Xe}^+[\text{RhF}_6]^-$ is a feasible formulation.

Rhodium hexafluoride has been found to react with oxygen but the reaction product has not been satisfactorily characterized, largely because of the small quantity of material available and its high reactivity.

3.2.3 The Reactions of Nitric Oxide with the Noble Metal Hexafluorides

The increase in the oxidizing power of the third transition series hexafluorides with increase in atomic number is borne out by their behaviour towards nitric oxide. The nature of the reactions of these hexafluorides with nitric oxide is summarized below:



*Present work.

It is seen that iridium and platinum hexafluorides form mixtures of pentavalent and quadrivalent complexes at low temperatures whereas under the same conditions WF_6 does not react⁹⁵ and the other hexafluorides form pentavalent complexes. This difference indicates that IrF_6 and PtF_6 are the most powerfully oxidizing and that WF_6 is the least oxidizing. Although tensimetric titrations of NO with IrF_6 and PtF_6 do not give pure 1:1 products it was nevertheless desirable to obtain these NOMF_6 salts pure. The isomorphism of the compounds provides for comparison of anion volumes in the series Ta to Pt and the unit cell being cubic indicates O_h or near O_h symmetry of the $[\text{MF}_6]^-$ ions, hence magnetic measurements on these compounds were more likely to be interpretable than for more complex ligand arrangements. Furthermore, the isomorphism of NOPtF_6 with O_2PtF_6 and the diamagnetism of the NO^+ cation promised a reliable measure of the contribution made by $[\text{PtF}_6]^-$ to the $\text{O}_2^+[\text{PtF}_6]^-$ susceptibility. From such a study, of course, it was hoped that a reliable assessment of the susceptibility of the O_2^+ ion could be made.

A promising alternative route for the preparation of the compounds NOMF_6 appeared to be controlled reaction in liquid tungsten hexafluoride. Tungsten hexafluoride proved to be a good solvent for these hexafluorides and is suitable for carrying out the reaction with nitric oxide because of its convenient liquid range (M.P. 2.3° , B.P. 17°) and inertness towards nitric oxide.⁹⁵ Since nitric oxide is admitted slowly to the hexafluoride system in this procedure the hexafluoride is generally in excess of NO and since the salt precipitates from solution there is less opportunity for the formation of $(\text{NO})_2\text{MF}_6$,

than in the gas-gas reaction. This technique proved to be a good one for the preparation of NOIrF_6 in quantity. In the case of platinum hexafluoride reaction, however, a mixed NOPtF_6 , $(\text{NO})_2\text{PtF}_6$ product was again obtained.

It was observed that the treatment of the mixture of the 1:1 and 2:1 NO-products of IrF_6 and PtF_6 with excess NO tends to the composition of the adducts to 2:1. This conversion is rapid in the case of platinum but slow in the case of iridium. The adduct NOOsF_6 does not consume NO even when the mixture is heated. The treatment of NOReF_6 with excess NO has not been done, but it is certain that $(\text{NO})_2\text{ReF}_6$ would not be formed. Thus, the oxidizing power of the hexafluorides of the third series appears to be increasing smoothly in the sequence $\text{WF}_6 < \text{ReF}_6 < \text{OsF}_6 < \text{IrF}_6 < \text{PtF}_6$.

The formation of NOReF_6 , NOOsF_6 , NOIrF_6 and NOPtF_6 indicates a minimum value of the first electron affinity of the hexafluorides of approximately 89 kcal/mole since the enthalpy of ionization of NO is 213^{36} kcal/mole and the lattice energy for each of these salts cannot be much more than 124 kcal/mole (Appendix IV). Since NOWF_6 is not formed, the first electron affinity of WF_6 is unlikely to be much more exothermic than 89 kcal/mole. The formation of $(\text{NO})_2\text{PtF}_6$ and $(\text{NO})_2\text{IrF}_6$, the lattice energies of which can be taken as 372 kcal/mole, indicates that the minimum value of the sum of the first and second electron affinities, $E_1 + E_2$ of PtF_6 and IrF_6 is 54 kcal/mole (Appendix IV). As $(\text{NO})_2\text{OsF}_6$ is not formed in these reactions the sum $E_1 + E_2$ for osmium hexafluoride cannot be more exothermic

than 54 kcal/mole. By extrapolation it can be said that $(\text{NO})_2 \text{ReF}_6$ would not be formed by the $\text{NO} + \text{ReF}_6$ reaction.

Although the NOPtF_6 salt was not prepared pure in quantity in this work a recent novel reaction has been discovered in these laboratories⁶² which provides an excellent preparation of the compound in quantity and high purity. This involves the reaction of NOF with the hexafluoride: $\text{NOF} + \text{PtF}_6 = \text{NOPtF}_6 + 1/2 \text{F}_2$.

The powder patterns of the 1:1 adducts closely resemble those of KSbF_6 ⁹⁶ and O_2PtF_6 .³⁴ The isomorphism of NOOsF_6 with O_2PtF_6 had been predicted by Bartlett and this was of value in supporting the ionic formulation of O_2PtF_6 .³⁴ The powder patterns of NOMF_6 ($\text{M} = \text{Ta}, \text{Re}, \text{Os}, \text{Ir}$ and Pt) and O_2PtF_6 are shown in Plate I. The unit cell parameters and the molecular volumes are compared in Table XXXI.

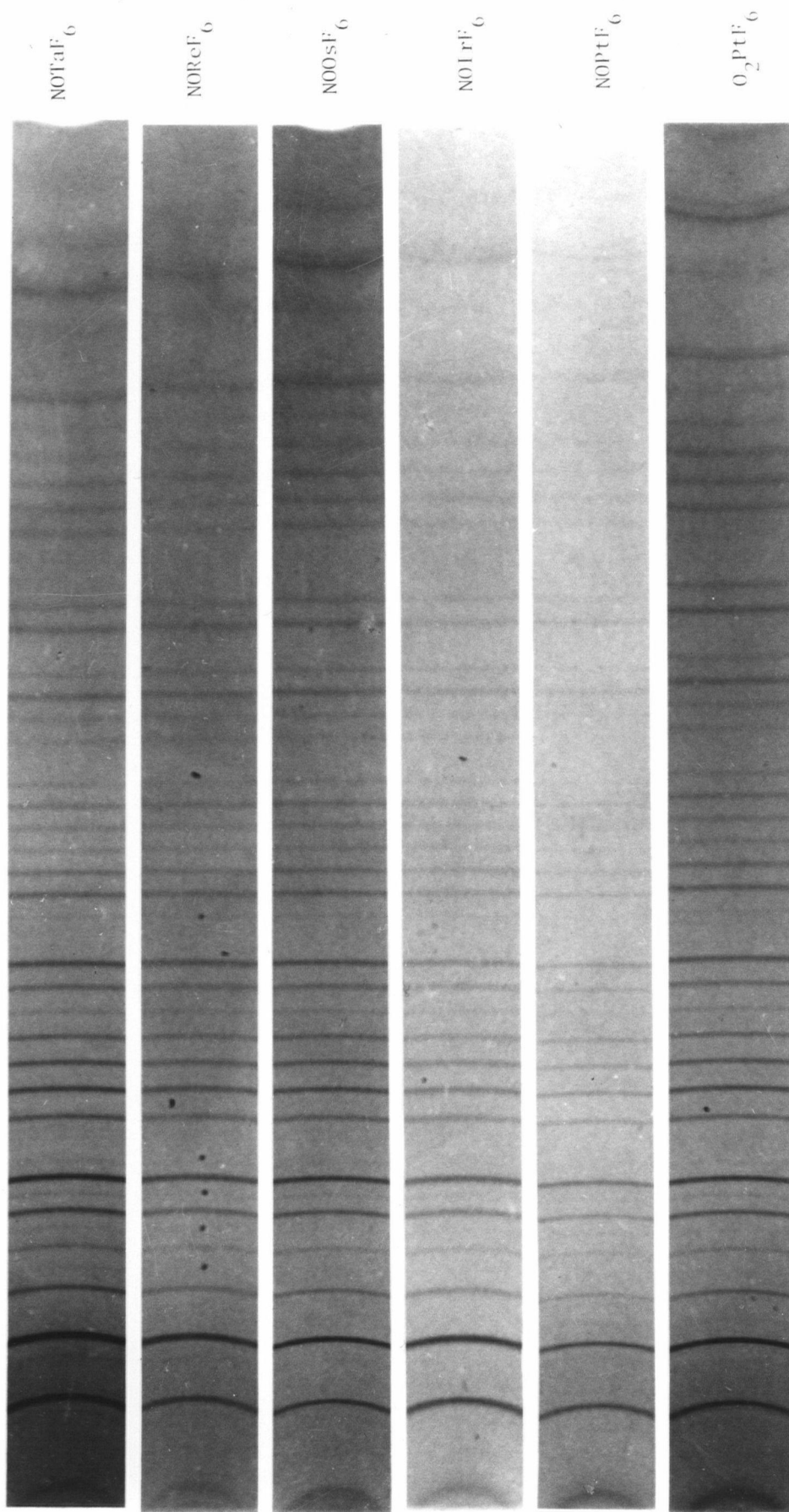
TABLE XXXI

Comparison of Unit Cell Parameters and Molecular Volumes
of NOMF_6 salts of the Third Transition Series

	NOTaF_6^*	NOReF_6^{62}	NOOsF_6^*	NOIrF_6^*	NOPtF_6^{62}	$\text{O}_2\text{PtF}_6^{34}$
$a, \text{\AA}$	10.22	10.151	10.126	10.114	10.112	10.032
Molecular Volume, \AA^3	133.4	130.7	129.8	129.3	129.2	126.2

*present work.

These compounds are undoubtedly salts, $\text{NO}^+[\text{MF}_6]^-$. A complete structural analysis of an NOMF_6 salt has not yet been done. It was considered unlikely that an unambiguous structure determination would be possible with the X-ray powder



X - RAY POWDER PHOTOGRAPHS

data since the light atom contributions to the line intensities are small and the difference between nitrogen and oxygen in scattering power in these salts is insignificantly small. The possibility of discerning whether the lattice has an ordered NO^+ or disordered NO^+ arrangement and the internuclear distance in NO^+ must rest on a neutron diffraction analysis. Such analyses have been undertaken with NOIrF_6 and NOPtF_6 samples by Dr. W. C. Hamilton at the Brookhaven National Laboratory.

The magnetic moment of NOOsF_6 is 3.36 B.M. at 297°K which is as expected for a third transition series d^3 system. Very simple theory predicts that a t_{2g}^3 configuration in an octahedral ligand field will possess a 4A_2 ground state. Such a state would, in a magnetically dilute system, possess a magnetic moment equal to the spin-only moment of 3.88 B.M. The lower value observed here can be attributed following Figgis, Lewis and Mabbs⁹⁷ in their interpretation of the $[\text{OsF}_6]^-$ results, to the large spin-orbit coupling in Os(V) . The data for other $[\text{OsF}_6]^-$ salts are compared with that for NOOsF_6 in Table XXXII.

TABLE XXXII

Magnetic Data for Some d^3 $[\text{MF}_6]$ Species.

Compound	μ_{eff} , B.M.	Reference
KOsF_6	3.34	97
CsOsF_6	3.23	97
NOOsF_6	3.36	present work
NaOsF_6	3.05	98
AgOsF_6	2.95	98
IrF_6	2.90	97

Iridium has a d^4 configuration in nitrosyl hexafluoroiridate (V). This compound has a magnetic moment of 1.23 B.M. at 297°K. The magnetic susceptibilities of a number of complexes of the metals of the second and third transition series having d^4 electronic configurations have been measured and the results have been discussed by Earnshaw, Figgis, Lewis and Peacock.⁹⁹ The d^4 configurations are of the low spin type (d_{t2g}^4) as a result of the high ligand field found commonly in third transition series compounds.

The temperature-independence of the paramagnetism, however, is a consequence of high spin-orbit coupling. The spin-orbit coupling evidently lifts the degeneracy⁹⁹ of the 3T_1 term (given by the Russell Saunders scheme as the lowest lying term). For $[\text{IrF}_6]^-$ the spin-orbit coupling is so great that only the lowest non-degenerate level of the system is occupied at available temperatures and the susceptibility arises only from the second order Zeeman effect between this and higher levels, the susceptibility being of the temperature-independent type with $\chi_M = 24N\beta^2/\zeta$ where N is Avogadro's number, β is Bohr Magneton and ζ is free-ion value of spin-orbit coupling. Earnshaw et al.⁹⁹ have calculated the expected value of χ_{Ir} in d^4 complexes, in which Ir is approximately in a cubic field of the ligands, to be nearly independent of temperature and to have a value of 650×10^{-6} c.g.s. units/mole. The value found for NOIrF_6 is about 650×10^{-6} c.g.s. units/mole and this is nearly independent of temperature. This value is also comparable to that of platinum hexafluoride which is also a d^4 system. The susceptibility of PtF_6 is approximately 700×10^{-6} c.g.s.

units/mole and again the susceptibility is nearly independent of temperature. The value of the magnetic moments of NOIrF_6 is compared with the values of some other related d^4 situations in Table XXXIII.

TABLE XXXIII

Magnetic Data for Some d^4 $[\text{MF}_6]$ Species.

Compound	μ_{eff} , B.M.	Reference
KIrF_6	1.27	99
CsIrF_6	1.29	99
NaIrF_6	1.23	98
AgIrF_6	1.24	98
NOIrF_6	1.23	present work
PtF_6	1.30	present work

The stronger oxidizing properties of PtF_6 and IrF_6 caused some difficulty in the synthesis of the 1:1 adducts but the preparation of pure 2:1 adducts was easier to effect. The 2:1 $\text{NO}:\text{MF}_6$ complexes, however, have not been as well characterized as the 1:1.

The characterization of $(\text{NO})_2 \text{PtF}_6$ is not straightforward. The sample prepared from solid-gas reaction of PtF_6 and NO gives rise to cubic NOPtF_6 plus another phase. This mixture, on treatment with excess NO , consumes more NO and a final product with stoichiometry $\text{NO}:\text{PtF}_6 :: 2:1$ is obtained. It was anticipated that $(\text{NO})_2 \text{PtF}_6$ would be isomorphous with K_2PtF_6 but this has not proved to be so. X-ray powder photographs show this phase to possess a hexagonal unit cell, $a = 10.01\text{\AA}$, $c = 3.53\text{\AA}$ and $U = 306.3\text{\AA}^3$. The reaction

product obtained from NO and PtF_6 in WF_6 also proved to be a mixture of the 1:1 and 2:1 phases on the basis of X-ray and magnetic evidence. Although the X-ray powder pattern of $(\text{NO})_2\text{PtF}_6$ has been indexed on the basis of a hexagonal unit cell, no structural details are available. The occurrence of sharp and diffuse lines in the pattern indicates that there will be some disorder in the lattice. Similar effects have been noted in UO_2F_2 ¹⁰⁰ and NaNdF_4 ,¹⁰¹ the diffuse reflections being associated with disorder in the planes giving rise to them.

The compound $(\text{NO})_2\text{IrF}_5$ has been reported,³⁸ that similar species are not present in the various reaction products of NO and PtF_6 has been demonstrated in two ways. Firstly the infrared spectrum of the residual gas following the reaction of NO with pure NOPtF_6 to give the 2:1 adducts, shows NOF and other nitrogen fluorides to be absent. This indicates that the $[\text{PtF}_6]$ group remains intact; it could only lose fluorine by interaction with the NO. Secondly treatment of the $\text{NO}(\text{PtF}_6)_x$ product from WF_6 solution with saturated aqueous potassium fluoride solution gives K_2PtF_6 . This again indicates that the $[\text{PtF}_6]$ group is present in the products.

The salt $(\text{NO})_2\text{IrF}_6$ has been reported by Robinson and Westland.³⁸ In the present case its identification depended on the similarity of its X-ray powder photograph with that characterizing $(\text{NO})_2\text{PtF}_6$.

Reference to Table XXXI shows that the effective molecular volume of NOOSF_6 , NOIrF_6 and NOPtF_6 decreases in that order. As they are isomorphous and contain the same cation, NO^+ ,

the decrease in the volume may be supposed to be due to the decrease in the volume of the hexafluoro-anions (V). A large number of other AMF_6 salts of the second and third transition series are known.⁸ The effective molecular volumes of a few AMF_6 salts have been computed and the volume trends are compared in Figure 18. Comparisons are made only for isomorphous series of salts containing the same cations; thus the effective molecular volumes of the hexafluoro-anions (V) are compared. It is seen in general, that (i) the volume of the hexafluoro-anion(V) decreases with increase in atomic number of the central atom in each series, (ii) the decrease in volume is sharper in second transition series than in the third, (iii) the volumes of the second series hexafluoro-anions are smaller than those of their sub-group relatives of the third series.

The same three features are seen in the comparison of the effective molecular volumes of the hexafluorides (both orthorhombic and cubic forms)³² of the second and third transitions series as shown in Figure 18.

It has already been remarked that the thermal stability of hexafluoride molecules decreases in each series with increase in atomic number of the central atom, PtF_6 ,²³ RuF_6 ²⁵ and RhF_6 ²⁶ having been found to dissociate to fluorine and lower fluorides rather readily. There is, therefore, a correlation of effective molecular volume, oxidizing power and thermal stability. The smaller the effective volume of the MF_6 species the more powerfully oxidizing it is. Presumably this correlation occurs as a consequence of the size

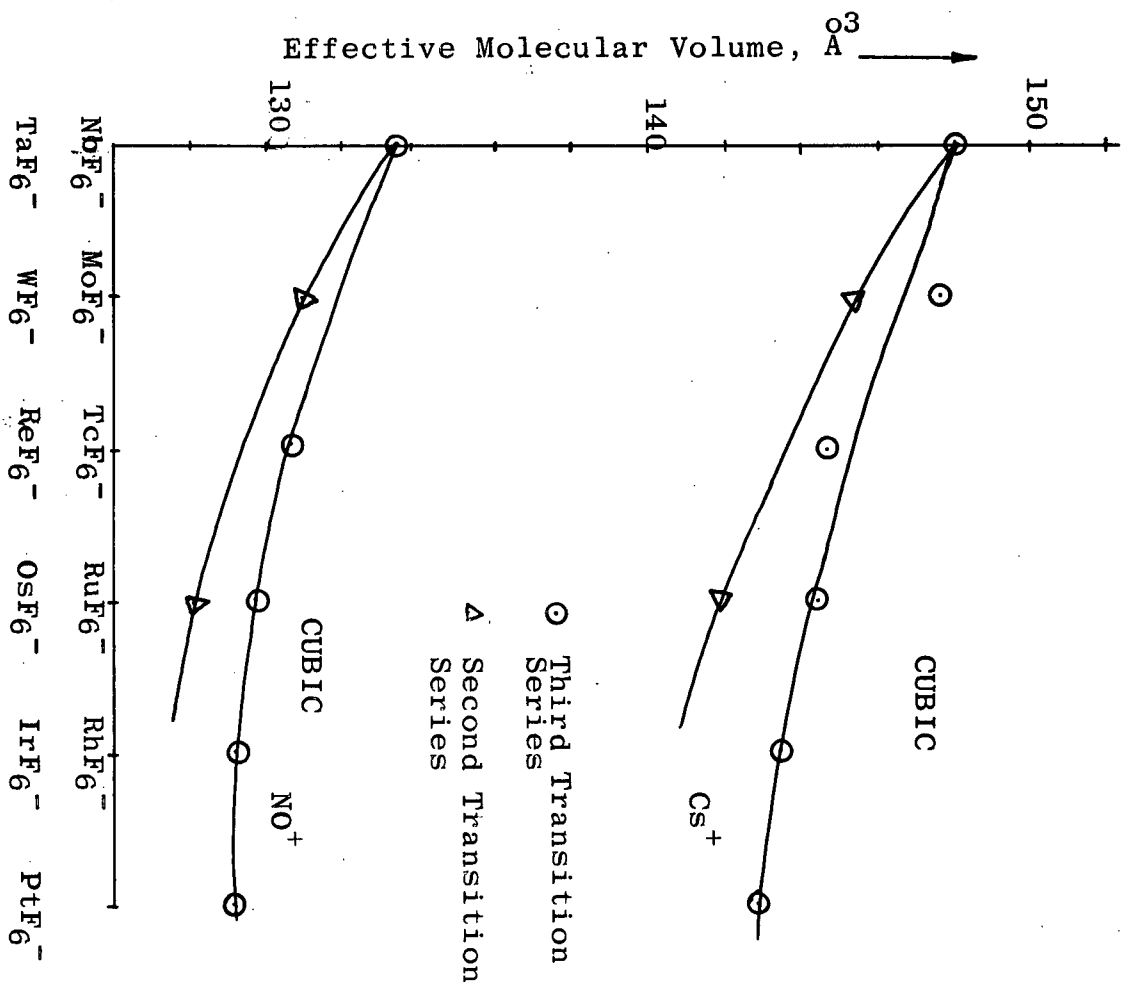
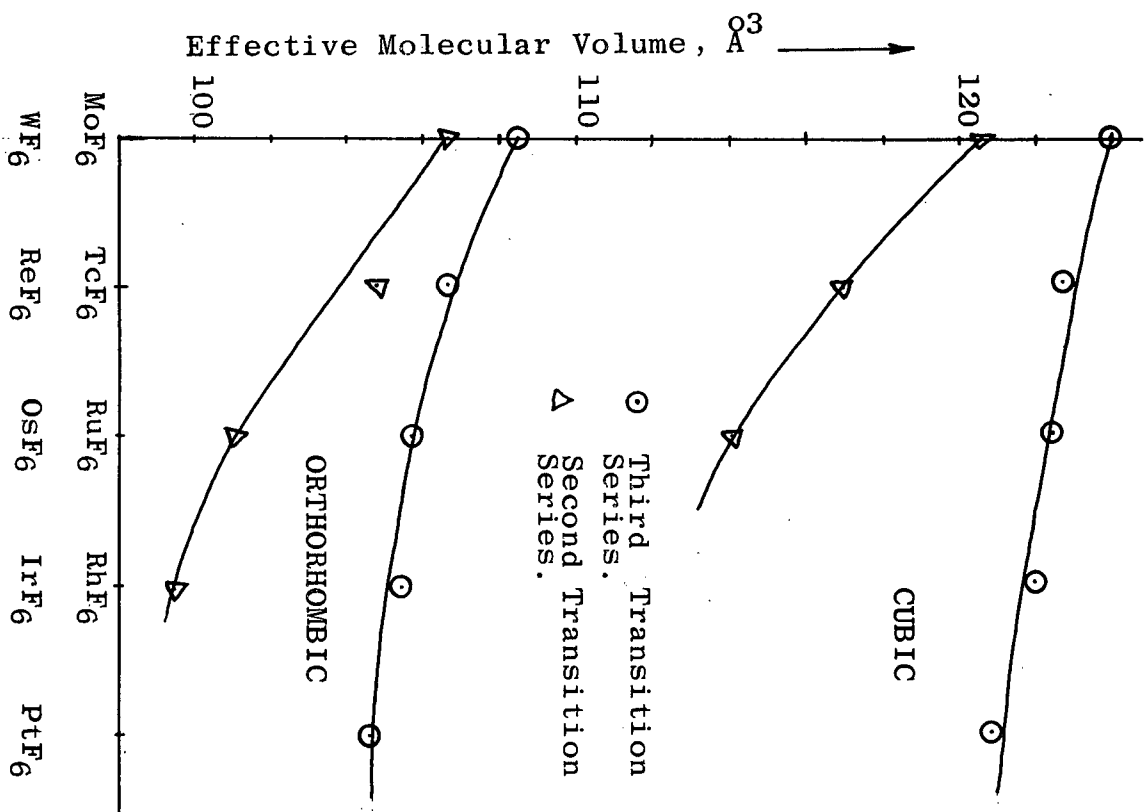


Figure 18. Comparison of Effective Molecular Volumes of MF_6 and $[\text{MF}_6]^-$ Species of the Second and Third Transition Series.

and electron affinity of MF_6 being dependent upon the polarizing power of the central atom. In Table XXIV d-electron configurations of hexafluoride molecules and hexafluoro-anions (V) are shown.

TABLE XXIV

d-Electron Configuration of Hexafluorides and Hexafluoro-anions(V) of the Second and Third Transition Series.

d^0	d^1	d^2	d^3	d^4	d^5
MoF_6	TcF_6	RuF_6	RhF_6		
WF_6	ReF_6	OsF_6	IrF_6	PtF_6	
NbF_6^-	MoF_6^-	TcF_6^-	RuF_6^-	RhF_6^-	
TaF_6^-	WF_6^-	ReF_6^-	OsF_6^-	IrF_6^-	PtF_6^-

In all of the hexafluorides except MoF_6 and WF_6 and in all of the hexafluoro-anions(V) except $[\text{NbF}_6]^-$ and $[\text{TaF}_6]^-$ non-bonding d-electrons are present which are located in the lower lying t_{2g} orbitals. These electrons do not effectively screen the ligands from the charge on the central atom, metal-ligand bond axes being in the nodal planes of the t_{2g} orbitals. Consequently the effective nuclear charge ($Z-S$) which is a measure of the polarizing power of the central atom increases with increase in atomic number (Z) as long as the non-bonding electrons are in t_{2g} orbitals. Both the decrease in volume and increase in oxidizing power with increase in Z in each series, is therefore accounted for. It must be supposed that in PtF_6 , RhF_6 , and RuF_6 , where ready dissociation to fluorine and a lower fluoride occurs, that the polarizing power of the central atom is so high that an electron is readily with-

drawn from the bonding region.

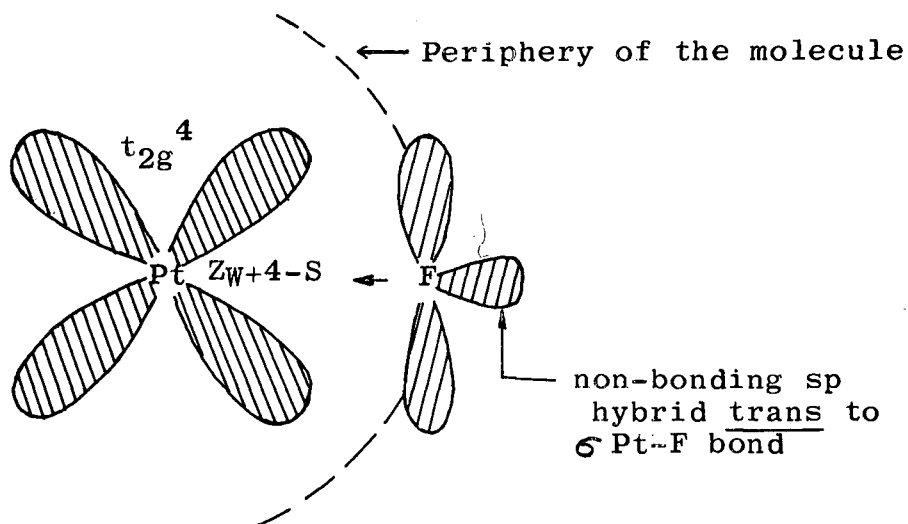
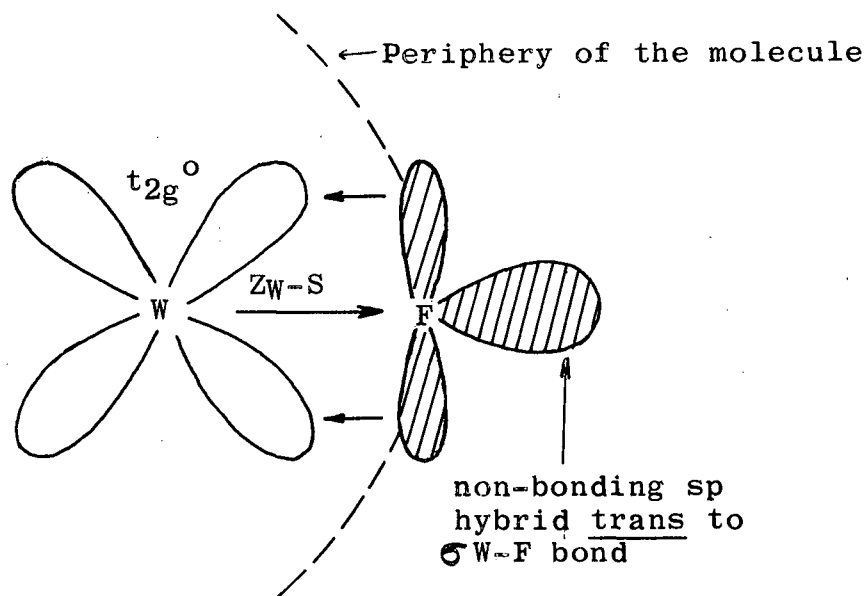
It is surprising in view of the decrease in hexafluoride effective molecular volume in the solid phase that the M-F distances given from electron diffraction studies are almost the same, the values being shown below⁵.

Compound	WF ₆	OsF ₆	IrF ₆
M-F distance, Å	1.833	1.831	1.830

An increase in the polarization of electrons in the σ -bond region with increase in Z of the central atom is to be expected although at the same time π -bonding involving unfilled t_{2g} orbitals of the central atom and filled orbitals of the fluorine ligands will of course decrease. It must be supposed, if the electron diffraction findings prove to be correct that these two effects roughly cancel, in their effect on bond length. The non-bonding sp electron pair of fluorine trans to the metal-fluorine bond will be polarized more in the case of Pt(VI) say, than in the case of W(VI) as shown in Figure 19. It is presumably the changes in size of these fluorine non-bonding electron pairs which are responsible for the changes in effective molecular volume of the hexafluorides.

3.2.4 The Reaction of Sulphur Tetrafluoride with the Noble Metal Hexafluorides.

The nature of the reactions of SF₄ with OsF₆, IrF₆ and PtF₆ indicates that the oxidizing (or fluorinating) power of the hexafluorides decreases in the order PtF₆ > IrF₆ > OsF₆.



Z_W = atomic number of tungsten

Figure 19. Bonding in the Noble Metal Hexafluorides

In the gas-gas reactions OsF_6 and IrF_6 do not react with SF_4 , whereas PtF_6 does, to give a product the X-ray powder photograph of which bears some resemblance to that of $(\text{NO})_2\text{PtF}_6$. Osmium and iridium hexafluorides need contact of the solid phase with excess of liquid sulphur tetrafluoride before they react.

The reaction products of excess liquid sulphur tetrafluoride with solid OsF_6 and IrF_6 are pentavalent complexes $\text{SF}_4, \text{OsF}_5$ and $\text{SF}_4, \text{IrF}_5$ which were found to be isomorphous with $\text{SF}_4, \text{SbF}_5$.¹⁰² It was found qualitatively that the heats of reaction increase in the order $\text{OsF}_6 < \text{IrF}_6 < \text{PtF}_6$. Platinum hexafluoride reacts violently with liquid SF_4 and the reaction product is amorphous. The analysis (see Section 2.3.7) rules out the composition $\text{SF}_4, \text{PtF}_5$. For pentavalent platinum (d_{t2g}^5) the expected magnetic moment is ~ 1.73 B.M.⁶² but this reaction product has a magnetic moment of 1.00 B.M. on the basis of a molecular weight of 398 ($\text{SF}_4, \text{PtF}_5$). This low value of the magnetic moment could arise from the presence of Pt(IV) in the reaction product, in addition to Pt(V). That the Pt(IV) compound present in this mixture cannot be $(\text{SF}_4)_2\text{PtF}_4$ is ruled out on the basis of analysis. The low percentage of fluorine and sulphur (Section 2.3.7) and the low value of the magnetic moment can be explained if the product is assumed to be a mixture of $\text{SF}_4, \text{PtF}_5$ and PtF_4 .

The room temperature magnetic moments of $\text{SF}_4, \text{OsF}_5$ and $\text{SF}_4, \text{IrF}_5$ are those expected for Os(V) and Ir(V) compounds respectively as may be seen by reference to Tables XXXII and XXXIII.

The X-ray powder photographs of these complexes indicate cubic symmetry with the platinum metal atoms lying in a simple cubic lattice with $a \sim 5.58 \text{ \AA}$. (this indicates a volume of 173.8 \AA^3 for the formula SF_4, MF_5 which is the volume expected on the basis of Zachariasen's method¹⁰³). Allowing each F ligand a volume of 18 to 19 \AA^3 the volume of SF_4, MF_5 should be between 162 and 171 \AA^3 . A preliminary X-ray study of the isomorphous $\text{SF}_4, \text{SbF}_5$ complex has been interpreted in terms of an ionic lattice composed of $[\text{SF}_3]^+$ and $[\text{SbF}_6]^-$ ions,^{102,104} this being the most satisfactory model to account for the cubic symmetry.

Hepworth, Robinson and Westland^{38,76} had prepared the complex $\text{SF}_4, \text{IrF}_5$ by the reaction of solid IrF_6 with liquid SF_4 and had observed that this complex hydrolysed completely to a colloidal iridium dioxide, sulphurous and hydrofluoric acids; there was no evidence of $[\text{IrF}_6]^{2-}$ in solution. The analogous selenium complexes $\text{SeF}_4, \text{OsF}_5$ and $\text{SeF}_4, \text{IrF}_5$ they formulated as $[\text{SeF}_3]^+ [\text{OsF}_6]^-$ and $[\text{SeF}_3]^+ [\text{IrF}_6]^-$ in that these compounds produced the $[\text{MF}_6]^{2-}$ ions on hydrolysis. Furthermore, they argued that SeF_3^+ was a feasible ion on the grounds that the conductivity of liquid SeF_4 was consistent with autoionization: $2 \text{ SeF}_4 \rightleftharpoons [\text{SeF}_3]^+ + [\text{SeF}_5]^-$. In view of the difference in behaviour of sulphur and selenium complexes towards hydrolysis it has been postulated^{76,105} that selenium complexes are ionic and the sulphur complexes may be coordination compounds, $\text{F}_4\text{S} \rightarrow \text{MF}_5$. Bartlett has pointed out,¹⁰⁶ however, that the difference in the hydrolytic behaviour in the two cases may well be attributable to the reducing nature of sulphurous acid. The

X-ray evidence obtained in this work supports this point and indicates the ionic formulation of the SF_4, MF_5 complexes. Plate II shows the X-ray powder photographs of NOOsF_6 , SF_3OsF_6 and SF_3IrF_6 .

It is of interest to assess the SF_3^+ cation volume. The anions being common, the difference in the molecular volumes of the isomorphous SF_3^+ and NO^+ salts can be taken to arise due to the difference in the effective volumes of SF_3^+ and NO^+ . The effective molecular volumes of some SF_3^+ and NO^+ salts are compared in Table XXXV.

TABLE XXXV

Comparison of Molecular Volumes (in \AA^3) of
Some SF_3^+ and NO^+ Salts.

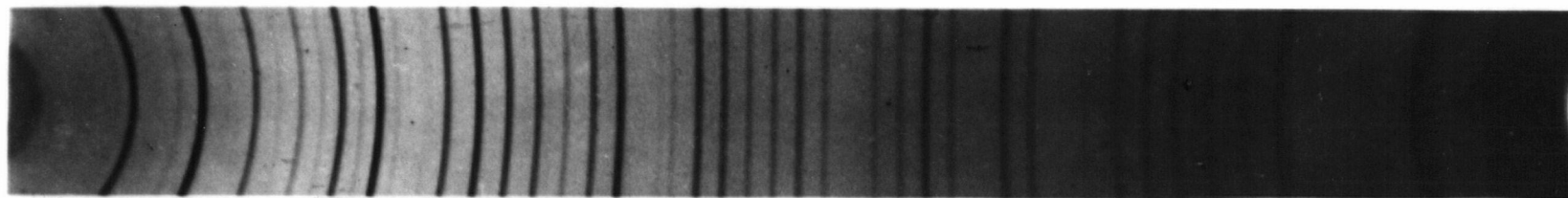
	Mol. Volume		Mol. Volume		Mol. Volume
$\text{SF}_3^+[\text{SbF}_6]^-$	178.0	$\text{SF}_3^+[\text{OsF}_6]^-$	173.8	$\text{SF}_3^+[\text{IrF}_6]^-$	173.8
$\text{NO}^+[\text{SbF}_6]^-$	132.4	$\text{NO}^+[\text{OsF}_6]^-$	129.8	$\text{NO}^+[\text{IrF}_6]^-$	129.3
Difference	45.6		44.0		44.5

From the above table it is seen that the SF_3^+ cation is about 45\AA^3 larger than the NO^+ cation. If the NO^+ is taken to have a volume of $\sim 20\text{\AA}^3$, as is indicated by its similarity to K^+ ¹⁰³ then the volume of SF_3^+ will be $\sim 65\text{\AA}^3$.

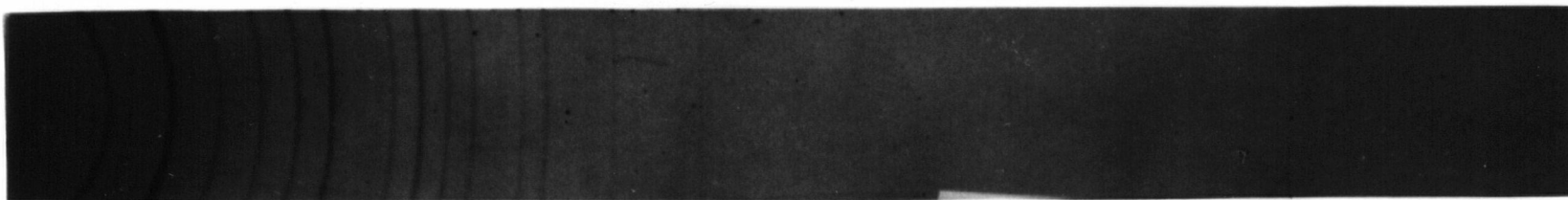
3.2.5 Other Oxidizing Reactions of the Noble Metal Hexafluorides

(i) Krypton and carbon monoxide

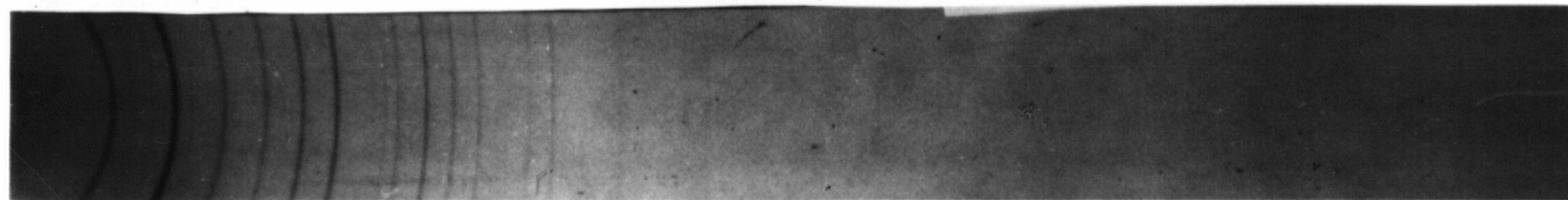
The reactions of krypton and carbon monoxide, which have higher ionization potentials³⁶ than oxygen or xenon, with platinum hexafluoride were examined in order to assess the



NOOsF₆



SF₃OsF₆



SF₃IrF₆

X - RAY FOWDER PHOTOGRAPHS

upper limit of the oxidizing power of PtF_6 . Assuming both Kr^+ and CO^+ to be akin in volume to O_2^+ the oxidation of Kr and CO to give $\text{Kr}^+[\text{PtF}_6]^-$ and $\text{CO}^+[\text{PtF}_6]^-$ would require that the electron affinity of platinum hexafluoride should exceed 198 kcal/mole (Appendix IV). Krypton did not combine with platinum hexafluoride but carbon monoxide reacted violently. Carbonyl fluoride, COF_2 and a mixture of platinum metal and platinum tetrafluoride were produced. It is not necessary to postulate $\text{CO}^+[\text{PtF}_6]^-$ or related species here, since an adequate explanation can be found in terms of oxidative fluorination by the PtF_6 . The formation of two C-F bonds in COF_2 will liberate considerable energy (the average C-F bond energy is ~ 105 kcal/mole)¹⁰⁷ and since the dissociation of PtF_6 to lower fluorides and fluorine occurs readily,²³ the exothermicity of the reaction with CO is easily understood. Moreover, if an intermediate is formed in the case of CO, it should also form in the case of krypton as both require the PtF_6 to have approximately the same oxidizing power. Presumably KrF_2 and PtF_4 do not form because of the low Kr-F bond energy. The experimental evidence indicates that krypton difluoride dissociates slowly to the elements, even at ordinary temperatures,¹⁰⁸ therefore the average bond energy cannot greatly exceed 18.4 kcal/mole,¹⁰⁹ which is the enthalpy of formation of atomic fluorine.^{1,2} The fact that xenon and oxygen are oxidized, whereas krypton is not, indicates that the electron affinity of platinum hexafluoride is unlikely to be greater than 198 kcal/mole. It is probably much less.

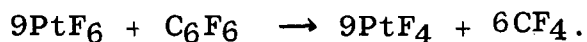
(ii) Nitrogen trifluoride.

The absence of any interaction between nitrogen

trifluoride and platinum hexafluoride is not surprising. The ionization potential of NF_3 is 13.2 e.v.¹¹⁰ and the NF_3^+ cation being large, the lattice energy for a salt $\text{NF}_3^+[\text{PtF}_6]^-$ would be smaller than in the cases of $\text{O}_2^+[\text{PtF}_6]^-$ and $\text{Xe}^+[\text{PtF}_6]^-$. It is significant that despite the strong oxidizing and fluorinating properties of PtF_6 there was no indication of the formation of NF_4 or NF_5 .

(iii) Hexafluorobenzene

It seemed worthwhile to attempt the oxidation by ionization of hexafluorobenzene in view of the remarkable electron affinity of platinum hexafluoride and low ionization potential of C_6F_6 (9.9 e.v.).¹¹¹ However, even at the outset it was recognized that a prime difficulty in effecting the reaction $\text{PtF}_6 + \text{C}_6\text{F}_6 \rightarrow [\text{C}_6\text{F}_6]^+ [\text{PtF}_6]^-$ would be the competition from the highly favourable alternative reactions:

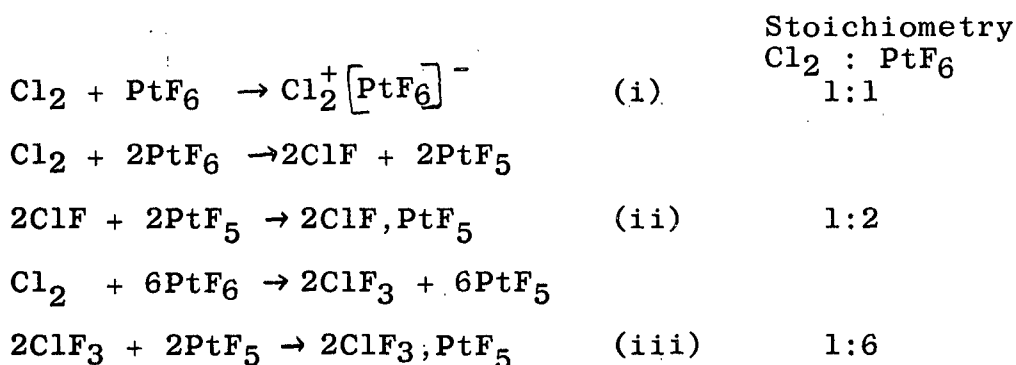


Unfortunately the reactions such as the latter predominated and there was no indication that the ionization reaction could occur.

(iv) Chlorine

The chlorine molecule has an ionization potential of 11.3 e.v.³⁶ and for the formation of $[\text{Cl}_2]^+ [\text{PtF}_6]^-$ the minimum value of the electron affinity of PtF_6 is therefore required to be at least 118 kcal.mole (Appendix IV). Apart from possible side reactions the formation of this compound appears to be favourable since for the O_2^+ case as we have seen the minimum

electron affinity of PtF_6 is required to be greater than 156 kcal/mole. The reaction product of Cl_2 and PtF_6 was amorphous but no evidence of free ClF_3 or ClF_5 was obtained in the infrared monitoring of the reaction. Absence of any free fluorinated species of chlorine indicates that chlorine is bound in the solid product. The various reactions which can be supposed to occur are given below along with the expected stoichiometry of the reactions.



The observed stoichiometry of the reaction was approximately 1:2.5 hence all three reactions could occur. Reaction (iii) is clearly not predominant. The solid product could not be characterized by X-ray powder photographs as it was amorphous. Incidentally $\text{ClF}_3, \text{PtF}_5$ normally yields sharp line X-ray powder photographs.⁸⁷ Obviously this reaction needs further investigation.

Though iridium hexafluoride fails to oxidize oxygen (observed in the present work) or xenon⁹⁴ it does react with nitric oxide not only to produce $\text{NO}^+ [\text{IrF}_6]^-$ which requires a minimum electron affinity of 89 kcal/mole but oxidizes more nitric oxide to yield $(\text{NO})_2\text{IrF}_6$ as well. This indicated that IrF_6 was perhaps capable of oxidizing chlorine. As in the

case for $\text{Cl}_2^+[\text{PtF}_6]^-$ the minimum value of E_1 of IrF_6 is required to be 118 kcal/mole. No free ClF or ClF_3 was formed during the observed reaction of chlorine with iridium hexafluoride. In two reactions the Cl_2 : IrF_6 stoichiometries were 1:1 and 1:1.4. The very pale yellow solid formed initially became a deeper yellow liquid in a few minutes. This liquid on keeping in an evacuated glass container for a period of a few weeks produced a yellow solid which was identified by X-ray powder photography to be iridium pentafluoride.⁵⁷ This last observation is in accord with the findings of Robinson and Westland who reported³⁸ that chlorine reacted with iridium hexafluoride at 55-60° to yield an oil which gives " IrF_4 " as a sublimate at 120-140°. The " IrF_4 " of Robinson and Westland has been recently identified in these laboratories as IrF_5 .⁵⁷ The sequence of changes observed in this work suggests that the first product may be $\text{Cl}_2^+[\text{IrF}_6]^-$, which decomposes perhaps to a $\text{ClF}_3, \text{IrF}_5$; IrF_5 mixture

$$6\text{Cl}_2 + [\text{IrF}_6]^- \rightarrow 2\text{ClF}_3, \text{IrF}_5 + 5\text{IrF}_5 + 5\text{Cl}_2$$

The $\text{ClF}_3, \text{IrF}_5$ adduct could have decomposed by interaction with the glass container: $4\text{ClF}_3, \text{IrF}_5 + 3\text{SiO}_2 \rightarrow 4\text{IrF}_5 + 3\text{SiF}_4 + 3\text{O}_2 + 2\text{Cl}_2$.

It will be necessary in further investigations of these interesting systems to work at lower temperatures and in non-silaceous containers, in order to preserve the initial products of reaction.

APPENDIX I

PROGRAM NUMBER 1

INVERSE MAGNETIC SUSCEPTIBILITY VS TEMP STRAIGHT LINE APPROXIMATION

SJOB

SIBFTC AAEM

C FORTRAN FOUR CONVERSION OF STRAIGHT LINE APPROXIMATION

C ESTIMATION OF PARAMETERS FOR A STRAIGHT-LINE APPROXIMATION

S3-6 1

C LET N = NUMBER OF OBSERVATIONS

S3-6 3

C LET X = INDEPENDENT VARIABLE

S3-6 4

C LET Y = DEPENDENT VARIABLE

S3-6 5

C THIS PROGRAM FITS LINE TO 1/MAGS VS TEMP

C LET Y(J) BE MAGS NOT 1/MAGS

C LET X(J) BE TEMP

14 SX = 0.

S3-6 6

SY = 0.

S3-6 7

SXX = 0.

S3-6 8

SXY = 0.

S3-6 9

SYY = 0.

S3-6 10

J=0

READ(5,1)N,AX,AY

1 FORMAT(16,2X,A4,2X,A4)

S3-6 12

DIMENSIONX(100),Y(100)

DO 2 I = 1,N

S3-6 13

J=J+1

READ(5,3)X(J),Y(J)

3 FORMAT(F7.0,F7.0)

Y(J)=1./Y(J)

SX = SX + X(J)

SY = SY + Y(J)

APPENDIX I CONTINUED

	SXX=SXX+X(J)*X(J)		
	SXY=SXY+X(J)*Y(J)		
2	SYY=SYY+Y(J)*Y(J)		
	READ(5,20)TEST		
20	FORMAT(A3)	S3-6	22
	CALL SETHOL(CHECK,3HEND)		
	IF(TEST-CHECK)11,12,11		
11	WRITE(6,13)		
13	FORMAT(51H WRONG NUMBER OF DATA CARDS OR LAST DATA CARD NOT ,		
1	32HFOLLOWED BY AN END-OF-DATA CARD)		
	STOP	S3-6	27
12	FN = N	S3-6	28
	DN = 1./FN	S3-6	29
	AVX = SX*DN	S3-6	30
	AVY = SY*DN	S3-6	31
	CALL SKIP TO (1)		
	WRITE(6,4)AX,AVX,AY,AVY		
4	FORMAT(16H MEAN VALUE OF A4,3H = E13.6/15X,A4,3H = E13.6)		
	DNN = 1./((FN - 1.))	S3-6	35
	S = SXX - SX*AVX	S3-6	36
	COVX = S*DNN	S3-6	37
	COVY = (SYY - SY*AVY)*DNN	S3-6	38
	COVXY = (SXY - SX*AVY)*DNN	S3-6	39
	STDY=SQRT(COVY)		
	WRITE(6,5)AX,STDY,AY,STDY		
5	FORMAT(//23H STANDARD DEVIATION OF A4,3H = E13.6/22X,A4,3H = E13.6		
1)			
12	CORR = COVXY/((STDY*STDY)	S3-6	44
11	WRITE(6,6)AX,AY,CORR		

APPENDIX I CONTINUED

6	FORMAT(/21H CORRELATION BETWEEN A4,4HAND A4,3H = F10.8)		
	A = COVXY/COVX	S3-6	47
	WRITE(6,7)A		
7	FORMAT(/32H SLOPE OF REGRESSION LINE = E13.6)		
	B = AVY - A*AVX	S3-6	50
	WRITE(6,8)B		
8	FORMAT(32H INTERCEPT OF REGRESSION LINE = E13.6)		
	R=SQRT((FN-1.)*(COVY-A*A*COVX)/(FN-2.))		
	WRITE(6,9)R		
9	FORMAT(32H STANDARD ERROR OF ESTIMATE = E13.6)		
	SI=R*SQRT(DN+AVX*AVX/S)		
	SS=R*SQRT(1./S)		
	WRITE(6,10)SS,SI		
10	FORMAT(31H CONFIDENCE INTERVAL PARAMETERS/21X10HSLOPE = E13.6/		
	121X10HINTERCEPT E13.6)		
	WRITE(6,22)		
22	FORMAT(////115H TEMP SUSC.(OBS) SUSC(CALC)		
1	DEVIATION (CGS*10E-6) 1/TEMP 1/SUSC(OBS) (1/CGS))		
	N=FN		
	J=0		
	DO42I=1,N		
	J=J+1		
	YCALC=A*X(J)+B		
	SCALC=1000000./YCALC		
	SOBSV=1000000./Y(J)		
	SDEVI=SOBSV-SCALC		
	TINV=1./X(J)		
	WRITE(6,33)X(J),SOBSV,SCALC,SDEVI,TINV,Y(J)		
33	FORMAT(F10.2,8H ,F10.2,9H ,F10.2,9H ,F10.2,		
116H	,F10.5,2H ,F10.2)		

APPENDIX I CONTINUED

```

42  CONTINUE
    WRITE(6,44)
44  FORMAT(///28H      TEMP          SUSC(CALC)///)
    TEMP=60.
    DO52I=1,12
    TEMP=TEMP+20.
    YCALC=A*TEMP+B
    SCALC=1000000./YCALC
    WRITE(6,55)TEMP,SCALC
55  FORMAT(F10.2,8H      ,F10.2)
52  CONTINUE
    GO TO 14
    END
$ENTRY

```

S3-6 61
S3-6 62

APPENDIX II

PROGRAM NUMBER 2

CALCULATION OF O,D,1/D*D,NFRN FROM ARC MEASUREMENTS

```

$JOB
$IBFTC INDEXX
44 BN=0.
   CN=0.
   SCP=0.
   SBP=0.
C   CALC OF BEAM STOP CENTRE BPA=AV(X1+X2/2)
C   DATA CARD WITH X1=X2=0 SIGNALS END OF DATA
1   READ(5,30)X1,X2
30  FORMAT(2F10.3)
   BP=(X1+X2)/2.
   SBP=SBP+BP
   IF(BP.EQ.0.)GO TO 3
   BN=BN+1.
   GO TO 1
3   BPA=SBP/BN
C   CALC OF COLLIMATOR CENTRE CPA=AV(X1+X2)/2
C   DATA CARD WITH X1=X2=0. SIGNALS END OF DATA
4   READ(5,30)X1,X2
   CP=(X1+X2)/2.
   SCP=SCP+CP
   IF(CP.EQ.0.)GO TO 5
   CN=CN+1.
   GO TO 4
12  5   CPA=SCP/CN
11  WRITE(6,75)

```

APPENDIX II CONTINUED

```

75  FORMAT(1X,10H      X1      ,20H      2THETA,20H      D
      1HKL      ,20H      1/D*D      ,30H      NREFN //
      2/)
C   FACTOR TO CONVERT ARC TO ANGLE
      ANGLE=3.1414/(CPA-BPA)
      IF(ANGLE.LT.0.)GO TO 7
      GO TO 13
7   ANGLE=-ANGLE
C   CALC OF 2THETA,DCORR,1/D*D
C   IF X FOR ALPHA1 ADD 100 TO X VALUE
C   IF X FOR ALPHA2, ADD 200 TO X VALUE
C   X1=0 SIGNALS END OF DATA + NO OTHER SET
C   X1=999 SIGNALS END OF DATA + ANOTHER SET FOLLOWING
13  READ(5,2)X1
2   FORMAT(F10.3)
      IF(X1.EQ.0.)GO TO 17
      IF(X1.EQ.999.)GO TO 70
      IF(X1.GT.200.)GO TO 14
      IF(X1.GT.100.)GO TO 15
      AMBDA=0.7709
      GO TO 16
14  X1=X1-200.
      AMBDA=0.77217
      GO TO 16
15  X1=X1-100.
      AMBDA=0.77025
      GO TO 16
16  X2=X1-BPA
      THETA2=X2*ANGLE
      IF(THETA2.LT.0.)GO TO 20

```

APPENDIX II CONTINUED

```

20      GO TO 21
21      THETA2=-THETA2
      THETA=THETA2/2.
      CTHETA=COS(THETA)
      STHETA=SIN(THETA)
      XTHETA=1./STHETA
      DHKL=AMBDA*XTHETA
      DINSQ=1./(DHKL*DHKL)
      XNRFN=0.5*((CTHETA*CTHETA/STHETA)+(CTHETA*CTHETA/THETA))
      THETA2=360./6.2828*THETA2
      WRITE(6,18)X1,THETA2,DHKL,DINSQ,XNRFN
18      FORMAT(1X,F10.3,10H          ,F10.3,10H          ,F10.5,10H
1      ,F10.6,20H          ,F10.3/)
      GO TO 13
70      CALL SKIP TO (1)
      GO TO 44 ,
17      STOP
      END
$ENTRY

```

APPENDIX III

PROGRAM NUMBER 3

CALCULATION OF $1/D^2$ FOR ASSUMED SET OF UNIT CELL PARAMETERS

```
$JOB
$TIME      15
$IBFTC DATAPR
C DATA PREPARATION FOR CRYSTAL STRUCTURE ANALYSIS
C X-RAY ANALYSIS GROUP CHEMISTRY DEPARTMENT UNIVERSITY OF
C BRITISH COLUMBIA
988 READ 989, IPR1, IOUT1
989 FORMAT (I2,I2)
REWIND IOUT1
GO TO (90,99), IPR1
90 READ 80, WAVE,A1,A2,A3,CSA1,CSA2,CSA3,SNA2,PHI0,FL1M
80 FORMAT(F5.4,4X,F6.6,F6.6,F6.6,2X,F7.5,F7.5,F7.5,F7.5,2X,F7.3,F3.2)
R1=WAVE*A1*SNA2
R2=WAVE*A2*(CSA3-CSA1*CSA2)/SNA2
R3=WAVE*A2*SQRT (1.-CSA1**2-CSA2**2-CSA3**2+2.*CSA1*CSA2*CSA3)
1 /SNA2
R4=WAVE*A1*CSA2
R5=WAVE*A2*CSA1
R6=WAVE*A3
FOVLS = 4.0/(WAVE**2)
READ 81, LSTRT,LNEG1,LNEG2,L,M,N,KIN,JIN,II,JJ,KK
81 FORMAT (I2,I2,I2,I2,I2,I2,7X,I2,I2,6X,I1,I1,I1)
JSIGN=1
69 KSIGN=1
70 DO 1 IP=LSTRT,50,L
11 FI=IP-1
```

APPENDIX III CONTINUED

```

71 DO 2 JP=1,50,M
   IF (JSIGN) 52,53,53
72 DO 3 KP=1,50,N
   IF (KSIGN) 56,59,59
73 X1=R1*FKD+ R2*FJ + 0.0000001
   X2=R3*FJ
   X3=R4*FKD+ R5*FJ + R6*FI
   DIMENSION LFI(3)
   SINSQ=0.25*(X1**2 + X2**2 + X3**2)
   OOVDS = FOVLS * SINSQ
   IF (SINSQ-FL1M) 8,9,9
9   IF (FKD) 2,10,2
10  IF (FJ) 1,20,1
8   TWOTH=114.59156*ATAN(SQRT (SINSQ/(1.-SINSQ)))
   CHI=57.29578*ATAN(X3/SQRT (X1**2 + X2**2))
   PHI=57.29578*ATAN(X2/X1) +PHI0
   IF (X1) 30,31,31
30  PHI=PHI + 180.
   GO TO 35
31  IF (X2) 32,35,35
32  PHI=PHI + 360.
35  LFI(1)=FKD
   LFI(2)=FJ
   LFI(3)=FI
   IF (PHI-360.) 3,37,37
37  PHI=PHI-360.
3   PUNCH 2011, LFI(II),LFI(JJ),LFI(KK),OOVDS
2011 FORMAT (10X,3I3,27X,F8.3)
12  2 CONTINUE
11  1 CONTINUE

```

APPENDIX III CONTINUED

```

20  IF (KSIGN) 21,22,22
22  KSIGN=KIN
    IF (KSIGN) 91,21,21
91  LSTRT=LNEG1
    GO TO 70
21  IF (JSIGN) 23,24,24
24  JSIGN=JIN
    IF (JSIGN) 92,25,25
92  LSTRT=LNEG2
    GO TO 70
23  IF (KSIGN) 69,25,25
25  PRINT 26
26  FORMAT (1X,14HSTARTING  SORT)
    GO TO 100
52  FJ =-JP+1
    GO TO 72
53  FJ = JP-1
    GO TO 72
56  FKD=-KP+1
    GO TO 73
59  FKD= KP-1
    GO TO 73
C 100  LIBRARY PROGRAM FOR SORTING DATA (IBSRT)
C      WITH FINAL OUTPUT ON PRINTER
C
100  GO TO 988
99  READ 101, WAVE,AA,BB,CC,CSA,CSB,CSG,NCURV,IFILE
101  FORMAT (F5.4,4X,F6.6,F6.6,F6.6,2X,F7.5,F7.5,F7.5,9X,I2,2X,I2)
12  WAVE2=WAVE**2
11  AHH=0.25 * WAVE2 * AA**2

```

APPENDIX III } CONTINUED

```

AKK=0.25 * WAVE2 * BB**2
ALL=0.25 * WAVE2 * CC**2
AHL=0.50 * WAVE2 * AA*CC*CSB
AHK=0.50 * WAVE2 * AA*BB*CSG
AKL=0.50 * WAVE2 * BB*CC*CSA
DIMENSION FCURV(8), FO(8), P(8), F(8,14)
DO 200 I=1,NCURV
200 READ 201, P(I), FO(I), (F(I,J),J=1,14)
201 FORMAT (16F5.3)
DO 400 I=1,8
400 FCURV(I)=0.
ONOLS = 1./WAVE2
C ROUTINE FOR WINDING OUTPUT TAPE TO PROPER FILE
ASSIGN 253 TO IENDF
CALL EOF (IOUT1,IENDF)
NFILE = IFILE
254 IF (NFILE - 1) 102,102,252
252 READ (IOUT1) II,IGPEN,SSOLS,FH,FK,FL,FOBS,FOBS2,(FCURV(I),I=1,8)
GO TO 252
253 NFILE = NFILE - 1
GO TO 254
102 READ 103,II,IGPEN,FH,FK,FL,FINT,VBS,S1NSM
103 FORMAT (I2,1X,I2,5X,F3.0,F3.0,F3.0,2X,F5.0,4X,F5.2,5X,F5.5)
IF (II) 300,301,300
301 IF (IGPEN) 300,302,300
300 SSOLS=0.
FREL=0.
FSQR=0.
DO 303 I=1,NCURV
11 303 FCURV(I)=0.

```

APPENDIX III CONTINUED

```

GO TO 105
302  FS1N2=AHH*FH**2 + AKK*FK**2 + ALL*FL**2 + AHL*FH*FL + AHK*FH*FK +
      1 AKL*FK*FL
      IF (FS1N2 -1.) 104,104,102
104  RCLOR=2.*SQRT ((1.-FS1N2)*(FS1N2-S1NSM))/(1.-2.*FS1N2+2.*FS1N2**2)
      FSQR = FINT * RCLOR * VBS
      FREL = SQRT (FSQR)
      SSOLS = FS1N2 * ONOLS
      STOLS = SQRT (SSOLS)
      IF (STOLS - 0.1) 203,204,204
203  DO 202 I=1,NCURV
202  FCURV(I) = FO(I)/EXP (P(I)*SSOLS)
      GO TO 105
204  IF (STOLS - 1.0) 205,206,206
205  K0 = 1
207  K1 = K0 + 1
      E1 = K1
      F1 = 0.1*E1
      IF (STOLS - F1) 40,41,41
41  K0 = K0 + 1
      GO TO 207
40  E0 = K0
      F0 = 0.1*E0
      K2 = K0 + 2
      K3 = K0 + 3
      RANGE = STOLS - F0
      DO 402 I=1,NCURV
402  FCURV(I) = F(I,K0) + (F(I,K1)-F(I,K0))*RANGE*10. + 50.*
      1 (F(I,K2)-2.*F(I,K1)+F(I,K0))*RANGE**2 + 166.667*
      2 (F(I,K3)-3.*F(I,K2)+3.*F(I,K1)-F(I,K0))*RANGE**3

```

APPENDIX III CONTINUED

```

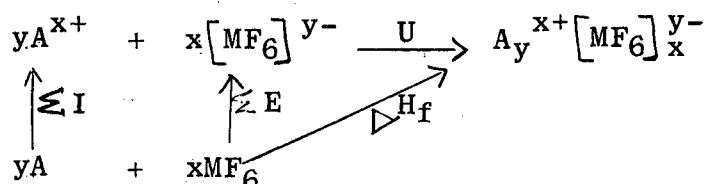
GO TO 105
206 KLOW = 10
209 KHIGH= KLOW + 1
      EHIGH= KHIGH
      FHIGH= 0.1 * EHIGH
      IF (STOLS - FHIGH) 42,43,43
43   KLOW = KLOW + 1
      GO TO 209
42   DO 502 I=1,NCURV
502   FCURV(I) = F(I,KHIGH) + (F(I,KLOW)-F(I,KHIGH))*(FHIGH-STOLS)*10.
105   PRINT 2013, II,IGPEN,SSOLS,FH,FK,FL,FREL,FSQR, (FCURV(I),I=1,8)
2013  FORMAT (1X,I2,1X,I2,1X,F7.4,2X,3F5.0,2X,F6.1,2X,F6.0,7(F6.3,1X),
      1 F6.3)
106   IF (II) 198,102,198
198   GO TO 99
      END
$ENTRY
0102
      1 2      1 1 1      -1      123

```

APPENDIX IV

Estimation of Minimum Electron Affinities of The Noble Metal Hexafluorides for Various $A_y^{x+}[MF_6]_x^{y-}$ Formulations.

The value of the minimum electron affinity of a noble metal hexafluoride, MF_6 has been derived by using a Born Haber cycle for the formation of salts $A_y^{x+}[MF_6]_x^{y-}$:



where A is a reagent like O_2, NO, CO etc.; $x = 1$ or 2 , $y = 1$ or 2 ; $\sum E$ is the total electron affinity of MF_6 molecule; $\sum I$ is the total enthalpy of ionization of A; U and ΔH_f are lattice energy and heat of formation of $A_y[MF_6]_x$ respectively. Lattice energies were calculated using Kapustinskii's equation,¹¹²

$$U = 287.2 \sum n \frac{z_1 z_2}{r_C + r_A} \left(1 - \frac{0.345}{r_C + r_A}\right) \text{ where } \sum n \text{ is the}$$

number of ions in the molecule $A_y[MF_6]_x$, z_1 and z_2 the ionic charges and $r_C + r_A$ is the sum of the radii of the anion and cation in the lattice when referred to coordination number six.

The values of $r_C + r_A$ for $O_2^+[PtF_6]^-$ and $NO^+[MF_6]^-$ were obtained by correcting the observed interionic distances for coordination number six.¹¹³ The interionic distances in these salts were calculated from the known unit cell parameters (CsCl type, 8:8 coordination).

The values of $r_C + r_A$ for other salts have been derived by subtracting 1.33 \AA (for the O_2^+ radius, taken to be equal to the

K^+ radius) from $r_C + r_A$ of O_2PtF_6 and then adding the appropriate value of the radius of A^{x+} .

The radii of Xe^+ and Xe^{2+} were taken to be 1.50 and 1.00 Å respectively on the basis of the calculated covalent radius of xenon in XeF_4 (1.31 Å, Xe having a positive charge of 1.36)⁹³ and on the basis of the bond length, Xe-F being 2.00 Å in XeF_2 .¹¹⁴

From the Born Haber cycle given in the last page, $\Delta H_f = \sum I + \sum E + U$. For the formation of $A_y[MF_6]_x$ ΔH_f should be exothermic and hence $\sum E$ should be more exothermic than $\sum I + U$. The minimum value of $\sum E$ has been taken as $\sum I + U$. The values for the minimum electron affinities of MF_6 for the formation of some $A_y[MF_6]_x$ salts, along with the values of ionization potentials of A and lattice energies of $A_y[MF_6]_x$ are tabulated below.

	U (kcal/mole)	$\sum I$ kcal/mole	Minimum $\sum E$ for exothermic ΔH_f (kcal/mole)	
			$[MF_6]^-$	$[MF_6]^{2-}$
$O_2^+[PtF_6]^-$	-125	281	-156	
$NO^+[MF_6]^-$	-124	213	-89	
$(NO^+)_2[MF_6]^{2-}$	-372	426		-54
$Cl_2^+[MF_6]^-$	-112	230	-118	
$CO^+[PtF_6]^-$	-125	323	-198	
$Kr^+[PtF_6]^-$	-125	323	-198	
$Xe^+[PtF_6]^-$	-120	280	-160	
$Xe^{2+}[PtF_6]_2^-$	-402	747	-172	
$N_2^+[PtF_6]^-$	-125	358	-233	

REFERENCES

1. A. G. Sharpe, Quart. Rev., 1957, 11, 49.
2. J. G. Stamper and R. F. Barrow, Trans. Faraday Soc., 1958, 54, 1592.
3. L. Pauling "Nature of the Chemical Bond", 3rd ed., Cornell University Press, Ithaca, N.Y., 1960, p.225 and p.514.
4. JANAF Thermochemical Tables, Thermal Research Lab., The Dow Chemical Company, 1960-1963.
5. B. Weinstock, Record of Chemical Progress, 1962, 23, 23.
6. B. Weinstock, Chem. and Eng. News, 1964, Sept. 21, 86.
7. R. D. Peacock, "Some Fluorine Compounds of the Transition Metals" in "Progress in Inorganic Chemistry", Vol. 2, Interscience Publishers, New York, 1960.
8. R. D. W. Kemmitt, D. R. Russell, and D. W. A. Sharp, J. Chem. Soc., 1963, 4408.
9. J. H. Holloway, R. D. Peacock, and R. W. H. Small, *ibid*, 1964, 644.
10. B. N. Figgis and J. Lewis, "The Magnetic Properties of Transition Metal Complexes" in "Progress in Inorganic Chemistry", Vol. 6, Interscience Publishers, New York, 1964.
11. W. Moffitt, G. L. Goodman, M. Fred, and B. Weinstock, Mol. Phys., 1959, 2, 109.
12. H. H. Claassen, J. Chem. Phys., 1959, 30, 968.
13. B. Weinstock, H. H. Claassen, and J. G. Malm, *ibid.*, 1960, 32, 181.
14. H. H. Claassen, H. Selig, and J. G. Malm, *ibid.*, 1962, 36, 2888.
15. H. H. Claassen, J. G. Malm, and H. Selig, *ibid.*, 1962, 36, 2890.
16. G. B. Hargreaves and G. H. Cady, J. Chem. Soc., 1961, 1563.
17. Wang Yi Ch'iu, Soviet Physics, Doklady, 1961, 6, 39.
18. E. L. Muetterties and W. D. Phillips, "The Use of NMR in Inorganic Chemistry", in "Advances in Inorganic Chemistry and Radiochemistry", Vol. 4, Academic Press, Inc., New York, 1962.

19. E. L. Muetterties and K. J. Packer, J. Am. Chem. Soc., 1964, 86, 293.
20. N. Bartlett, S. Beaton, L. W. Reeves, and E. J. Wells, Can. J. Chem., 1964, 42, 2531.
21. C. A. Hutchison, Jr., and B. Weinstock, J. Chem. Phys. 1960, 32, 56.
22. I. J. Solomon, et al., Inorg. Chem., 1964, 3, 457.
23. (a) B. Weinstock, H. H. Claassen, and J. G. Malm, J. Am. Chem. Soc., 1957, 79, 5832.
(b) B. Weinstock, J. G. Malm, and E. E. Weaver, *ibid.*, 1961, 83, 4310.
24. H. Selig, C. L. Chernick, and J. G. Malm, Inorg. Nuclear Chem. 1961, 19, 377.
25. H. H. Claassen, H. Selig, J. G. Malm, C. L. Chernick, and B. Weinstock, J. Am. Chem. Soc., 1961, 83, 2390.
26. C. L. Chernick, H. H. Claassen, and B. Weinstock, *ibid.*, 1961, 83, 3165.
27. (a) J. G. Malm, H. Selig, and S. Fried, *ibid.*, 1960, 82, 1510.
(b) J. G. Malm, and H. Selig, J. Inorg. Nuclear Chem. 1961, 20, 189.
28. O. Ruff and F. W. Tschirch, Ber. 1913, 46, 929.
29. B. Weinstock and J. G. Malm, J. Am. Chem. Soc., 1958, 80, 4466.
30. M. A. Hepworth and P. L. Robinson, J. Inorg. Nuclear Chem. 1957, 4, 24.
31. G. B. Hargreaves and R. D. Peacock, J. Chem. Soc., 1960, 2618.
32. S. Siegel and D. Northrop, private communication to N. Bartlett.
33. B. Weinstock and H. H. Claassen, J. Chem. Phys., 1959, 31, 262.
34. N. Bartlett and D. H. Lohmann, J. Chem. Soc., 1962, 5253.
35. N. Bartlett, Proc. Chem. Soc., 1962, 218.
36. F. H. Field and J. L. Franklin "Electron Impact Phenomena". Academic Press, Inc., New York, 1957.

37. H. H. Hyman, ed., "Noble Gas Compounds", The University of Chicago Press., Chicago, 1963.
38. P. L. Robinson and G. J. Westland, J. Chem. Soc., 1956, 4481.
39. E. E. Aynsley, N. N. Greenwood, and D. H. W. Wharmby, J. Chem. Soc., 1963, 5369.
40. D. H. Lohmann, Ph.D. Thesis, University of British Columbia, Canada, 1961.
41. G. A. Welch and N. Parker, U.K.A.E.A. unclassified report WSL-R-36, 1959.
42. J. D. Rushmere and H. Messon, U.K.A.E.A. unclassified report SCS-R-392, ARDC/P-84, 1959.
43. Page 2620 in Reference 33.
44. R. Gilchrist and E. Wichers, J. Am. Chem. Soc., 1935, 57, 2567.
45. A. I. Vogel, "A Textbook of Quantitative Inorganic Analysis", Longman's Green & Co., Toronto, 1955, 261.
46. H. H. Willard and O. B. Winter, Ind. Eng. Chem., Anal. Ed., 1933, 5, 7.
47. S. Cromer, USAEC, MDDC-803, 1944, June 20.
48. H. C. Clark and R. J. O'Brien, Can. J. Chem., 1961, 39, 1033.
49. B. N. Figgis and R. S. Nyholm, J. Chem. Soc., 1959, 331.
50. B. N. Figgis and R. S. Nyholm, *ibid.*, 1958, 4190.
51. P. W. Selwood, "Magnetochemistry", 2nd ed., Interscience Publishers, New York, 1956, 92.
52. J. B. Nelson and D. P. Riley, Proc. Phys. Soc., 1945, 57, 160.
53. N. Bartlett, "Fluorine Compounds of the Platinum Metals" in "Preparative Inorganic Reactions", Vol. 2, W. L. Jolly, ed., Interscience Publishers, New York, 1965. 319.
54. (a) L. A. Woodward and H. L. Roberts, Trans. Faraday Soc., 1956, 52, 615.
(b) N. J. Hawkins, and W. W. Sabol, J. Chem. Phys., 1956, 25, 775.
55. J. H. Holloway and R. D. Peacock, J. Chem. Soc., 1963, 527.

56. J. H. Hollway, P. R. Rao, and N. Bartlett, Chem. Comm. 1965, 306.
57. N. Bartlett and P. R. Rao, *ibid*, 1965, 252.
58. N. Bartlett and M. Akhtar, unpublished work.
59. B. C. Eggleston, D. F. Evans, and R. E. Richards, J. Chem. Soc., 1954, 943.
60. H. H. Claassen, C. L. Chernick, and J. G. Malm, J. Am. Chem. Soc., 1963, 85, 1927.
61. M. A. Hepworth, K. H. Jack, and G. J. Westland, J. Inorg. Nuclear Chem., 1956, 2, 79.
62. N. Bartlett and S. P. Beaton, unpublished work.
63. O. Glemser, Paper read at "The Symposium on Fluorine Compounds" at the meeting of American Chemical Society, Chicago, July, 1964.
64. H. v. Wartenberg, Ann., 1924, 440, 97.
65. E. E. Aynsley, R. D. Peacock, and P. L. Robinson, J. Chem. Soc., 1950, 1622.
66. N. Bartlett and J. Trotter, to be published.
67. G. H. Cady and G. B. Hargreaves, J. Chem. Soc., 1961, 1568.
68. Page 99 in Reference 10.
69. H. Selig, F. A. Cafasso, D. M. Gruen and J. G. Malm, J. Chem. Phys. 1962, 36, 3440.
70. B. J. Brisdon and G. W. A. Fowles, unpublished results as quoted in Reference 10.
71. R. G. Williams and G. W. A. Fowles, unpublished results as quoted in Reference 10.
72. E. G. Ippolitov, Zh. Neorgan. Khim., 1962, 7, 940.
73. J. Lewis and G. Wilkinson, J. Inorg. Nuclear Chem. Soc., 1958, 6, 12.
74. G. B. Hargreaves and R. D. Peacock, Proc. Chem. Soc., 1959, 6, 12.
75. J. R. Geichman, E. A. Smith, and P. R. Ogle, Inorg. Chem., 1963, 2, 1012
76. M. A. Hepworth, P. L. Robinson, and G. J. Westland, Chem. and Ind., 1955, 1516.

77. M. A. Hepworth, Ph. D. Thesis, University of Durham, 1956.
78. M. A. Hepworth, P. L. Robinson, and G. J. Westland, J. Chem. Soc., 1954, 4268.
79. M. A. Hepworth, P. L. Robinson, and G. J. Westland, *ibid.*, 1958, 611.
80. J. A. Ibers and W. C. Hamilton, to be published.
81. A. C. Hurley, J. Mol. Spect., 1962, 9, 18.
82. D. P. Mellor and N. C. Stephenson, Austral. J. Sci. Res., 1951. A4, 406.
83. N. Bartlett, to be published.
84. "Interatomic Distances and Configurations in Molecules and Ions", Chemical Society, (London), Special Publication No. 11, 1958 and Supplement to the above, Special Publication No. 18, 1965.
85. G. Herzberg, "Spectra of Diatomic Molecules", 2nd ed., D. Van Nostrand Co., New York, 1950.
86. T. H. Jordan, H. W. Smith, W. E. Streib, and W. N. Lipscomb, Acta, Cryst., 1964, 17, 777.
87. N. Bartlett and D. H. Lohmann, J. Chem. Soc., 1964, 619.
88. R. D. Peacock and D. W. A. Sharp, J. Chem. Soc., 1959, 2762.
89. A. J. Edwards, J. H. Holloway, and R. D. Peacock, Proc. Chem. Soc., 1963, 275.
90. R. Hoppe, H. Mattauch, K. M. Rödder, and W. Dähne, Z. anorg. allg. Chem., 1963, 325, 214.
91. F. Mahieux, Compt. Rend., 1963, 257, 1083.
92. F. Mahieux, *ibid.*, 1964, 258, 3497.
93. R. T. Sanderson, Inorg. Chem., 1963, 2, 661.
94. C. L. Chernick, et al., Science, 1962, 138, 136.
95. J. R. Geichman, E. A. Smith, S. S. Trond, and P. R. Ogle, Inorg. Chem., 1962, 1, 661.
96. H. Bode and E. Voss, Z. anorg. Chem., 1951, 264, 144.
97. B. N. Figgis, J. Lewis, and F. E. Mabbs, J. Chem. Soc., 1961, 3138.

98. R. D. Peacock, *Rec. trav. Chim.*, 1956, 75, 576.
99. A. Earnshaw, B. N. Figgis, J. Lewis, and R. D. Peacock, *J. Chem. Soc.*, 1961, 3132.
100. W. H. Zachariasen, *Acta, Cryst.*, 1948, 1, 277.
101. J. H. Burns, *Inorg. Chem.*, 1965, 4, 881.
102. N. Bartlett and P. L. Robinson, *J. Chem. Soc.*, 1961, 3417.
103. W. H. Zachariasen, *J. Am. Chem. Soc.*, 1948, 70, 2147.
104. N. Bartlett and K. H. Jack, personal communication.
105. Page 236 in Reference 7.
106. N. Bartlett, Ph. D. Thesis, University of Durham, 1958, 25.
107. Page 85 in Reference 3.
108. R. D. Mackenzie, *Science*, 1963, 141, 1171.
109. N. Bartlett, *Endeavour*, 1964, 3, 23.
110. R. M. Reese and V. H. Dibeler, *J. Chem. Phys.*, 1956, 24, 1175.
111. J. R. Majer "Mass Spectrometry of Fluorine Compounds", in "Advances in Fluorine Chemistry", Vol. 2, Butterworths, London, 1961, 83.
112. A. F. Kapustinskii, *Quart. Rev.*, 1956, 10, 283.
113. Page 522 in Reference 3.
114. H. A. Levy and P. A. Argon, *J. Am. Chem. Soc.*, 1963, 85, 241.